NASA CR-134885

# SEMICONDUCTING POLYMERS

## FOR

## GAS DETECTION

by N. R. Byrd and M. B. Sheratte

MCDONNELL DOUGLAS CORPORATION
DOUGLAS AIRCRAFT COMPANY

prepared for

NATIONAL AERONAUTICS AND SPACE ADMINISTRATION

PRICES SUBJECT TO CHANGE

| 1. Report No<br>NASA CR 134885 | 2. Government Accession No. | 3. Recipient's Catalog No. |
|---|---|---|
| 4. Title and Subtitle<br>Semiconducting Polymers for Gas Detection | | 5. Report Date<br>December 1975 |
| | | 6. Performing Organization Code |
| 7. Author(s)<br>N. R. Byrd & M. B. Sheratte | | 8 Performing Organization Report No. |
| 9. Performing Organization Name and Address<br>McDonnell Douglas Corporation<br>Douglas Aircraft Company<br>3855 Lakewood Boulevard<br>Long Beach, California 90846 | | 10. Work Unit No. |
| | | 11. Contract or Grant No.<br>NAS 3-18919 |
| 12. Sponsoring Agency Name and Address<br>National Aeronautics & Space Administration<br>Washington, D.C. 20546 | | 13. Type of Report and Period Covered<br>Contractor Report |
| | | 14. Sponsoring Agency Code |

15 Supplementary Notes

NASA Project Manager, Richard E. Gluyas, Materials and Structures Division
NASA Lewis Research Center, Cleveland, Ohio 44135

16. Abstract

Four conjugated polyenes, and two polyesters containing phthalocyanine in their backbone, were synthesized. These polymers were characterized by chemical analysis, thermogravimetric analysis, spectral analysis, and X-ray diffraction studies for crystallinity, as well as for their film-forming capability and gas/polymer interactions. Most of the polymers were relatively insensitive to water vapor up to 50 percent relative humidity, but the polyester/phthalocyanine (iron) polymer was relatively insensitive up to 100 percent RH. On the other hand, poly(p-dimethyl-aminophenylacetylene) was too conductive at 100 percent RH. Of the gases tested, the only ones that gave any evidence of interacting with the polymers were $SO_2$, $NO_x$, HCN and $NH_3$. Poly(imidazole)/thiophene responded to each of these gases at all relative humidities, while the other polymers gave varying response, depending upon the RH. Thus, since most of these gases were electron-accepting, the electron-donating character of poly(imidazole)/thiophene substantiates the concept of electronegativity being the operating principle for interaction effects. Of the six polymers prepared, poly(imidazole)/thiophene first showed a very good response to smoldering cotton, but it later became non-responsive; presumably due to oxidation effects. However, poly(imidazole)/ferrocene generally gave consistent responses. The other four did not. The reason for this is not known.

| 17. Key Words (Suggested by Author(s))<br>Polymeric Fire Detector<br>Gas Sensing Polymers<br>Semiconducting Polymers | 18. Distribution Statement<br><br>Unclassified Unlimited |
|---|---|

| 19. Security Classif. (of this report)<br>Unclassified | 20. Security Classif. (of this page)<br>Unclassified | 1/: | Price* |
|---|---|---|---|

NASA-C-168 (Rev. 6-71)

BLANK PAGE

## FOREWORD

This document represents the final report for the work accomplished between
1 July 1974 and 29 June 1975 by McDonnell Douglas Corporation for the
National Aeronautics and Space Administration, Lewis Research Center,
Cleveland, Ohio; under Contract NAS3-18919 on Semiconducting Polymers for
Gas Detection. This work was under the technical direction of Dr. Richard
E. Gluyas, NASA Project Manager.

Work in the program was conducted at McDonnell Douglas Corporation's
Douglas Aircraft Company and McDonnell Douglas Astronautics Company, Long
Beach and Huntington Beach, California. Dr. N. R. Byrd was the McDonnell
Douglas Program Manager, and the work was performed by Dr. M. B. Sheratte.

BLANK PAGE

# TABLE OF CONTENTS

TABLE OF CONTENTS (Cont'd.)

# LIST OF TABLES

BLANK PAGE

# LIST OF FIGURES

Preceding page blank

BLANK PAGE

# LIST OF PLATES

BLANK PAGE

SEMICONDUCTING POLYMERS

FOR

GAS DETECTION

BY

N. R. BYRD

M. B. SHERATTE

## SUMMARY

The objective of this program was to synthesize six conjugated polyenes of
varying electronegativity and having film-forming capability. For this purpose,
poly(imidazole)/thiophene (I), poly(Schiff's base)/thiophene (II), poly(imidazole)
/ferrocene (III), polyester/phthalocyanine (metal-free) (IV), polyester/phthalo-
cyanine (iron)(V), and poly(p-dimethylaminophenylacetylene) (VI) were to be
synthesized. These semiconducting polymer films were to be deposited on a
lock-and-key type of electrode sensor and checked for their response behavior
to a number of gases, as well as to gases from a smoldering cotton fire. In
addition, the polymers prepared were to be evaluated by thermogravimetric
analysis (TGA) and isothermal (35°C) gravimetric analysis.

All of the six polymers were prepared. In the case of the homopolymers, i.e.,
polymers I, II, III and VI, the characterization and analysis of the intermediates
in their preparation, as well as the polymers, themselves, resulted in excellent
values, thereby unequivocally establishing their identity. In the preparation
of the phthalocyanine used as a comonomer for polymers IV and V, the inter-
mediates, and the phthalocyanine, also analyzed very well. It was only in the
preparation of the copolymer that any discrepancies resulted, and here, again,
the analysis for the hydrogen, nitrogen and iron atoms was in fairly good agree-
agreement with structure. Infrared spectral analysis of all compounds and
polymers also correlated very well with structure.

The molecular size distribution, by gel permeation chromatography (GPC), for those
polymers that were soluble in chloroform, correlated quite well with the relative
viscosity data. A further interesting feature is the fact that the polyester
/phthalocyanine polymer had a higher relative viscosity value than the conjugated

polyenes. This might be related to an actually higher molecular size or that the polyenes are more rod-like and, therefore, show less resistance to flow.

X-ray crystallographic analysis of the polymers showed only the poly(Schiff's base) to be crystalline, as a powder.

Film deposition of the various polymers could only be effected by a dipping technique. A one percent solution gave films varying in thickness, depending upon the polymer, from 0.57 microns to 13.64 microns. In some cases the films were uniform and coherent, in others they were non-uniform and cracked.

The thermogravimetric analysis (TGA) data and isothermal weight loss data showed excellent correspondence. A striking anomaly was found in the excellent stability of the polyester/phthalocyanine polymers, as shown by their TGA data.

With regard to their gas interaction responses, polymers I and V were least affected by moisture due to changes in relative humidity; with polymer V being the best. Polymer VI, however, was the most affected by water vapor at the high (75 percent and 100 percent) relative humidities. The only gases that elicited major response were $NH_3$, $SO_2$, $NO_x$ and HCN. The responses were generally related to the relative humidity, for most polymers. For example, $NO_x$ was most readily detected by polymer IV at 25 percent RH, but at 50 percent and 75 percent RH, polymer VI gave the greatest response to $NO_x$. Sulfur dioxide, on the other hand, was most interactive with polymer III at 25 percent, 50 percent and 75 percent RH, but at 100 percent RH, polymer II gave the greatest response. On an overall basis, however, polymer I was responsive to $SO_2$ at each RH, albeit not at the magnitude of II or III. From the data, it was observed that polymer I was more responsive to those gases that elicited a response than was any other polymer. Thus, based upon the gases that caused a signal to be generated, and considering the structure for polymer I, it appears that the concept of electron-donor polymer with electron-accepting gas, i.e., electronegativity factor, is still a viable operating principle in forming charge-transfer complexes in gas detecting polymers.

# 1.0 INTRODUCTION

Fires, whether in private dwellings or in aircraft, are a matter of great concern . The annual loss in lives and property is very large, and because of this, numerous programs have been undertaken to study the cause, propagation, prevention and detection of fires. The President's National Commission on Fire Prevention and Control, after a lengthy study relating to fires in various dwellings, issued a report in 1973 listing a number of priorities regarding efforts to minimize fire hazards; and number two on that list (after fire prevention) was the need for early warning fire detectors. Thus, the probem of early warning fire detection in order to save lives and property in nursing homes, hospitals, private dwellings, office buildings, mines and aircraft is of paramount importance. To this end, a fire detector capable of monitoring the atmosphere and rapidly detecting the presence of any contaminant buildup is needed.

Recently, there has been a proliferation of fire and/or gas detecting devices on the commercial market that are claimed to be able to detect fires either by heat evolution or combustion products generated. The detection techniques are varied, using either infrared, thermal (low-melting alloys), photoelectric, ionization chambers, and heated surface semiconducting sensors (TGS). Essentially, each system has its own merits in being able to detect a fire. Both the ionization chamber and TGS device can detect a fire in the incipient stage from the gases generated. The photoelectric system detects visible smoke particles by obscuration or by scattering of the light by the smoke when the light is picked up by a light-sensitive element. In the later stages of a fire, i.e., the flame and heat stages, the detection method is by infrared or thermal detectors. However, in none of these systems is there any degree of specificity.

A promising approach that could obviate the difficulties of the other techniques is an outgrowth of earlier NASA sponsored programs (References 1-3), and consists of a solid state device that uses polymeric organic semiconductors, either alone or in conjunction with an inorganic semiconductor. Initially, polymeric, film-forming organic semiconductors, e.g., substituted polyacetylenes (polyphenylacetylene and its derivatives) were used as the detecting materials in a solid-state sensor (Reference 1). This was further expanded upon in Contract NAS3-17515 (Reference 2) with other polyacetylenes, e.g., poly(ethynylferrocene),

poly(etnynylcarborane) and poly(ethynylpyridine), among others. They act as semiconductors, and can also be chemically modified so that the effect of substituents, on their conduction and complexing capability, can be observed. The basic principle upon which the polymeric organic semiconductors depend for their detection capability is a relationship between their electronegativity, adsorption characteristics, complexing behavior, and a change in some of their electrical properties.

The objective of this program was to synthesize six (6) conjugated polyenes of varying electronegativity and having film-forming capability. These semiconducting polymer films were to be deposited on a lock-and-key type of electrode sensor and checked for their gas response behavior. In addition, the polymers prepared were to be evaluated by thermogravimetric analysis (TGA) and isothermal (35°C) gravimetric analysis in order to establish their long term stability and feasibility for use as fire detectors.

Essentially, the synthesis of a poly(imidazole) from thiophene-2,5-dialdehyde (I), a poly(Schiff's base) from the same dialdehyde (II), a poly(imidazole) from ferrocene - 1, 1'-dialdehyde (III), a poly(phthalocyanine) polyester (metal-free)(IV), a poly(phthalocyanine) polyester with an Fe++ atom (V), and poly(p-dimethylaminophenylacetylene) (VI) was attempted. Films were prepared and they were evaluated for their response to water vapor, carbon monoxide, ammonia, sulfur dioxide, HCN, nitrogen oxides, acetylene, crotonaldehyde, cigarette smoke and the gases from a smoldering cotton fire.

4

## 2.0 THEORETICAL BACKGROUND

## 2.1 TYPES OF POLYMERS CONSIDERED FOR DETECTOR

The concept behind the development of an early warning fire detector is basically to use organic semiconductors of varying electronegativity so that gases generated by an incipient or smoldering fire, e.g., carbon monoxide, hydrocarbons and water vapor, among others, would be detectable by at least three of these semiconductors in order to have a fire detector. There are many organic polymers that have been shown to possess a semiconducting capability, but they are, generally, intractable substances having no capability for being fabricated other than in the form of pressed discs. However, during the course of this, and other programs (References 1 and 2), intrinsic polymeric semiconductors having film-forming capability and varying electronegativity have been developed.

The primary requirement of any of the polymers chosen was that they be electrically conducting, and that the conductivity be low. [If the conductivity is high, the charge-transfer complex between gas and polymer is not as readily detectable due to the relatively small changes in conductance with small concentrations of gas (Reference 2).] With these criteria in mind, it was possible to consider many substances that are electrically conducting, but are not truly totally conjugated polymers. Thus, the following were considered:

1.  Poly(imidazole) from thiophene-2, 5-dialdehyde and 1,4-bis(phenylglyoxyloyl)-benzene (I) (See Figure 1).

2.  Poly(Schiff's base) from thiophene-2,5-dialdehyde and p-phenylenediamine (II) (See Figure 2).

3.  Poly(imidazole) from ferrocene-1,1'-dialdehyde and 1,4-bis(phenylglyoxyloyl) benzene (III) (See Figure 3).

4.  A poly(phthalocyanine) polyester metal-free (IV) (See Figure 4).

5.  A poly(phthalocyanine) polyester with an $Fe^{++}$ atom (V) (See Figure 5).

6.  Poly(p-dimethylaminophenylacetylene) (VI) (See Figure 6).

## 2.2 RATIONALE FOR CHOICE

### 2.2.1 Characteristics of Organic Semiconductors and their Complexing Behavior

It is possible to affix to polymeric chains certain groups giving them ionic conductivity, or to introduce long sequences of conjugated double bonds to produce electronic conduction. Therefore, organic semiconductors are capable of supporting electronic conduction by nature of the presence of conjugated carbon-carbon double bonds. In addition to having alternating double and single bonds, these semiconducting materials also obey the relationship

$$\sigma = \sigma_0 e^{-\Delta E/2kT} \tag{1}$$

where k = Boltzmann's constant, $\sigma$ = conductivity and $\sigma_0$ and E are constants for the particular material, their values being obtained from a plot of log versus $1/T$, with $\sigma_0$ being the intercept and E being the slope.

Intrinsically, most organic semiconductors have comparatively low conductivity. To increase it, either the temperature is raised or a complex is formed. In complex formation, one component is an electron-donating substance and another is an electron-attracting material; chloranil-p-phenylenediamine or anthracene-iodine complexes being representative examples. Although the exact mechanism of conduction in the charge-transfer complex is not explicit, it is presumed to be the sharing of electrons, which, in effect, removes the electrons somewhat from the sphere of the electron-donor. This delocalization of electrons subsequently results in a smearing out of the electron cloud throughout the complex which, in turn, can more readily result in a p- or n-type semiconductor. In other words, once the complex is formed, the electrons are more easily excited to an activated singlet or triplet state with consequent availability for electronic conduction.

In order to elucidate the concept of electron delocalization in a conjugated system, let us examine the structure of butadiene. The double bonds involve pi-bond orbitals which consist of an unpaired electron in a p-orbital perpendicular to the molecular axis. It is the interaction of these perpendicular p-orbitals that forms the pi orbital, or what the chemist calls, "a double bond."

Figure 7 depicts the bonds in the butadiene molecule showing the sigma and pi bonds, and the resultant "streaming" effect due to the pi bonds. This electron delocalization (uniform distribution of the electron cloud over the entire molecule) occurs in all organic semiconductors, whether simple charge-transfer or polymeric. If one now considers the streamer electrons of a polyacetylene as represented in Figure 8, it can be seen that there is no localization of electrons, and that they are theoretically capable of being readily displaced in an electric field.

One of the important criteria upon which our conduction-detection method is based is the presence of a conjugated unsaturated system either alone or in conjunction with non-bonding p-electrons as found on nitrogen, sulfur, etc. Proof of this structure was obtained by color, infrared and ultraviolet spectroscopy and the presence of unpaired electrons. In an isolated double bond, there is little opportunity for resonance stabilization of any radical (or diradical); a large amount of energy being required to unpair the pi electrons. Increasing the length of the conjugation path lowers the energy for excitation to a triplet state. From Figures 9 and 10 there is strong evidence for the presence of free radicals in the polymers poly(phenylacetylene) and poly(p-nitrophenylacetylene), respectively. This, in conjunction with the deep brown color of the solution, is very indicative of conjugation. In other words, once the conjugated path is long enough, the electrons can readily become delocalized, and unpairing can occur at room temperature. This, for example, is the reason for the stability of diphenylpicrylhydrazyl - a free radical stable in powder or solution.

Before we consider the chemical aspects of the polymers prepared in this program, let us first examine the general effects of impurities on semiconducting organics and see how this relates to our concept of fire detection, viz., charge-transfer complexes between compounds of different electronegativities. One of the sources of uncertainty regarding the mechanism of conduction in organics is that little is known about the effect of "impurities" on the conducting species. For example, Labes, et al, found that the bulk dark conductivity of anthracene was increased when exposed to iodine vapor and was dependent upon the pressure of iodine (a change in pressure of 30 mm caused an increase by one order of magnitude) (Reference 4), and the p-chloranil, in the presence of amine vapors, showed an increase in its bulk dark conductivity (Reference 5).

Heilmeir (Reference 6) and Schneider (Reference 7) both indicated that oxygen played an important role in the conductivity of the phthalocyanines and anthracene,

respectively, and Aftergut (Reference 8) found that trace impurities affected the conductivity of phenothiazine. Terenin (Reference 9) has also discussed the effect of the ambient gas atmosphere on the photoconduction of organic dyes. Thus, the sign of the majority carrier is equivocal in organics until one removes the last trace of "impurity" from the system. However, it is the very nature of this problem which allows considering the use of organic semiconductors as probes for the detection of these contaminants.

The theoretical aspects of signal generation involve either formation of a charge-carrier at the polymer-electrode interface in the space - charge region with a subsequent migration through the bulk of the polymer to the opposite electrode interface or formation of a charge-transfer complex throughout the bulk of the polymer with a consequent change in the bulk resistivity. The literature is not clear on this point, and it still has to be resolved. However, it is agreed that either mechanism will have a similar effect, i.e., generation of a signal.

By itself, the change in resistance of a polymer subjected to "impurities" is of little consequence, for this is what has been observed by others with the simple organics (References 4 and 5). What is important is to be able to relate this to the complexing behavior of gases with the semiconducting polymers and to correlate this with "impurity" detection.

Organic chemistry is replete with examples describing electrophilic and nucleophilic reactions. It is from this wealth of information that the analogies to the electronegativity effects of these semiconducting polymers are drawn. An example of an electrophilic group is the carbonyl moiety. This group is best represented by the resonance hybrid forms a and b:

$$-C \overset{\frown}{=} \overset{..}{O}: \longleftrightarrow -\overset{\oplus}{C} - \overset{\ominus}{\underset{..}{O}}:$$
$$\text{a} \qquad\qquad \text{b}$$
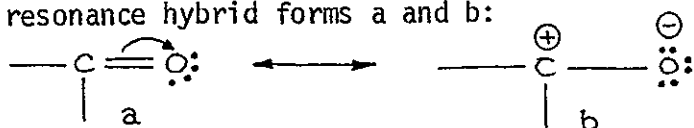
and under the influence of some reagents, an electromeric shift may occur in the direction of b so as to further enhance the electron-attracting (electronegativity) nature of the carbon atom. An order of reactivity for the carbonyl group has been established, and it has been found that the reactivity of a carbonyl group with a compound having a high-electron density decreases in the order (Reference 10)

$$R-\overset{O}{\overset{||}{C}}-H > R-\overset{O}{\overset{||}{C}}-R' > R-\overset{O}{\overset{||}{C}}-OR' > R-\overset{O}{\overset{||}{C}}-NH-R' > R-\overset{O}{\overset{||}{C}}-O^-$$
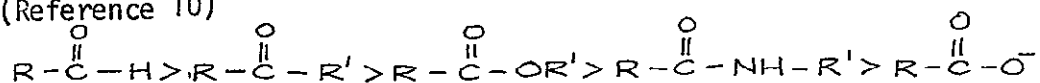
In other words, the decreasing positive character of the carbonyl carbon is

responsible for the decreasing order of reactivity. An analogous picture may be developed for electropositive compounds, such as amines, ethers, etc.

This may now be related to the electronegativity effects in organic semiconductors and the differences in their conductivities. Thus, the more electron-donating one substance is, and the more electron-withdrawing its complexing partner is, the greater should be the difference in conductivities between the base substance and its complex. Conversely, a strong electron-donating material and a weak electron-attracting partner should result in a lower spread in the conductivity between the base substance and its complex. This is amply borne out by the values obtained in parent polyacenes versus their complexes (Reference 11). Thus, perylene had a $\sigma_0$ of $10^{-1}$ ohm$^{-1}$ cm$^{-1}$; perylene-bromine complex had a $\sigma_0$ of 1 ohm$^{-1}$ cm$^{-1}$; violanthrene was $10^{-7}$ ohm$^{-1}$cm$^{-1}$; violanthrene-iodine complex was $10^{-1}$ ohm$^{-1}$cm$^{-1}$; pyranthrene was $10^{-7}$ ohm$^{-1}$cm$^{-1}$; pyranthrene-bromine complex was $3 \times 10^{-2}$ ohm$^{-1}$cm$^{-1}$. Thus, the $\Delta c$(change in conductivity between base substance and complex) is 10 for perylene-bromine complex, $10^6$ for the violanthrene-iodine complex, $10^5$ for the pyranthrene-bromine complex, and $10^9$ for a chloranil-p-phenylenediamine complex. In this latter case, chloranil is strongly electron-withdrawing and p-phenylenediamine is strongly electron-donating. It is very likely that with these complexes, as has been reported with others (References 12-14), there are unpaired electrons that may be the contributing factor to their electrical conduction. For a detailed theoretical discussion of charge-transfer complex formation, see Appendix A.

## 2.2.2 Theoretical Relationship of Polymer Structure to Electrical or Gas Response Behavior

In previous programs (Reference 1 and 2), the polymers studied were predominantly of the poly(acetylene) addition-type of polymer with the conjugation in the backbone and a functional moiety in the appendage. In the present program, the conjugated polyene was predominantly a condensation polymer with the conjugation and functional moiety both as part of the conducting electron (or hole) backbone. In almost all cases their syntheses were well established and little difficulty was anticipated in their preparation.

The preparation of a poly(imidazole) from thiophene-2,5-dialdehyde has been detailed by Krieg and Manecke (Reference 15). They report the reaction of thiophene-2,5-dialdehyde with the 1,4-bis(phenylglyoxyloyl) benzene and ammonia to yield a poly(imidazole), shown in Figure 1, with an electrical resistivity of $10^{12}$ ohm-cm. The synthetic approach is shown in Figure 11. The unique-

9

ness of this structure is the high electron density from the nitrogen and the sulfur and the relative ease for the sulfur to donate its electrons. This is evidenced by the fact that the thiophene sulfur can readily undergo oxidation-reduction reactions. Thus, a priori, it was presumed this would have excellent capability of detecting nitrogen oxides, aldehydes or hydrocarbons.

Another sulfur/nitrogen polymer prepared was the poly(Schiff's base) from thiophene-2, 5-dialdehyde and p-phenylenediamine, shown in Figure 2. Its reaction sequence is given in Figure 12. The anil structure of this compound was exo to the rings and not part of a ring system, as for I. Thus, it was presumed it would be more capable of donating its electrons more readily for complexing with such oxidizable substances as carbon monoxide.

It had been shown previously (References 1 and 2) that conjugated polymers that contain aromatic appendages lose some of their interactive capability between the appendage and the backbone due to non-coplanarity between the ring and the backbone. It was also observed that ferrocenylacetylenes gave very good responses in a smoldering cotton fire (Reference 2). Thus, to get around the problem of poor interactive ability between the appendage and the backbone, and to further enhance the gas response capability of the ferrocene moiety, it was proposed that the ferrocenyl moiety be made a part of the backbone. Since ferrocene dialdehyde had been prepared by Osgerby and Pauson (Reference 16), it was decided to prepare the poly(imidazole), shown in Figure 3, comparable to that of the thiophene-2,5-dialdehyde compound. The synthesis is depicted in Figure 13. This polymer should be more electropositive than for the case where the ferrocenyl moiety is an appendage, and it could be used for detecting carbon monoxide, aldehydes and unsaturated hydrocarbons.

There are numerous reports in the literature on the electrical conductivity of phthalocyanine and some of its derivatives including both the non-metal complexed and the metal complexed. Recently, there has been a considerable effort put forward towards making polymers with phthalocyanine as part of the polymer backbone. One such reference is that given by Zeschmar (Reference 17) where he uses phthalocyanine dicarboxylic acid with a glycol to get a polyester and the resultant polymer is photoconductive. It is quite likely this class of polymers can show conductivity from phthalocyanine moiety to phthalocyanine moiety through interchain interaction. Thus, preparing two polymers of this type, one with a metal atom, e.g., iron (See Figure 5), and one without (See Figure 4) would

10

give polymers capable of detecting HCN, $CO_2$, $NH_3$ or $SO_2$, depending upon whether the metal-chelated or non-metal chelated polymers are used. Figures 14 and 15 describe the method used for preparing the metal-free and the metallated polymers, respectively.

Finally, in view of the fact that it had been reported by Senturia (Reference 3) that poly(p-aminophenylacetylene) was quite responsive to fire conditions, it was decided to enhance its responsiveness by attempting to increase its electropositive character by preparing the dimethylamine derivative. Preparation of poly(p-dimethylaminophenylacetylene) should be possible by methylating the poly(p-aminophenylacetylene) with dimethylsulfate. Figure 16 depicts its preparation. This dimethyl amino polymer should be a much stronger base than the parent compound and very capable of detecting nitrogen oxides, sulfur dioxide, and aldehydes, among others.

Thus, to sum up the use of these electrically conducting organics as part of an early warning fire detecting system, it is interesting to quote Garrett (Reference 18), "Here we have an electrical component (organic semi-conductors) which can perform any of the basic logic functions, and perform them at a voltage level of kT/e (25 mv at room temperature) - a voltage level that is very much of the order of the membrane potentials found in living organisms."

## 2.3 EVALUATION OF POLYMERS FOR USE IN EARLY WARNING FIRE DETECTOR

Once the various polymers were prepared, they were subjected to different tests to determine their feasibility for use in a fire detection system. Subsequent to their synthesis, the polymers were characterized by means of elemental composition, infrared and ultraviolet spectroscopy, inherent viscosity, thermogravimetric analysis (TGA) and isothermal gravimetric analysis.

The elemental composition and spectroscopic data would help identify the polymers unequivocally. The TGA and isothermal data would establish the long term stability feature of these polymers for extended use in an ambiance.

Next to be studied were the film properties and their responsiveness to gases. For this purpose, films were prepared by the best method possible, e.g., dipping or spinning, depending upon solubility characteristics. Since it had been adequately demonstrated that gas/polymer interactions were maximized in the bulk of the polymer, as opposed to the surface (Reference 1), thick films were given more serious consideration. Furthermore, polymer crystallinity was also given consideration. It is well established that physical properties of

11

bulk polymers depend to a considerable extent on their ability to orient at the molecular level. Thus, it is anticipated that crystallinity effects, whether in the molecular domain, or higher levels, will also enhance the electrical conduction effects.

Finally, in order to know the capability of each polymer with regard to its ability to be used as part of a fire detection system, it is necessary to know its responsiveness to each of the following gases:

1. Dry air
2. Gas from incipient combustion of cellulosic material, e.g., cotton
3. Water vapor
4. Carbon monoxide
5. Hydrocarbons, e.g., acetylene
6. Aldehydes, e.g., acrolein or crotonaldehyde
7. Ammonia
8. Sulfur dioxide
9. HCN
10. Nitrogen oxides

It should be borne in mind that any fire detector built will be not a single sensor (polymer) device, but rather a multiple sensor (polymer) system wherein each sensor will be relatively more specific to a particular contaminant (gas) than any of the others, but the combination of sensors will represent the fire detector. Thus, the question of the probability of any one sensor responding

preferentially to a gas must be given serious consideration. It had been established previously (Reference 1) that in a two-sensor system where one was coated with poly(p-aminophenylacetylene) and the other coated with poly(p-nitrophenylacetylene), when upon exposure to either $SO_2$ or $NH_3$ in an open circuit, balanced network, the amino polymer responded preferentially to the $SO_2$ and the nitropolymer to the $NH_3$. For a more detailed analysis regarding decision mechanisms for contaminant recognition, see Appendix

## 3.0 EXPERIMENTAL

It had been demonstrated, previously, that conjugated polyenes of the poly-(acetylene) (addition type) could be made to respond differently to various gases (References 1 and 2), but it was believed there existed a minimalization of interaction between the electronegative group on the appendage and the conducting electrons (or holes) of the backbone due to a lack of coplanarity. Therefore, it was decided to prepare condensation type polyenes where the functional moiety, e.g., a nitrogen, oxygen, sulfur atom, etc., could be in resonance interaction with the conjugated polyene. Once prepared, they were all subjected to characterization studies consisting of viscosity measurements, spectroscopic analyses, thermogravimetric analyses, and gas/polymer interaction effects, as determined by changes in electrical conductance. This section, will, therefore, contain only experimental methods, while Section 4 will consist of a detailed discussion of the results.

### 3.1  Synthesis of Polymers

In choosing the polymers for this program, consideration was given to their ease of synthesis, any reported electrical conduction, functional moiety, e.g., N, O, S, Fe, etc., for possible interaction with a reactive gas, and possibility of being a film former. To this end, a poly(imidazole) based upon thiophene aldehyde (I), a poly(Schiff's base) based upon the same aldehyde (II), a poly(imidazole) based upon ferrocene aldehyde (III) two phthalocyanine polymers (one without, and with a metal atom) (IV and V, respectively), and poly(p-dimethylaminophenylacetylene) (VI) were considered.

### 3.1.1  Poly(imidazole) from Thiophene Aldehyde (I)

To prepare this polymer, whose synthesis has been described elsehwere (Reference 19), two starting materials first had to be prepared, viz., thiophene-2, 5-dialdehyde (IA) and 1,4-bis(phenylgloxylolyl) benzene (IB).

### IA

The preparatation of thiophene-2, 5-dialdehyde derived from the commercially available thiophene-2-aldehyde by first preparing the diethyl acetal of this aldehyde via its reaction with ethyl orthosilicate (Reference 20).

Thiophene-2-carboxaldehyde (180 g) and 340 g of ethyl orthosilicate were dissolved in 120 cc of ethanol plus 400 cc benzene in a 2 liter flask. To this mixture was added 3 cc of 85% $H_3PO_4$ and the mixture heated at reflux for 16 hours. It

13

was then allowed to cool and left standing about two weeks.

The solution was then treated with 60 g NaOH dissolved in 250 cc of water and refluxed for two hours. It was decanted from the gel [it never dissolved, although literature (Reference 20) claims it does dissolve] and the solvent removed under vacuum to yield a dark liquid. The first rough distillation gave a pale straw liquid and then distillation at 105°C/20mm [literature claims 116°C/35mm (Reference 20)] gave a 90% yield of a liquid with a refractive index, $n_D^{20}$ 1.4868 [literature $n_D^{20}$ 1.4876 (Reference 20)]. The material is not stable at room temperature, but goes yellow overnight and dark brown within three days.

The thiophene-2-carboxaldehyde diethyl acetal, prepared above, was converted to thiophene-2,5-dialdehyde (IA) via the following procedure:

Butyl lithium was prepared in ether solution from 8.6 g lithium and 68.5 g (0.5 mole) n-butyl bromide (Reference 21). The butyl lithium was treated with 51.0 g (0.3 mole) thiophene-2-carboxaldehyde diethyl acetal at -20°C for one hour. The mixture was then allowed to stand at room temperature for three hours. The resultant solution was cooled to -30°C and 60 g (1.0 mole) of dimethylformamide (DMF) added. The resulting exotherm was controlled with a dry ice/acetone bath. The brown suspension that formed was allowed to come to room temperature gradually by stirring overnight. The entire mixture was then poured over a large amount of ice to hydrolyze the excess lithium alkyl.

The product was extracted into ether, dried over sodium sulfate and the solvents removed under vacuum. The brown oily residue, presumed to be crude thiophene-2, 5-dialdehyde diethyl acetal was suspended in 500 ml of 50% acetone/dilute hydrochloric acid and stirred overnight at room temperature. A pale yellow solid suspension resulted. After recrystallizing from aqueous ethanol, the product [thiophene-2,5-dialdehyde (IA)] had a mp 114-116°C [Goldfarb (Reference 22) reported 114°C].

Analysis:  Calc. for $C_6H_4O_2S$:     C = 51.43; H = 2.86; S = 22.86%
           Found:                    C = 51.22; H = 2.95; S = 22, 48%

To 400 cc tetrahydrofuran (THF) was added 50g benzyl chloride and 10g magnesium to prepare benzylmagnesium chloride. To this solution (at 0°C) was added slowly, with stirring, a solution of 27g terephthaldehyde in 250 cc THF. The exothermic reaction was complete in about 1/2 hour. The suspension of complex product was heated under reflux for 1/2 hour, cooled to 0°C and hydrolyzed with 15g ammonium chloride dissolved in 100 cc water. Precipitated magnesium salts were dissolved by addition of a small quantity of HCl and the solution extracted with 3 x 100 cc ether. The organic layer was separated and dried over potassium carbonate. Removal of the ether left 60g (84% yield) of a pale yellow paste, which, when recrystallized from methanol, yielded white crystals; mp. 173-5°C. This product, $\alpha$, $\alpha'$ (para-phenylene)bis($\beta$-phenylethanol), shown in Figure 17, is the precursor to 1,4-bis(phenylglyoxyloyl) benzene (IB).

To 32g (0.1 mole) of $\alpha$, $\alpha'$ (para-phenylene)bis($\beta$-phenylethanol) dissolved in 300 cc acetic acid and 100 cc acetic anhydride at 10°C was added a solution of 20g chromic acid in 150 cc acetic acid and 20 cc water. The addition took about one hour and the temperature was kept below 15°C. When the addition was complete, the solution was stirred overnight at room temperature and then poured into a large excess of water. The resultant white precipitate was washed extensively with water to remove chromium salts and recrystallized from ethyl acetate. The melting point of this diketone was 170-172°C. [Literature (Reference 23) gives mp 172-174°C.]

To 4.8g of the above diketone, dissolved in 30 cc acetic acid, was added a solution of 3.5g selenium dioxide in 30 cc water. The mixture was stirred, under reflux, for two hours and then filtered hot from the precipitated selenium. Addition of water to the acetic acid solution gave a yellow precipitate which was recrystallized from ethyl acetate to yield 3.1g of buff crystals, mp 124-126°C [literature value (Reference 23) 125-126°C].

Analysis: Calc. for $C_{22}H_{14}O_4$:  C=77.19; H = 4.09%
Found:  C=77.30; H = 4.18%

The poly(imidazole) (I) was prepared by dissolving 2.1g of IB, 0.86g of IA and 3g of ammonium acetate in 100 cc acetic acid and stirring under reflux in a

nitrogen atmosphere for 24 hours. The mixture was then poured into a large volume of water to yield a bright yellow precipitate of I. The complete reaction sequence from thiophene aldehyde to I is depicted in Figure 11.

Analysis: Calc. for $C_{28}H_{18}N_4S$: C=76.02; H=4.07; N=12.67; S=7.24%

Found: C=76.48; H=4.41; N=12.08; S=6.93%

### 3.1.2 Poly(Schiff's base) from Thiophene Aldehyde (II)

Thiophene-2,5-dialdehyde (IA) [1.40g (0.01 mole)] and 1.08g (0.01 mole) of p-phenylenediamine were melted together under a nitrogen atmosphere at 120°C. The temperature was slowly raised to 150°C over a period of six hours and held at that point overnight. Finally, the temperature was raised to 200°C and the mixture evacuated for six hours. The resulting polymeric mass was a hard orange solid. Its preparative sequence is shown by Figure 12.

Analysis: Calc. for $C_{12}H_8N_2S$: C=67.92; H=3.77; N=13.21; S=15.09%

Found: C=68.24; H=3.81; N=12.95; S=14.97%

### 3.1.3 Poly(imidazole) from Ferrocene Dialdehyde (III)

The preparation of the ferrocene/imidazole polymer (III) first required the preparation of ferrocene -1,1' -dicarboxaldehyde followed by its reaction with 1,4-bis(phenylglyoxyloyl) benzene.

1,1' -Dihyroxymethyl ferrocene (49g, 0.2 mole) was dissolved in 2000 cc dry chloroform, and 1000g of freshly precipitated, and dried, manganese dioxide were added. The mixture was stirred under nitrogen for five days at room temperature and then filtered. The filtrate was evaporated to dryness and divided into ten portions of 5g each. Each portion was chromatographed on an alumina column that was approximately 1 1/2" x 40" using benzene as the eluent. From each fraction, the leading band on the column yielded about 3g of ferrocene-1, 1'-dicarboxaldehyde, while the second band consisted mainly of unchanged dihydroxymethyl ferrocene, which was eluted with ether. Total yield of ferrocene-1, 1'dicarboxaldehyde was 28.5g, mp 181-83° ([Osgerby and Pauson (Reference 16) gave a mp 183-84°C]. Its analysis is as follows:

Calc for $C_{12}H_{10}O_2Fe$: C=59.54, H=4.13, Fe=23.09%

Found: C=59.38, H=4.18, Fe=22.79%

Ferrocene dicarboxaldehyde (6.05g, 0.025 mole), 1,4-bis (phenylglyoxyloyl benzene (8.55g, 0.025 mole) and excess ammonium acetate (10g) were dissolved in 300 ml acetic acid, and stirred under reflux under a nitrogen atmosphere for 48 hours. The mixture was poured into a large volume of water to yield a brown precipitate. Yield was 10.5g of the ferrocene/imidazole polymer (III). Figure 13 depicts the preparation sequence.

Analysis: Calc. for $C_{34}H_{24}N_4Fe$: C=75.00; H=4.41; N=10.29; Fe=10.29%
Found: C=74.38; H=4.10; N=9.85; Fe=10.61%

### 3.1.4 Polyester/phthalocyanine Copolymer (Metal-Free) (IV)

In order to prepare the polyester/phthalocyanine copolymer, it was first necessary to synthesize phthalocyanine dicarboxylic acid. To do so, aminoisoindolenine, and trichloroisoindolienine carbonylchloride, shown as part of the preparative sequence in Figure 14, were first prepared. Subsequently, they were reacted together to get the phthalocyanine dicarboxylic acid which was then copolymerized to the polyester, as given in Figure 14.

Phthalonitrile (100g, 0.78 mole) was suspended in 600 cc methanol and cooled to -20°C. To this suspension, 200 cc of liquid ammonia, cooled to -50°C, were slowly added. The mixture was rapidly divided into six portions and poured into six stainless steel pressure reaction vessels which were immediately sealed. (Note: It is advantageous to precool the vessels to prevent rapid boiling of the ammonia when the solution first enters the vessel. Otherwise, considerable care must be exercised to prevent frothing up and overflow during the filling.)

The sealed vessels were heated at 100°C for six hours and then allowed to cool overnight. The pale blue solution that was obtained was filtered through charcoal, and the almost colorless filtrate was evaporated to dryness, yielding 110g of pale tan powder, mp 195-6°C, turning green upon melting. [Linstead, et al, gave a mp of 193°C (Reference 24).]

Phthalimide-5-carboxylic acid (70g, 0.33 mole) and 220g (1.05 mole) of $PCl_5$ were heated in 300g of o-dichlorobenzene for 16 hours at 100°C, under nitrogen. The resultant $POCl_3$, excess $PCl_5$ and o-dichlorobenzene were distilled out to yield trichloroisoindolenine carbonylchloride as a pale green oily product that was stored under dry nitrogen. After about one week, it solidified to a white solid that fumed strongly in air.

Using the method of Zeschmar (Reference 25), the phthalocyanine dicarboxylic acid was synthesized from the aminoiminoisoindolenine and 1,1,3-trichloroiso-indolenine -6-carboxylic acid chloride, prepared above.

To 28.3g of 1,1,3-trichloroisoindolenine-6-carboxylic acid chloride dissolved in 200 cc benzene were added, dropwise, a solution of 14.5g of 1,3-diminoiso-indolenine and 60g triethylamine dissolved in 200 cc dimethylformamide (DMF). An ice/salt bath was used to maintain the temperature below 50°C.

After the addition was complete, the cooling bath was removed and the temperature was allowed to rise slowly to 90°C. After about 15 minutes, the temperature began to fall and the solution was heated for 24 hours at 90-110°C. The benzene was removed under vacuum, and the brown suspension that resulted was poured into an excess of water. The deep purple product was purified by repre-cipitation from concentrated sulfuric acid.

The phthalocyanine diacid, prepared above, was incorporated into a copolymer comprising 10% of phthalocyanine dicarboxylic acid and 90% terephthalic acid with ethylene glycol. The two acids were dissolved, under nitrogen, in a 10 molar excess of ethylene glycol, together with 0.1% zinc oxide to act as a transesterification catalyst. The temperature was slowly raised to 270°C over a 5-hour period, and held at 270°C for 2 hours. During this time water and excess ethylene glycol distilled out. While still hot, the polymer was poured onto a teflon sheet, and on cooling, the polymer solidified to a dark glass. The presence of 2.01 percent nitrogen in the non-metalated polymer confirms the incorporation of the phthalocyanine moiety into the polyester polymer.

18

Analysis: Non-metalated polymer;*  C≈66: H≈4.2: N=2.38%

Found:                                  C = 63.12; H = 4.58; N=2.01%

*Note: See Section 4.1.1 for discussion of analysis and possible molecular weight.

## 3.1.5  Polyester/phthalocyanine Copolymer (Metalated with Iron) (V)

A portion of the above polymer was dissolved in DMF and stirred overnight with excess ferrous citrate. The supposedly metalated polymer was precipitated by pouring the solution into excess water to obtain a pale tan powder.  The 1.98 percent nitrogen in the metalated polymer confirms the incorporation of the phthalocyanine moiety into the polyester polymer.  Furthermore, the metalated polymer was found to contain 1.86 percent iron, which corresponds to about 80 percent of the phthalocyanine molecules being metalated.

Analysis:  Metalated polymer:*  C≈64; H≈4.1; N = 2.32; Fe = 2.32%

Found:                            C = 66.43; H = 4.31; N = 1.98; Fe = 1.86%

*Note: See Section 4.1.1 for discussion of analysis.

## 3.1.6  Poly(p-dimethylaminophenylacetylene) (VI)

To prepare VI, the scheme shown in Figure 16 is followed.  In sequence, poly(phenylacetylene) is prepared first followed by poly(p-nitrophenylacetylene), poly(p-formamidophenylacetylene), and then poly(p-aminophenylacetylene) all prepared by the methods discussed elsewhere (References 1 and 2).  Subsequently poly(p-dimethylaminophenylacetylene) (VI) is prepared, as shown in Figure 16.

The poly(p-aminophenylacetylene) (5g), prepared from poly(phenylacetylene) (References 1 and 2), was dissolved in 100 cc DMF and 50 cc dimethylsulfate (about a 10 molar excess) were added, together with about 2g of sodium hydroxide. The mixture was heated at 100-120°C, with stirring, under nitrogen, for 24 hours.  About 30 cc of the DMS were distilled off under vacuum, and the remaining dark brown solution was poured into an excess of water. The glutinous precipitate was coagulated by adding sodium chloride and then filtered.  After extensive washing to remove  adsorbed salts, 2.7g of brown powder were isolated. In order to determine whether a monomethyl or dimethyl derivative had been

obtained, a comparison was made between the calculated values for the mono-methyl and dimethyl derivatives, and the experimentally found values. The found values and the infrared spectra seemed to indicate that the product was the dimethyl derivative.

Analysis: Calc. for monomethyl derivative: $C_9H_9N$: C=82.44; H=6.87; N=10.69%

Calc. for dimethyl derivative: $C_{10}H_{11}N$: C=82,76; H=7.59; N=9.66%

Found: C=82.10; H=7.82; N=9.49%

## 3.2  CHARACTERIZATION STUDIES

Subsequent to the preparation of the polymers, various physical and chemical properties were evaluated. Their structures were determined by infrared and ultraviolet absorption spectra. Relative viscosities were obtained as a rough determination of molecular weight, and molecular weight distributions were also determined. Film properties were studied, and thermal analytical data, e.g., thermogravimetric analyses and isothermal stabilities were also obtained. Finally, gas/polymer interactions were determined for pure gases under different relative humidities, as well as gases generated by a burning cigarette and from smoldering cotton.

### 3.2.1  Physical Data

### 3.2.1.1  Film Properties:  Preparation and Thickness Determination.

In order for the polymers prepared in this program to be capable of being incor-porated into a useful device, they had to be able to be put down as a film on the electrode substrate. The method that consistently gave good films for most of the polymers was via the technique described elsewhere (References 1 and 2). The sensor was kept in a vertical position and then dipped into a one percent solu of the polymer in dimethylformamide. By withdrawing the sensor from this slowly, and as gradually as possible, the surface tension of the solution pulled the excess liquid off the surface. The sensor was then stood on edge on a piece of absorbent paper and allowed to dry. While in this position, the paper pulled off any bead which might form at the bottom edge of the sensor. In view of the fact that dimethylformamide (DMF) was about the best solvent for the polymers prepared in this program, the DMF could only be removed by vacuum in order to get films. An alternative method for obtaining films on the electrode substrate was to place a drop of the DMF solution on a horizontally placed sensor, evenly distributing it over the surface and then pumping it dry.

The film thicknesses were measured with an Etec "Autoscan" Scanning Electron

20

Microscope (SEM) of all the polymers prepared. Since the polymer is non-conducting, it will give a "charging" effect, even at very low voltages when examined in the SEM. Therefore, a thin layer of carbon, followed by a thin layer of gold-palladium, was used as a shadowing material.

After selecting an area on the microscope slide where the film thickness was relatively flat, continuous and non-fragmented, the specimen was rotated and tilted so that the polymer film and glass slide coincided exactly 90 degrees with the electron beam. The optical axis, tilt axis and the surface of the specimen were adjusted to coincide with one intersection. After making these final adjustments of the specimen and stage, a series of photographs were made at different magnifications. The thickness of the polymer film and glass slide were then measured from the resultant photograph. For comparison, the measurements were made with a caliper rule utilizing a 20X binocular microscope, and related to the SEM measurement of the slide to assure maximum accuracy. At the same time the film thickness determinations were being made, it was decided to examine the edge of the polymer with relation to its surface. This was done by tilting the glass slide 45 degrees and examining the edge-surface structure at 400X and 4000X. In addition to the 45 degree tilt, the 90 degree tilt was also done at 4000X. Figure 18 shows the 90 degree edge view of polymer I, and from this view, the thickness measurement was made. It measures 13.64 microns. Figures 19 and 20 are the 400X and 4000X, respectively, of the 45 degree view of the edge and surface of this polymer. Figure 21 is the 90 degree view of polymer II, and its thickness measures 0.572 microns. Figures 22 and 23 are the 400X and 4000X 45 degree view of polymer II. Figure 24 depicts the edge of polymer III from which its thickness measures 2.67 microns. The 400X and 4000X 45 degree pictures are given by Figures 25 and 26. Figure 27 gives the 90 degree picture for polymer IV, and its thickness calculates to be 11.18 microns. The 45 degree tilt view at 400X and 4000X of polymer IV are shown in Figures 28 and 29. For polymer V, the thickness was calculated from Figure 30 to be 6.99 microns, while the 45 degree 400X and 4000X pictures are shown in Figures 31 and 32. Finally, the 90 degree view of polymer VI is depicted in Figure 33, and its thickness is 1.9 microns. Figures 34 and 35 are the 400X and 4000X pictures of the 45 degree edge surface view.

## 3.2.1.2 Crystallinity Studies

An attempt was made at crystallizing the polymers by either annealing the films from a temperature slightly below the melting point and/or in the presence of a field. In most instances were was no evidence for any crystallinity developing as determined via a polarizing microscope. Thus, it was decided to look at the degree of crystallinity the polymers might intrinsically have; and to do this, X-ray diffraction studies were run. Using a powder method, in which the sample to be studied was reduced to a fine powder, and placing the sample in a beam of monochromatic X-rays from an XRD-6 General Electric diffractometer employing a nickel filter, with the target tube of Cu $K_\alpha$ at 45 kva at 20 milliamps, and with Cu $K_\alpha$=1.54050A, the Bragg equation (2) was used to determine the extent of crystallinity.

$$\lambda = 2 d \sin \theta \qquad (2)$$

Here, $\lambda$=wavelength, d is the crystal lattice spacing and $\theta$ is the incident angle of the X-rays. Table I lists the polymers tested and the qualitative indication of crystallinity. Table II lists the $2\theta$ and d (Å) values for the only truly crystalline polymer, i.e., poly(Schiff's base) from thiophene-2,5 -dicaboxaldehyde and p-phenylenediamine (polymer II). The polyester/phthalo- cyanine (iron) polymer (V) and poly(p-dimethylaminophenylacetylene) (VI) gave indications of some trace crystallinity, but a spectrographic analysis (Table III) showed this to be due to minor amounts of inorganic ions.

## 3.2.1.3 Viscosities and Molecular Weight Distribution

Table IV gives the values for the relative viscosities for polymers I - VI run in DMF at a 0.05 percent solution concentration. In addition, the molecular size distribution was determined by means of gel permeation chromatography (GPC) with a Waters Associates Ana-Prep Chromatograph. Figures 36 to 38 are the molecular size distribution curves for poly(imidazole)/thiophene (I), polyester/phthalocyanine (IV) and polyester/phthalocyanine plus iron (V), respectively. The other polymers could not be run as they were not soluble in tetrahydrofuran or chloroform. The results show V to have the largest size (160 Å), IV, next (140 Å), and I, least (90 Å).

3.2.1.4  Infrared and Ultraviolet Absorption Spectra

3.2.1.4.1  Infrared Spectra

One way of characterizing the chemical structure of an organic compound and/or polymer is its infrared absorption spectrum. Thus, in following the synthesis of the various polymers, the infrared spectrum of the starting materials and/or intermediates were obtained and the subsequent appearance or disappearance of characteristic absorption peaks followed.

(Note:  All IR spectra were obtained on a Perkin-Elmer Model 521 Infrared Spectrophotometer.)

In the course of preparing the poly(imidazole) from thiophene-2,5-dialdehyde, the first compound prepared was the thiophene-2-aldehyde diethylacetal, which was obtained from thiophene-2-carboxaldehyde whose infrared spectrum is shown in Figure 39.  The diethyl acetal spectrum is Figure 40.  This was converted to the thiophene-2,5-dialdehyde/diethylacetal, shown in Figure 41, and then hydrolyzed to the thiophene-2,5-dialdehyde, whose infrared spectrum is depicted in Figure 42.

To prepare the 1,4-bis (phenylglyoxyloyl) benzene needed in the preparation of the poly(imidazole)/thiophene, the precursor, $\alpha, \alpha'$ (para-phenylene)bis($\beta$-phenyl ethanol), whose infrared spectrum is shown in Figure 43 was oxidized to a diketone, the infrared spectrum being depicted by Figure 44, and finally to the 1, 4-bis (phenylglyoxyloyl) benzene whose infrared spectrum is shown in Figure 45, and which was compared to the infrared spectrum of an independently synthesized compound, shown in Figure 46 (Reference 25).  These compounds led to the preparation of polymer I, whose infrared curve is depicted by Figure 47.

The infrared spectrum of the poly(Schiff's base) (Polymer II) prepared from thiophene-2,5-dialdehyde is shown in Figure 48.

The preparation of the poly(imidazole) from ferrocene-1, 1'-dialdehyde, whose infrared spectrum is shown in Figure 49, resulted in a polymer (polymer III), the infrared spectrum of which is given by Figure 50.

The synthesis of the polyester/phthalocyanine polymer involved the preparation of aminoiminoisoindolenine, trichloroisoindolenine carbonyl chloride and the phthalocyanine dicarboxylic acid as intermediates. Their infrared spectra are shown in Figures 51, 52, and 53, respectively. From the phthalocyanine di-carboxylic acid, the polyester/phthalocyanine (metal-free) polymer (IV)was obtained and this was converted to the metalated (with iron)polymer (V), whose infrared curves are shown in Figures 54 and 55, respectively.

Finally, the infared spectrum for poly(p-dimethylaminophenylacetylene)(VI) is depicted by Figure 56.

### 3.2.1.4.2 Ultraviolet Spectra

Generally, ultraviolet absorption spectra are obtained by dissolving a compound in a solvent that has a low cut-off in the ultraviolet region, such as alcohol. In the case of the polymers prepared in this program, their solubility in alcohol is questionable. However, they were suspended in methanol and allowed to sit until a slight color developed in the methanol. This was presumed to be indicative of some dissolution; and it was this solution that was used for the ultraviolet spectra. (Note: All UV spectra were obtained with a Cary 14 recording spectrophotometer.) Figures 57 to 62 are the ultraviolet absorption spectra for polymers I to VI.

### 3.2.2 Thermal Stability Measurements

Quite germane and critical to the program are thermal stability measurements, i.e., stability to high temperatures and to a particular temperature for an extended period of time. For this purpose, thermogravimetric analysis (TGA) curves were run in air using a duPont 950 Thermogravimetric Analyzer, 990 Thermal Analyzer and a Cahn Time Derivative Computer. In the figures

containing these curves, there are two types of curves shown. The upper
curve represents the rate of weight change with time and temperature while the
lower curve shows the absolute weight loss. Figures 63 to 68 are the TGA
curves for all polymers, and Table V gives the isothermal weight losses.

## 3.3 GAS MEASUREMENTS

Since one of the necessary aspects of this program is to determine gas/polymer
interaction effects for possible use in fire detecting devices, the various
polymers prepared were applied as films onto a lock-and-key electrode
substrate and placed into a 7000 cc stainless steel vacuum chamber which was
connected to a gas input tube.

The lock-and-key (interdigitated) electrodes were prepared on Corning 7059 glass
slides that were 1" x 1" x 0.048". These glass slides were degreased in hot
(60°C) trichloroethylene then acetone at room temperature, followed by hot
(60°C) methyl alcohol, rinsed with deionized (D.I.) water and blown dry with
nitrogen. They were then cleaned in concentrated (48%) hydrofluoric acid
for two seconds and those substrates that remained clear were kept for processing
into the sensor; all others were discarded. The good slides were then given a
deionized water rinse for 30 minutes, blown dry with nitrogen and baked for ten
minutes at 180°C in a vacuum oven prior to metallization.

The slides were placed in a vacuum system and the surfaces were reverse sputtered
for 30 seconds followed by the sputtering of nickel for 1-1/2 minutes (to get a
film 50-100 Å thick) and then gold was sputtered on for eight minutes to a
thickness of 2000 Å. Filtered Hunt photoresist was spun onto the gold surface
at 5000 rpm for 40 seconds and then dried in a dessicator, under nitrogen,
for 30 minutes, followed by a bake in a vacuum oven for 60 minutes at 66°C.
The slides were then masked with the lock-and-key pattern and exposed for eight
seconds, developed and then rinsed in deionized water. This was followed by baking
at 125°C for 30 minutes under infrared lamps.

The next step was to etch the gold pattern on the slide with KI gold etchant

(consisting of four parts of KI, one part of $I_2$ and 14 parts of water) at 60°C and then etching the nickel at room temperature in a mixture of one part nitric acid, one part acetic acid and one part acetone. The photoresist was then removed with Room Temperature Hunt Microstrip.

After completion of the above steps, the sensors were tested for shorts and then 0.002" x 0.010" gold ribbon leads were soft soldered to the electrodes. Frequently, incomplete removal of the nickel subsurface or some other conducting short would result and the surface conduction was too high. However, after overcoming these difficulties in obtaining good lock-and-key electrode sensors, gas measurements were made on all polymers that were prepared and that could be put down as films on the electrodes. In all cases, the applied voltage across the 5 mil spacing between the electrodes was 90 volts, d.c.

Plate I shows the overall system with the chamber, its connection to the vacuum rack, and the electrometer used for electrical measurements. Figure 69 depicts the circuit diagram of this setup. Plate II shows the inside of the chamber with a coated sensor and Plate III shows the lock-and-key electrode sensor without the polymer coating on it.

Initially, the set-up shown schematically in Figure 70 was assembled. The stainless steel lid on top of the 7000 cc chamber (Plate I) was placed on top so that it almost closed the top of the chamber, but still permitted a flow of air through the chamber. The sensor, inside the chamber, rested on a 1/4" teflon sheet that lay on top of an inverted 1000 ml polypropylene beaker. Leads went through the chamber wall to the usual external circuits, and a 90 volt potential drop was applied across the sensor.

A 15mm O.D. glass tube passed through the chamber wall, and the end of the tube was about three inches away from the sensor and about one inch below it. The various test gases were carried into the chamber and to the sensor by blowing them through this tube using a small fan. The gas to be tested was injected into the fan from a hypodermic syringe placed about 1/2" away from the fan. In the case of cigarette smoke, a smoldering cigarette was held about one inch away from the fan. In the case of smoldering or burning cotton, the more elaborate setup shown in Figure 71 was employed. The ignition coil, in this latter setup, was made of nicrhome wire that had been wound on a 3mm glass rod and then slipped off the rod. Cotton was wrapped around the coil and either

26

caused to smolder or burn at the appropriate moment. By using a variac (variable transformer), the voltage was controlled such that 12-15 volts caused smoldering and 15-18 volts caused burning.

Usually, when an "active" gas was injected towards the fan, the sensor was seen to respond within less than one second, and reach a maximum response in less than two seconds. Thereafter, decay back to the original baseline generally took anywere from one to fifteen minutes, depending on the gas and the size of the dose. For the data shown in Tables VI-VIII for polymers I-III respectively, the smoldering cotton exposure is for about 30 seconds, and when the response levels off, the cotton is ignited and the subsequent value given in the Tables is for the burning cotton. When cigarette smoke was held in front of the blower, the response was about five seconds later. It then took about 30 seconds to reach a maximum value. Presumably, the slowness of response could be attributed to adsorption of the vapors on the walls of the tube and chamber and then a gradual desorption.

Initially, the gas responses of polymers I-III were evaluated in this system, and their responses are shown in Tables VI-VIII. By way of explanation of the technique used in putting the gases into the chamber with the sensor, all those substances that are liquids are stored in flasks fitted with serum caps. A hypodermic needle was inserted through the serum caps and the atmosphere above the liquid was withdrawn into the hypodermic. Then, based on the partial pressure of the gas at ambient conditions (50% relative humidity), it was this volume of gas, mixed with air, that was injected into the fan.

Subsequent to the preparation of all six polymers, the technique used to make the necessary gas measurements is that shown in the schematic of Figure 72. In this modification, the flask shown at one end had an air inlet tube and had different concentrations of sulfuric acid in it for the various relative humidities (RH) used. Thus, from Lange's Handbook of Chemistry (1961), p. 1423, at 25°C, a 55 percent sulfuric acid solution gave an atmospheric RH of 25 percent. A 43 percent sulfuric acid solution gave a 50 percent RH, and a 30 percent sulfuric acid solution gave 75 percent RH. For 100 percent RH, water was used. The port marked "to aspirator" was where suction was applied to pull the various vapors through the chamber and on to the sensor. The rubber septum was used as an injection site for introducing all the vapors. At this point, a funnel was also put, to which was attached a hypodermic needle that was inserted

into the rubber septum. The cotton was burned inside this funnel and the gases sucked through the hypodermic needle into the tube that led to the sensor.

All the gas measurements, cigarette smoke and burning cotton data generated with this system are given in Tables IX-XII. Table XIII shows the minimum quantity of gas used in order to obtain a response. In some instances, however, no response was observed even up to 100 cc of gas used.

Experimentally, the procedure was to use a water aspirator to draw air through the sulfuric acid solutions (or pure water) and after equilibrium had been reached ($E_0$ values in Tables IX- XII, the particular gas tested was injected through the rubber septum. Usually, for all polymers except IV and V, a response was noted within less than one second and it reached a maximum within two to three seconds. It was this maximum that is recorded as E (in mv). Polymers IV and V were considerably more sluggish and they took about 30 seconds to respond. Generally, the original $E_0$ value was obtained after about 15 to 30 minutes, depending upon the gas and its concentration; that is if the response was very high. Otherwise, it returned within two to three minutes.

# 4.0 DISCUSSION OF RESULTS

## 4.1 ANALYSIS OF PHYSICAL PROPERTIES

### 4.1.1 Molecular Weight and Viscosity Data

Since the relative viscosity ($M_{rel}$) of each polymer was obtained at the same concentration, it is possible to compare the apparent molecular weights from the viscosity data. This makes it possible to relate the molecular weights of all the polymers prepared since the gel permeation chromatographic data for molecular weight could not be obtained for the poly(Schiff's base) from thiophene-2,5-dialdehyde (polymer II), the poly(imidazole)/ferrocene (polymer III), and poly(p-dimethylaminophenylacetylene) (VI) due to poor solubility in chloroform or tetrahydrofuran (THF).

One interesting fact presents itself from the data in Table IV for the relative viscosity of poly(p-dimethylaminophenylacetylene) (VI). It is noted that its relative viscosity of 1.34 compares very favorably with the value of 1.31 found for its precursor [poly(p-aminophenylacetylene)], reported previously (Reference 2.) Thus, the reproducibility of preparation plus the excellent chemical analysis attest quite well to the degree of purity of this compound. Furthermore, it had previously been shown (Reference 2) that the relative viscosity of the parent compound to this series, viz., poly(phenylacetylene), had a relative viscosity of 1.19, and by reaction to give the amine derivative the viscosity increased. This might be attributable to the fact that the poly(phenylacetylene) was more ordered and rod-like while the interaction of the amino and dimethylamino groups would cause the chains to develop some bulk to what was previously termed the trans-unaligned structure (References 1 and 2). By so doing, the molecular volume would increase and therefore the viscosity would increase. Similarly, the structures of polymers I, II and III could also be more rod-like (particularly polymer II) and their relative viscosities would also be low; while the polyester/phthalocyanines (polymer IV and V) could have a coiled structure, as well as a possibly high molecular weight, and thus exhibit a higher viscosity.

As a further point of interest in regard to the molecular weights of IV and V, is their chemical analysis data. It was indicated earlier (Sections 3.1.4 and 3.1.5) that the calculated carbon and hydrogen analysis data for IV and V were $C \approx 66$, $H \approx 4.2$ and $C \approx 64$, $H \approx 4.1$, respectively. The reason for this approximation was the fact that it was difficult to exactly determine the extent of copolymerization between the phthalocyanine moiety and the polyester portion. However, if an assumed molecular copolymer formula is given, an exact calculated analysis can be obtained for each polymer. Thus, for the

non-metalated polymer (IV), we can write:

$$\left[(\text{Phthalocyanine})-COO\left(CH_2 CH_2 OCO\, C_6 H_4 COO\right)_{30} CH_2 CH_2 OCO\right]_n$$

or

$$-\left(C_{334}\, H_{262}\, N_8\, O_{124}\right)_n$$
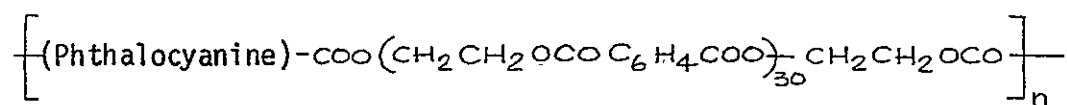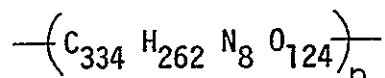
A

This calculates to:

$$\left. \begin{array}{l} C = 62.96 \\ H = 4.11 \\ N = 1.76 \end{array} \right\} \text{ Formula A}$$

On the other hand, if we write:

$$\left[(\text{Phthalocyanine})-COO\left(CH_2 CH_2 OCO\, C_6 H_4 COO\right)_{20} CH_2 CH_2 OCO\right]_n$$

or

$$-\left(C_{234}\, H_{182}\, N_8\, O_{84}\right)_n$$
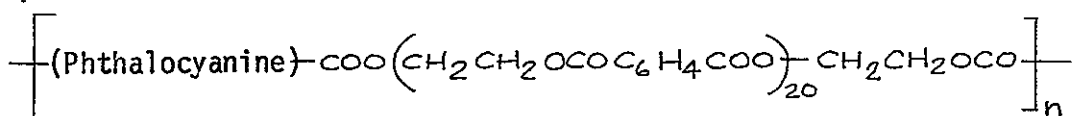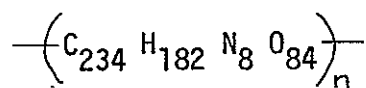
B

This calculates to:

$$\left. \begin{array}{l} C = 63.15 \\ H = 4.09 \\ N = 2.51 \end{array} \right\} \text{ Formula B}$$

Since the found values were:

$$\begin{array}{l} C = 63.12 \\ H = 4.58 \\ N = 2.01 \end{array}$$

It would appear that Formula B is more likely correct. Furthermore, if we examine the data for the metalated polymer (V), we get for Formula A:

$$-\left(C_{334}\, H_{260}\, N_8\, O_{124}\, Fe\right)_n$$
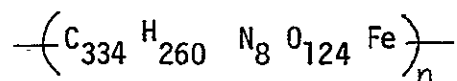
A plus Iron

and this calculates to:

$$
\left.\begin{array}{l}
C = 62.43 \\
H = 4.05 \\
N = 1.74 \\
Fe = 0.87
\end{array}\right\} \quad \text{Formula A plus iron}
$$

Alternatitively, if we use Formula B, we get:

$$-\left(C_{234} \ H_{180} \ N_8 \ O_{84} \ Fe\right)_n-$$
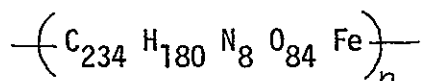
B plus Iron

which calculates to:

$$
\left.\begin{array}{l}
C = 62.40 \\
H = 4.00 \\
N = 2.49 \\
Fe = 1.24
\end{array}\right\} \quad \text{Formula B plus, iron}
$$

Since the found values were:

$$
\begin{array}{l}
C = 66.43 \\
H = 4.01 \\
N = 1.98 \\
Fe = 1.86
\end{array}
$$

It would again seem that Formula B would most likely be correct. It will be recalled tha in Sections 3.1.4 and 3.1.5, the calculated values for carbon and hydrogen were given as approximate values. This was due to the fact that it is not actually known to what extent the phthalocyanine moiety did go into the copolymer; particularly, since there is a large discrepancy between the calculated and found carbon analysis. In addition, it should be noted that the high iron and carbon and lower nitrogen found could be attributable to ferrous citrate being trapped.

It is of interest to note that the curves given in Figures 36 to 38 show the molecular sizes of the phthalocyanine polymers (IV and V) to be considerably larger than, the poly(imidazole)/thiophene polymer (I). This is also borne out from the relative viscosity data of Table IV. Furthermore, the curves of IV and V (Figures 37 and 38) show them to be skewed, thereby implying a non-Gaussian distribution with a large amount of lower molecular size polymer being present. The curve for polymer I (Figure 36), on the other hand is skewed in the other direction, implying more of the larger molecular size

31

polymer. It would appear from this, therefore, that the polymerization process of the imidazole polymer is more efficient than the polyester/phthalocyanine system.

## 4.1.2 Spectral Analysis

In discussing the various spectra obtained (both infrared and ultraviolet), it would be well to briefly point up the relationship between the synthesis and the spectra. For example, where one polymer was derived from another, it is of interest to show how the appearance (or disappearance) of a particular functional group can be followed spectroscopically. This applies equally well to the preparation of a polymer from its monomer, wherein the characteristic absorption peaks attributable to the monomer disappear as it is converted to the polymer. Furthermore, when we consider the excellent chemical analyses obtained, as well as the good melting points, the infrared spectra become further absolute identification of chemical structure of the individual componds and polymers.

As mentioned previously, the preparation of poly(imidazole)/thiophene (I) proceeded from thiophene-2-aldehyde, whose infrared spectrum is given by Figure 39. This spectrum has all the characteristic thiophene absorption peaks, such as at 3100 $cm^{-1}$, 1510 $cm^{-1}$, 1425 $cm^{-1}$, 1080 $cm^{-1}$, 1050 $cm^{-1}$, 860 $cm^{-1}$, and 725 $cm^{-1}$. In addition, it has the carbonyl absorption at around 1650-1700 $cm^{-1}$. This shifting to the 1650 $cm^{-1}$ region is possibly due to conjugation with the conjugate electrons in the ring. By preparing the diethyl acetal derivative, whose infrared spectrum is shown in Figure 40, the majority of the thiophene peaks remained, but the carbonyl absorption at 1650 $cm^{-1}$ is completely gone. Then, coverting this to the thiophene-2-carboxaldehyde diethyl acetal-5-carboxaldehyde, the infrared spectrum (Figure 41) of this compound shows the return of the carbonyl absorption at 1675 $cm^{-1}$. Finally, hydrolysis of the acetal group results in a spectrum that has a stronger absorption for the carbonyl, and with some of the absorption peaks found in the mono carboxaldehyde (Figure 39), but shifted due to the longer path of conjugation because of the two aldehyde groups being conjugated with the ring double bonds (Figure 42).

The other compound needed in the synthesis of polymer I was 1, 4-bis(phenyl-glyoxyloyl) benzene. The preparation of this started with $\alpha, \alpha''$ (para-phenylene) bis ($\beta$-phenylethanol) (or alternatively named, $\alpha, \alpha'$-dibenzyl-p-xylene-$\alpha,\alpha'$-diol), whose infrared spectrum is shown in Figure 43. The characteristic bonded OH

32

absorption at 3350 cm$^{-1}$, the three aromatic absorptions at 1600-1500 cm$^{-1}$, taken in conjunction with the absorption in the 3100-3000 cm$^{-1}$ region plus the fingerprint absorptions for substituted aromatics in the 2000 cm$^{-1}$ to 1600 cm$^{-1}$ are all indicative of the correctness of structure for this compound. The conversion of this to the 1, 4-bis(phenylacetyl)benzene, was shown to proceed as expected by elimination of the OH absorption at 3350 cm$^{-1}$ and the development of a carbonyl absorption at 1675 cm$^{-1}$, as seen in the infrared spectrum given in Figure 44. This was oxidized to the 1,4-bis(phenylglyoxyloyl) benzene, whose spectrum is shown in Figure 45. The OH absorption of 3350 cm$^{-1}$ has completely disappeared, as would be expected, and the carbonyl at 1675 cm$^{-1}$, as well as the aromatic peaks at 1500 and 1600 cm$^{-1}$ are all present. By way of comparison to indicate the purity of this compound, Figure 46 is the infrared spectrum of this same compound prepared and reported by another investigator (Reference 26), and it is interesting to see the strong OH absorption they have at 3435 cm$^{-1}$ where no absorption should be present. Finally, the preparation of polymer I by combining thiophene-2,-5-dialdehyde and 1,4-bis(phenylglyoxyloyl) benzene, in the presence of NH$_3$ results in a polymer whose spectrum is given by Figure 47. It is interesting to note the shifting of the peak at 1675 cm$^{-1}$ to 1650 cm$^{-1}$ which depicts the elimination of the carbonyl and the formation of the imidazole ring, i.e., the NH and/or C=N absorption which ties in with the broad shoulder from 3100-3300 cm$^{-1}$ for the NH. The thiophene moiety and the substituted benzenes are also all present, with the thiophene absorption peaks shifted due to the conjugation with the imidazole ring. (See also Figures 42 and 45).

Polymer II, the poly(Schiff'sbase) from p-phenylenediamine and thiophene-2,5-di-aldehyde has its infrared spectrum shown in Figure 48. The absorption at 1650 cm$^{-1}$ is indicative of the CH=N group, and the peak at 1190 cm$^{-1}$ is relatable to the thiophene moiety. In addition, there are the absorptions at 1500 and 1600 cm$^{-1}$ for the aromatic group, thereby indicating the structure for the polymer to be correct.

Polymer III was derived from the reaction of ferrocene-1,1'dialdehyde, whose infrared spectrum is seen in Figure 49, and 1,4-bis(phenylglyoxyloyl)benzene. The spectrum for the ferrocene compound compares favorably with that of the spectrum of acetyl ferrocene that has been reported elsewhere (Reference 2). The 1450 cm$^{-1}$, 1350 cm$^{-1}$, 1375 cm$^{-1}$, 1275 cm$^{-1}$ and the double peaks between 1000 and 1050 cm$^{-1}$, among others, are related to the ferrocene moiety. The 1650-1660 cm$^{-1}$ absorption is attributable to the aldehyde group.

The spectrum for polymer III, given in Figure 50, shows some similarity to Polymer I (thiophene/imidazole polymer) at around 1250 to 1300 $cm^{-1}$, 950 $cm^{-1}$, 750 $cm^{-1}$, 700 $cm^{-1}$ for the phenylimidazole/ferrocene moieties and at 1650 $cm^{-1}$ for the C=N or NH absorption, as well as the broad shoulder at 3000 to 3300 $cm^{-1}$ for the NH absorption.

In the course of preparing polymers IV and V, two of the required intermediates, viz., aminoiminoisoindolenine and trichloroisoindolenine carbonyl chloride had to be characterized. Their spectra are given in Figures 51 and 52, respectively. Figure 51 has an absorption at 3300 to 3000 $cm^{-1}$ for bonded NH groups and for the C=N structure, as well as the strong doublet at 1600-1650 $cm^{-1}$ for the conjugated C=C group. There is also the strong absorption at 1525 to 1550 $cm^{-1}$ for the cyclic, conjugated C=N group. Figure 52 has the acyl halide absorption as a doublet at 1725 to 1775 $cm^{-1}$ and the C-Cl group absorbing in the 600 to 800 $cm^{-1}$ region plus the broad absorption from 3300 to 3000 $cm^{-1}$ for the bonded NH group.

The infrared spectrum of the resultant phthalocyanine dicarboxylic acid from the preceding two compounds is shown in Figure 53. The OH from the carbonyl as well as the NH group, shows its absorption at 3400 $cm^{-1}$, as well as the absorption at 1690 $cm^{-1}$ for the aryl acid. In addition, there is a weak, broad absorption from 2450-2700 $cm^{-1}$ for the COOH group. For the NH group, there is another absorption at 1600 $cm^{-1}$. The rest of the spectrum has comparable absorptions for the phthalocyanine molecule, as compared to that given in Sadtler Standard Spectra, Midget Edition of 1959 Spectrogram 8760, i.e., the triplet is between 1300 and 1400 $cm^{-1}$ and the five peaks between 1200 and 1000 $cm^{-1}$

When the phthalocyanine dicarboxylic acid was copolymerized with ethylene glycol and terephthalic acid, the infrared spectrum of the resultant polyester is shown in Figure 54. The ester carbonyl absorption is quite pronounced at 1700-1725 $cm^{-1}$, as well as the OH from COOH end groups or glycol end groups at 3500 $cm^{-1}$. The aliphatic $CH_2$ at 2990 $cm^{-1}$ and the aromatic CH at 3100 $cm^{-1}$ are also indicative of the presence of both the ethylene glycol and terephthalic acid moieties, respectively. The 1440 $cm^{-1}$ and 1600 $cm^{-1}$ are probably related to the phthalocyanine structure.

The metalated (iron) polymer of the polyester/phthalocyanine (V) has its infrared spectrum in Figure 55. It is almost identical to Figure 54. Since the spectrum for copper phthalocyanine reported in Sadtler, Spectrogram 8776,and the

34

previously mentioned spectrum for phthalocyanine in the same reference were available for comparison, it was seen that they are very similar, and it is difficult to determine where the N - metal absorption peak is.

For polymer VI the infrared spectrum (Figure 56) of the dimethylated poly(p-aminophenylacetylene) was found to have lost the $NH_2$ absorptions at 3250 $cm^{-1}$, as found previously (Reference 2), and to have an absorption at 2900 $cm^{-1}$ that might be attributable to the $CH_3$ group.

In addition to the infrared spectra, an attempt was made at obtaining ultraviolet (UV)absorption spectra, as well. However, the polymers were not soluble in solvents that could be used for UV spectra. In order to get some evidence of their ultraviolet absorption capability, they were suspended in methanol and left there a few hours at room temperature. Then the colored supernatant liquid was used, but the resultant curves, given in Figures 57 to 62, are probably not representative of the polymers since the polymers did not dissolve. Rather, the alcohol only extracted some low molecular weight component that could have been present as an impurity. In view of the lack of definition,and little indication of an absorption peaks in these curves, no explanation of their structure will be given.

### 4.1.3  Film Properties and Crystallinity Studies

Of the various techniques that might be available for putting films of these polymers onto the electrodes used in this program, two may be considered: (1) spinning (analogous to the deposition of photoresist in electron device fabrication); and (2) dipping. Due to the fact that these polymers (I to VI) were not soluble in readily volatilized solvents, the spinning technique could not be used. Thus, the dipping process was considered, and the solvent (dimethylformamide) was removed, at as rapid a rate as possible, under vacuum. The resultant films were examined under the scanning electron microscope for thickness measurements and characteristic surface features, if any. In Figures 18 to 35, the magnifications used were mostly 4000X for the 90 degree view, and 400X and 4000X for the 45 degree view, except for Figures 18 and 20 (for polymer I), where the 90 degree picture is at 2000X and one of the 45 degree pictures is 800X; also Figure 30 is at 4500X, Figure 31 is at 450X and Figure 32 is at 4500X. Furthermore, in all pictures, number 1 on the photograph depicts the edge of the polymer film, number 2 is the top surface of the film (as seen when the slide is tilted 45 degrees), and number 3 is the glass surface.

By examining the films, in detail, considerable information was obtained that could be useful towards understanding some of the gas/polymer interaction effects to be discussed. Thus, polymer I was found to have a uniform thickness (Figure 18) and to be quite thick (13.64 microns). It also had a relatively smooth, nonporous surface (Figure 19).

Polymer II had a thin, non-uniform film, as seen in the thickness view (Figure 21) (thickness of about 0.572 microns) and an unevenly textured surface (Figure 22). Polymer III exhibited a cracked and peeling edge (Figures 24 and 26) and a highly cracked surface (Figure 25). Its thickness was found to be 2.67 microns. Polymer IV had a uniform thickness of about 11.18 microns (Figures 27 and 28) and a relatively smooth, non-porous surface, but with a few small surface pit marks (Figure 29). Polymer V was also relatively uniform in thickness (Figure 30) with an average thickness of about 6.99 microns. The fragments seen in Figure 30 are due to fracturing of the glass. The surface also looks relatively smooth, as seen in Figures 31 and 32. Finally, polymer VI exhibits a very uneven film (edge view) (Figure 33) with a thickness of about 1.9 microns, and a highly cracked surface (Figures 34 and 35).

Although an attempt was made to crystallize the various polymers prepared so that ordered structures could be obtained that might affect both the electrical conductance and the gas response behavior, little success was realized in this regard. If the polymers could be made to crystallize, their gas-interaction effects could probably be more sensitive in that the forces operating in forming a charge-transfer complex could be more easily transmitted through a crystalline polymer than an amorphous one. The only polymer that showed any degree of crystallinity, as observed by X-ray diffraction studies, was the poly(Schiff's base) from thiophene-2,5-dialdehyde (polymer II); and its crystallinity was inherent in the polymer, not induced, as seen in Table.II.

## 4.1.4 Thermal Analysis
In order to determine which polymers would have the necessary long term stability when used in a fire detector, they were subjected to thermogravimetric analysis (TGA), as well as isothermal weight loss studies of 35°C. By examining Table V and Figures 63 to 68, an interesting correlation can be seen between the isothermal weight loss and TGA data. That polymer which suffered the greatest weight loss at 35°C, i.e., poly(p-dimethylaminophenylacetylene) (VI), also showed the greatest ultimate weight loss at 105°C (about 6 percent) (See Figure 68).

This might be due to oxidative degradation of the methyl groups on the nitrogen. A further interesting example of correlation between structure and thermal properties is the similarity in stability between the poly(imidazole)/thiophene (I) and the poly(imidazole)/ferrocene (III). The isothermal weight losses are comparable (noticeable, but small), and the TGA data also show comparable values, i.e., about 2.5 percent at 110°C for I (Figure 63) and about 2.5 percent for III at 110°C (Figure 65). Thus, it may be that the thiophene and ferrocene moieties show equivalent stability, but the weak structure is the imidazole portion of the chain. This may be attributable to a delocalization of the hydrogen atom on the nitrogen in the imidazole ring and the bonding of this hydrogen with the sulfur atom on the thiophene ring.

The poly(Schiff's base) (II), as might be expected, shows an extremely low weight loss (see Figure 64). This could be related to the fact that a highly conjugated, linear structure exists that is strongly stabilized by being able to form a crystalline polymer, as discussed previously in Section 4.1.3. Thus, thermal energies would first have to break down the crystallinity before the bond energies would be affected in the polymer.

One of the most striking anomalies observed has been the apparently excellent thermal stability of the polyester/phthalocyanine polymers (IV and V). It is observed from Table V and Figures 66 and 67 that the weight losses were negligible, even though there are a large number of $-CH_2-$ groups in the polymer. Apparently, the phthalocyanine moiety exerts some stabilizing influence on the total molecule; albeit what is actually occurring is unknown, at the moment.

## 4.2  GAS SENSOR INTERACTIONS

Once the synthesis and characterization of the polymers was completed, the next step was to determine the gas detecting capability of the various polymers, and the potential for being used in a fire detecting system.  To this end, the first series of gas detecting tests were performed in a chamber set up as shown in Figure 70, with the gases being drawn through a blower fan  and passed down a tube about 25 cm long into a 7000 cc stainless steel chamber with the stainless steel lid partly off.  The first three polymers that were prepared (I, II and III) were tested for their response to $NH_3$, CO, HCN, $NO_x$, an aldehyde, e.g., croton-aldehyde, $SO_2$, cigarette smoke, and smoldering (burning) cotton.  The smoldering (burning) cotton tests were run with the blower end of the tube modified, as shown in Figure 71.

In this first series of tests, polymer I showed  a negative response to ammonia, an amine (diethylamine), and cigarette smoke, but it gave a positive response to the burning cotton (see Table VI).  None of the other gases including water vapor, elicited any response.  Polymer II, on the other hand, gave a response to every gas tested, except water vapor as seen in Table VII.  Furthermore, its response to ammonia and cigarette smoke, as well as the other gases tested, was positive.  Polymer III also showed responsiveness to some of the gases, such as ammonia, crotonaldehyde and nitrogen oxides, in addition to cigarette smoke and burning cotton (Table VIII).

From this early work, two striking developments were noted.  In all cases, both smoldering cotton and burning cotton were detectable with the three sensors shown (Tables VI - VIII, but these responses were not due to water vapor.  This was amply proven when a drying agent was used in the tube between the fire and the sensor.  With and without the drying agent, the response was the same.  Furthermore, it is seen from the Tables that water vapor gave no response with any of these sensors.  In fact, about 0.1 ml of liquid water was also injected directly into the fan that was directing the air to the sensor, and there was absolutely no response.  Thus, fires were being detected by means of the gases evolved, not water vapor; and which gases is still a moot point.

Additionally, a most dramatic observation was made that led us to believe that a fire detector that will not be affected by cigarette smoke or water vapor could be a likely possibility.  If we examine Figure 73, we find an interesting set of data.  Figures 73a and 73b are data for the effect of cigarette smoke and smoldering cotton on the thiophene/imidazole polymer (I).  However, by comparison to those

tests where the cigarette smoke and smoldering cotton were some distance away from the sensor (and the gases had to travel down a tube, as shown in Figures 70 and 71), in this instance the cigarette smoke and the cotton fire were in relatively close proximity to the sensor. Thus, the cotton fire was generated inside the chamber, a short distance away from the sensor, and the cigarette smoke was just outside the chamber, with the fan drawing the air through the chamber from the lid rather than into the chamber through the tube attached to it, as was done for the data generated in Tables VI-VIII. Obviously, the concentration of gases generated would be much higher when the smoke was close to the sensor than that found in the cases where the gases were blown down a long path tube and had a chance to get lost on the walls of the tube, as would be for the data given in Tables VI-VIII. However, it is not the concentration of gases that is important, (this would only affect the magnitude of the response), but it is the speed and direction of response; and this is affected by the proximity to the sensor plus the type of gas present. For example, in Figure 73, (which is a reproduction of an actual real time strip chart recording), cigarette smoke invariably gave a negative response. This was the same type of response observed for the thiophene/imidazole polymer when the gases were blown down the tube, (as seen in Table VI). The direction of response for amines is also negative, (see Table VI). Thus, it may be amines in cigarette smoke that are making this detector specific for cigarette smoke.

Thus, setting the sensor's baseline value on a center zero scale, and applying cigarette smoke, the sensor instantly responded in the negative direction. As soon as the cigarette was removed, the sensor immediately returned to the center zero value; and this occurred numerous times (Figure 73a). In the case of the smoldering and/or burning cotton, it, too, responded immediately, but in the positive direction, and when the cotton fire was extinguished, it immediately started to return to the original value (Figure 73b.)

It appeared from these data that a discriminating sensor had been developed that could be used as a fire detector in most normal environments. However, when all the polymers (I-VI) were completely synthesized and available for testing, they were evaluated under slightly different conditions. Instead of testing them only at 50 percent RH, they were also tested at 25 percent, 75 percent and 100 percent RH, as well. To obtain these conditions, the setup shown in Figure 72 was used. In addition, any one gas was tested at the same concentration for all polymers, viz., ammonia was at 10 cc, carbon monoxide was at 40 cc, acetylene at 20 cc, etc. Since 1 cc is equivalent to 140 parts per million (in a 7000 cc chamber), it is relatively simple to convert all the cc values to parts per million.

The first set of data obtained, shown in Table IX, are for polymers I, II and III, using the setup shown in Figures 70 and 71. These data were obtained under relatively dry conditions(as low a relative humidity, as possible) using calcium sulfate (drierite) in the air stream. However, the responses were minimal, possibly due to adsorption of some of the gases on the drierite. These data are all compiled in Tables IX to XIII, and Table XIV shows the minimum quantity of gas used to determine the responsiveness of any polymer. Thus, for example, the poly(imidazole)/thiophene (I) with ammonia at 25 percent RH was responsive at a level of 10μL while the nitrogen oxides evoked a response with this polymer and the same RH at 5μL. However, in some instances, no response was noted even up to 100 cc of gas used (see Table XIV).

In the Tables IX to XIII, the $I_0$ value is that for the particular polymer at a certain RH, but with no gas present, and the I value is that response generated by the gas. All polymers, except IV and V, responded in less than one second and reached a maximum within two to three seconds. Polymers IV and V were very sluggish and took 30 seconds to respond.

Before a discussion is undertaken relative to gas effects, it would be well to consider the effects of water vapor on the sensor due to changes in the relative humidity. In the first tests run on polymers I, II and III, as described earlier, it was shown that water vapor produced no effect on the sensor. Those results were obtained on water vapor concentrations that probably did not get much above 60 percent RH.

It was then decided to study gas/polymer interactions under controlled humidity conditions. Measurements were first made with either drierite in the gas flow path or under dry nitrogen, as shown in Table IX, to get approximately zero percent RH, but the data were not reproducible. Therefore, it was decided to use a 55% solution of sulfuric acid to give 25 percent RH as the lowest value. This always gave reproducible results. Use of 100 percent sulfuric acid, to get zero percent RH, would not have been reproducible, since the first passage of air would have changed the concentration of the sulfuric acid so that the RH would no longer have been zero percent. The amount of moisture passing through the solution used to give 25 percent RH, however, would not show as great an incremental change. [Note: The technique for obtaining various RH values, according to Lange's Handbook of Chemistry (1961), p. 1423, uses varying concentrations of sulfuric acid. It is interesting to note that there is no value given for zero percent RH.]

40

If we next look at the data given in Tables IX to XIII, we observe an interesting fact. Averaging the $I_0$ value in each polymer at each RH, it is seen that the relative change of $I_0$ from 25 percent RH to 100 percent RH is least for polymer V. The next to be least affected by water vapor due to RH changes is polymer I. Polymer II also was insensitive to water vapor from 25 percent RH to 75 percent RH, and then it showed an increase of $I_0$ at 100 percent RH. However, this is not as great an increase as that observed for polymer III, which increases most pronouncedly from 25 percent RH to 50 percent RH. The two polymers that showed the most change though, were polymers IV and VI. Polymer IV jumped markedly in response from 50 percent to 75 percent RH; but its response was most pronounced at 100 percent RH. Polymer VI, on the other hand, went off scale between 75 percent RH and 100 percent RH and could not be used at 100 percent RH.

It is difficult, at this time, to completely explain the reason for one substance being more affected by water vapor than another. Part of the explanation might reside in the chemistry, and part might be due to film thickness and film continuity effects. For example, Figures 34 and 35 depicting the surface structure of the film from poly(p-dimethylaminophenylacetylene) (VI), shows a highly cracked surface. Apparently, water molecules can, at a high RH, most easily go through this film to the substrate and cause a shorting effect. In the case of the poly(imidazole)/thiophene (I), this polymer's film, as seen in Figures 18 to 20, is depicted as a thick, uniform film, thereby minimizing water permeation. On the other hand, though, the film for polymer IV (see Figures 27 to 29) is very similar in thickness and surface texture to that of polymer I, but its response to water vapor at 75 percent and 100 percent RH is much more pronounced. In this case, the chemistry may be making the contribution. In other words, if there are a number of free carboxyl and/or hydroxyl end groups, they may be interacting with the water to allow facile migration through the film. In addition, the center of the metal-free phthalocyanine moiety is relatively large, and it, too, could accommodate a water molecule, thereby allowing easy migration through the polymer.

Why polymer V, which is derived from polymer IV and differs only in that it has an iron atom in it, shows little tendency to be affected by water is a moot point. One argument that might be put forward is that the hole in the center of the phthalocyanine moiety is plugged with an iron atom, and now the water is less likely to migrate through this region.

Polymers II and III are thin films (see Figures 21 and 24, respectively), and, in addition, polymer III has a highly cracked surface (see Figures 25 and 26), while

polymer II has an unevenly textured surface (Figures 22 and 23). Each of these polymers shows a similar water effect, as given by their change in $I_0$ with respect to a change in RH. However, it may be that if they were thicker films and uniformly spread, they might be relatively impervious to the effect of water vapor. The only anomalous result that is inexplicable, to date, is the fact that the $I_0$ value for polymer III decreased at 75 percent RH and then went up again at 100 percent RH.

Presently, it appears that water vapor may be making a contribution to the $I_0$ value for each polymer due to migration through the film to the substrate. Considerable more work has to be done in this area before it can be unequivocally resolved. However, Labes (Reference 4) also observed that moist air (60 percent RH) had no effect on the bulk dark conductivity of anthracene. Our data is somewhat analogous. Up to 50 percent RH, little effect is observed for most of the polymers. It's between 50 percent and 75 percent when most of the changes begin to show up.

The next problem to consider is the relationship between a particular gas and a particular polymer with respect to any interaction effects. Since the basic concept of the fire detector is to develop a multiplicity of sensors, each having specificity to a particular gas, it is easy to see how this specificity exists when comparing a particular gas with each polymer at a particular concentration of gas. Thus, for example, looking across any one line in Tables X to XIII, for any RH and for any one gas, e.g., $SO_2$, it can be seen that the electronegativity concept is operating through a charge-transfer complex that results in a greater electron interaction to give a greater $\Delta I$ (where $\Delta I = I - I_0$).

If we examine the data in Tables X to XIII, we find that the response to ammonia is not very great at 25 percent and 50 percent RH, for polymer III, but at 75 percent RH polymer III is exceptionally responsive (about a 20-fold increase in I), polymer II is next (about a 15-fold increase in I) and polymer VI is next (about a 10-fold increase in I). At 100 percent RH, polymer III drops in responsiveness to ammonia compared to polymers I (about a 30-fold increase in I), IV 16-fold increase in I) and II (15-fold increase in I). Polymer I, on the other hand, has shown a greater responsiveness to ammonia at all relative humidities, (except 75 percent RH). Therefore, it would appear that poly(imidazole/thiophene)(I) is the system to consider for ammonia in this group of polymers.

Since both polymers I and III each have the imidazole moiety as part of their polymer structure, a likely explanation for the greater responsiveness to ammonia of polymer I over polymer III might lie in the fact the hydrogen attached to the imidazole nitrogen could become delocalized and be bridging the thiophene ring and the imidazole ring by hydrogen bonding to both the sulfur

42

and the nitrogen. By so delocalizing itself, it can be considered to be a pseudo proton, and the ammonia could complex with this causing an ammonium ion to form. In effect, this should cause the conductance to decrease, as the electrons will be more tightly bound up with the ammonium ion; and this is essentially what did occur in the early phase of the program (see Figure 74 and Table VI ). However, the fact that the conductance did not decrease in this later work with the same polymer I might be attributable to a possible aging effect on the sulfur atom of the thiophene group causing it to possibly act as a sulfoxide. In this form, it could compensate for the electron-attracting nature of the ammonium ion and force electrons back into the conduction band.

The poly(imidazole)/ferrocene polymer (III), though, cannot form a hydrogen-bonded bridge between the imidazole ring and the ferrocene ring. Thus, its electronic interaction with ammonia, at the high relative humidities might be related mostly to the porosity of the polymer film (see Figures 25 and 26), thereby allowing the ammonia and water molecules to react on the surface of the substrate and become an ionic conductor. The conductance of polymer I, however, is more likely due to a bulk electronic effect in the polymer. This idea of a surface ionic conduction phenomenon is also borne out by the high conductance of polymer VI with ammonia. It, too, has a large number of cracks in the film (see Figures 34 and 35), and it could also allow the ammonia and water vapor to pass through to the substrate.

The next two gases to effect any major response were sulfur dioxide and nitrogen oxides, i.e., "acidic" gases. Again, responses were variable. For example, at 25 percent RH, polymer III gave an extremely large response to $SO_2$ and less so to $NO_x$. Polymer IV however, gave a small response to $SO_2$ and a large one to $NO_x$. At 50 percent RH, polymer III again gave a large response to $SO_2$ and a larger response to $NO_x$ than at 25 percent RH, while the polymer IV response to $NO_x$ at 50 percent RH dropped way down and its $SO_2$ response remained about the same as at 25 percent RH. In addition, the $SO_2$ response for polymer II shot way up at 50 percent RH, so that it was most responsive to this gas at this relative humidity. At 75 percent RH, almost all the polymers showed a good response to $SO_2$, but at 100 percent RH, polymer II was not responsive to $SO_2$. On an overall basis, though, polymer I was responsive to $SO_2$ at each RH level, and with a fairly large $\Delta_I$ . Thus, it could be said that polymer I was probably most responsive to $SO_2$.

For $NO_x$, it would appear that from 50 percent RH to 75 percent RH, polymer II was most responsive. (Its value for 100 percent RH was not measured.) However, once again, for a consistent responsiveness to $NO_x$, polymer I was the best one. By comparing its responsiveness to $SO_2$ and $NO_x$, it seems, though, that Polymer I is somewhat more responsive to $SO_2$.

One other gas response that was noticed was that for HCN. Here, only polymer I showed any interaction capability; its responsiveness increased with increasing RH. Although the exact mechanism for this response capability is not known, it appears likely to have something to do with the thiophené moiety, since polymers I and III both have the imidazole structure.

Finally, with regard to cotton smoke and cigarette smoke, only polymer III seemed to show any significant response whatever. This appears strange in the light of the data shown in Tables VI to VIII as well as the strip chart recording shown for polymer I, in Figure 73. Apparently, as mentioned earlier, polymer I may have undergone some oxidative change from the time the first data were obtained, and it was no longer capable of responding to the "fire" gases as it had before. However, another interesting fact is noted in that the response of poly(imidazole)/ferrocene (III) to the fire gases is somewhat comparable to what had been observed previously for poly(ethynylferrocene) (Reference 2). In that previous case, it was the ferrocenyl polymer that appeared to be the most responsive to "fire" gases.

## 5.0 CONCLUSIONS

Conjugated polymeric polyenes are feasible for early warning fire detector sensors. The polymers, conjugated and non-conjugated, viz., poly(imidazole)/thiophene (I), poly(Schiff's base)/thiophene (II), poly(imidazole)/ferrocene (III), polyester/phthalocyanine (metal-free) (IV), polyester/phthalocyanine (iron) (V), and poly(p-dimethylaminophenylacetylene) (VI), are all capable of responding to certain gases when exposed to them under different relative humidities. In most instances, the responses were greatest to $SO_2$, $NO_x$ and $NH_3$, particularly at high relative humidities. Furthermore, all show varying responses when exposed to different amounts of water vapor; and their responsiveness may be, in some cases, attributable to their film properties.

Since there were very slight differences in electronegativity due to the fact that most of the polymers were electron-donating, the gas/polymer interactions were relatively similar at low relative humidities. It was at high relative humidities that a mixture of surface and bulk effects became noticeable.

For most polymers, other than I or V, it is difficult to separate the reasons for their responsiveness and the magnitude of the response to the various gases. That is, is it due to a bulk electronic interaction effect, a surface effect due to migration of ions, or a combination of both? However, since polymers I and V were least affected by changes in RH, it might be that their response to the gases is due to a bulk electronic interaction effect. Furthermore, since polymer I is more conjugated than V, it should be more electropositive. This is borne out by the consistently greater response it shows with the gases used. This further substantiates the concept of developing a fire detector that would have a multiple sensor system for detecting the different gases expected to be present in a fire.

Finally, with regard to the detection of gases generated by smoldering cotton, it is unclear why polymer III was the only one to show any significant response. It is not known, at this time, what the exact composition of the products of combustion are from a smoldering fire, nor the relative percentage of each gas. Thus, it is difficult to explain the response behavior of the various polymers to smoldering cotton. Too many variables enter into the process to increase the complexity of the system. For example, the temperature of combustion, the amount of air present, the extent to which gases can be adsorbed on the walls (Note: If water vapor condenses on the walls of the tube, shown in Figure 72, some of the gases that may be soluble in water, as well as the water generated in the combustion, may remain on the walls of the tube.), and the responsiveness of the particular polymer to these gases will all enter into the detectability.

BLANK PAGE

## 6.0 RECOMMENDATIONS

To further develop and optimize the system necessary for developing an early warning fire detector an in-depth study has to be made utilizing the concepts already established, notably, the preparation of electrically conductive compounds capable of forming charge-transfer complexes with gaseous substances, and the technique for measuring the electrical signal generated. Therefore, further studies should be performed on the chemistry and electronics.

Background information has begun to accumulate that shows a poly(imidazole)/thiophene structure to be a potentially good detector for certain acidic gases, e.g., $NO_x$, $SO_2$, HCN, and that poly(ethynylferrocene) is a good "fire" gas detector (Reference 2). It is recommended, therefore, that these polymers among others, be further investigated by having a poly(imidazole)/thiophene with a nitro group built into the polymer, for strong electronegativity effects. As an adjunct, a dimethylamino group should be considered in the same polymer for strong electropositive effects. To develop the electronegativity series in the poly(ethynylferrocene) system, poly(ethynylnitroferrocene) plus poly(ethynylcobaltacene) and poly(ethynylnitrocobaltacene) are to be considered.

With regard to the electronics, consideration should be given to other types of measurement than conductance. Capacitance measurements should be very sensitive and responsive to gas/polymer interactions. Absorption of gases into polymers should change the dielectric constant of the medium, which should be readily detectable by capacitance measurements. Furthermore, water vapor may not be a serious problem because polymers such as poly(imidazole)/thiophene) are insensitive to changes in relative humidity. The use of discriminatory or compensatory circuits should eliminate interference where the polymer is sensitive to water vapor.

Another important practical problem is to study the response behavior of various polymers prepared for use in sensors when exposed to smoldering of other materials, e.g., nylon, wool, urethanes; acrylics, vinyl, phenolics, etc. In addition, these measurements should be made at different temperatures, e.g., 0°C, 25°C, 50°C, 100°C, etc.

Preceding page blank

47

A spectral (infrared and ultraviolet) study should be made of the various polymers upon exposure to gases. A correlation between spectral changes (upon exposure to various gases at different partial pressures) and electrical response should indicate which polymer, and the functional group in that polymer, is responsible for greatest specificity with a particular gas.

Tied in with this study, would be a detailed study of the ultraviolet absorption spectra of the various compounds, and their relationship to conductivity and complexing capability. This information would more readily enable the design of a polymer which would show maximum interactions with gases. For example, the UV spectrum of a conjugated polyene will be different if it is isolated from the appendage attached to it or in resonance interaction with the appendage; if in interaction, it will be more related to the electronegativity of the appended moiety and therefore more capable of maximum interaction effects.

The effect of film thickness is a problem that bears further investigation. By varying the film thickness, it would be possible to determine whether bulk or surface effects are operating. Along with this, a variation in electrode spacing should be considered. Decreasing the electrode spacing should enhance electrical response.

Finally, another area of importance to investigate is the molecular weight of the polymers prepared. A detailed study should be undertaken with regard to molecular weight distribution and electrical conductance. Increasing the molecular weight of a conjugated polyene should probably increase the electrical conductance due to the fact there will be fewer hoppings necessary from chain-to-chain.

## TABLE I
## X-RAY ANALYSIS OF POLYMERS FOR DEGREE OF CRYSTALLINITY

| POLYMER | DEGREE OF CRYSTALLINITY |
|---|---|
| Poly(imidazole)/thiophene (I) | Amorphous |
| Poly(Schiff's base)/thiophene (II) | Crystalline |
| Poly(imidazole)/ferrocene (III) | Amorphous |
| Polyester/phthalocyanine (metal-free) (IV) | Amorphous |
| Polyester/phthalocyanine (iron) (V) | Minor amount of crystallinity* |
| Poly(p-dimethylaminophenylacetylene) (VI) | Minor amount of crystallinity* |

*Minor amount of crystallinity appears to be due to inorganic impurities in the polymer (See Table III).

## TABLE II
## THE d-SPACINGS FOR THE POLY(SCHIFF'S BASE)/THIOPHENE (II)

| $2\theta$ | $d(\overset{\circ}{A})$ |
|---|---|
| 15.3 | 5.786 |
| 25.3 | 3.490 |
| 19.5 | 4.572 |
| 29.0 | 3.076 |
| 32.5 | 2.753 |

## TABLE III

### SPECTROGRAPHIC ANALYSIS OF POLYMERS

| | I<br>Poly(imidazole)/thiophene | II<br>Poly(Schiff's base)/thiophene | III<br>Poly(imidazole)/ferrocene | IV<br>Polyester/phthalocyanine(metal-free) | V<br>Polyester/phthalocyanine (Iron) | VI<br>Poly(p-dimethyl-aminophenyl-acetylene) |
|---|---|---|---|---|---|---|
| Minor Amounts | | | Fe | | Na, Fe | Ca, Na, Mg, Fe |
| Trace Amounts | Si, Fe, Mg, Al, Na, Ca | Si, Fe, Mg, Al, Na, Ca | Si, Mg, Al, Na, Ca | Si, Mn, Fe, Mg, Al, Na, Zr, Ca, Cr | Si, Mn, Mg, Al, Cu, Zn, Ni, Ca, Cr | Si, Mn, Sn, Ph, Al, Ca, Cd, Zn, Ag, Ni, Cr |

TABLE III

SPECTROGRAPHIC ANALYSIS OF POLYMERS

| | I<br>Poly(imidazole)/<br>thiophene | II<br>Poly(Schiff's base)/<br>thiophene | III<br>Poly(imidazole)/<br>ferrocene | IV<br>Polyester/<br>phthalocyanine(metal-free) | V<br>Polyester/<br>phthalocyanine<br>(Iron) | VI<br>Poly(p-dimethyl-<br>aminophenyl-<br>acetylene |
|---|---|---|---|---|---|---|
| Minor Amounts | | | Fe | | Na, Fe | Ca, Na, Mg, Fe |
| Trace Amounts | Si, Fe, Mg, Al, Na, Ca | Si, Fe, Mg, Al, Na, Ca | Si, Mg, Al, Na, Ca | Si, Mn, Fe, Mg, Al, Na, Zr, Ca, Cr | Si, Mn, Mg, Al, Cu, Zn, Ni, Ca, Cr | Si, Mn, Sn, Ph, Al, Ca, Cd, Zn Ag, Ni, Cr |

## TABLE IV
## POLYMER RELATIVE VISCOSITIES

<u>Solvent:</u>  Dimethylformamide

Temp.:    20°C $\pm$ 0.1°  .

<u>Concentration:</u>  0.05%

| <u>Polymer</u> | Relative Viscosity $(t/t_0)$ |
|---|---|
| Poly(imidazole)/thiophene (I) | 1.12 |
| Poly(Schiff's base)/thiophene (II) | 1.15 |
| Poly(imidazole)/ferrocene (III) | 1.08 |
| Polyester/phthalocyanine (metal-free) (IV) | 2.10 |
| Polyester/phthalocyanine (iron) (V) | 1.95 |
| Poly(p-dimethylaminophenylacetylene) (VI) | 1.34 |

TABLE V

ISOTHERMAL WEIGHT LOSS AT 35°C

| POLYMER | TIME (HRS) | PERCENT WEIGHT LOSS |
|---------|-----------|---------------------|
| Poly(imidazole)/thiophene (I) | 100 | 0.5% ± 0.1% |
| | 300 | 0.5% ± 0.1% |
| Poly(Schiff's base)/thiophene (II) | 100 | <0.1% ± 1% |
| | 300 | <0.1% ± 1% |
| Poly(imidazole)/ferrocene (III) | 100 | 0.2% ± 0.1% |
| | 300 | 0.2% ± 0.1% |
| Polyester/phthalocyanine (IV) | 100 | <0.1% ± 0.1% |
| | 300 | <0.1% ± 0.1% |
| Polyester/phthalocyanine plus Iron (V) | 100 | <0.1% ± 0.1% |
| | 300 | <0.1% ± 0.1% |
| Poly(p-dimethylaminophenylacetylene)(VI) | 100 | 1% ± 0.1% |
| | 300 | 0.8% ± 0.1% |

## TABLE VI

SENSITIVITY OF POLY(IMIDAZOLE) FROM 1,4-BIS (PHENYLGLYOXYLOYL) BENZENE AND THIOPHENE -2,5- DICARBOXALDEHYDE SENSOR TO GASES

| GAS | VOLUME | INITIAL CURRENT (amp) | MAX. CURRENT (amp)** |
|---|---|---|---|
| $NH_3$ | 10cc | $2.30 \times 10^{-10}$ | $1.57 \times 10^{-10}$ |
| $NH_3$ | 2cc | $2.30 \times 10^{-10}$ | $2.10 \times 10^{-10}$ |
| Diethylamine | 2cc (1) | $2.25 \times 10^{-10}$ | $1.85 \times 10^{-10}$ |
| $H_2O$ | 10cc (1) | $2.20 \times 10^{-10}$ | $2.20 \times 10^{-10}$ |
| CO | 10cc | $2.15 \times 10^{-10}$ | $2.15 \times 10^{-10}$ |
| $CO_2$ | 10cc | $3.20 \times 10^{-10}$ | $3.20 \times 10^{-10}$ |
| Nitrogen Oxides | 10cc | $3.20 \times 10^{-10}$ | $3.20 \times 10^{-10}$ |
| HCN | 10cc | $2.25 \times 10^{-10}$ | $2.35 \times 10^{-10}$ |
| $CH_3CH{:}CH.CHO$ | 10cc (1) | $2.23 \times 10^{-10}$ | $2.23 \times 10^{-10}$ |
| *Cigarette | - | $2.20 \times 10^{-10}$ | $2.05 \times 10^{-10}$ |
| ·Cigarette | - | $2.20 \times 10^{-10}$ | $1.85 \times 10^{-10}$ |
| Smoldering Cotton | - | $2.10 \times 10^{-10}$ | $2.15 \times 10^{-10}$ |
| Burning Cotton | - | $2.10 \times 10^{-10}$ | $5.20 \times 10^{-10}$ |

*Current reaches $2.05 \times 10^{-10}$ amps within 5 secs.

**Maximum deviation obtained after about 30 secs.

(1) Air saturated with vapor above liquid

Note: Relative humidity for all measurements was 50%

## TABLE VII

SENSITIVITY OF POLY(SCHIFF'S BASE) FROM P-PHENYLENE DIAMINE AND THIOPHENE -2,5-DICARBOXALDEHYDE SENSOR TO GASES

| GAS | VOLUME | INITIAL CURRENT (amp) | MAX. CURRENT (amp)* |
|---|---|---|---|
| $NH_3$ | 1cc | $1.25 \times 10^{-10}$ | $2.50 \times 10^{-10}$ |
| $NH_3$ | 0.1cc | $1.05 \times 10^{-10}$ | $1.25 \times 10^{-10}$ |
| $NH_3$ | 10μL. | $0.95 \times 10^{-10}$ | $1.00 \times 10^{-10}$ |
| CO | 5cc | $0.90 \times 10^{-10}$ | $1.00 \times 10^{-10}$ |
| CO | 1cc | $0.86 \times 10^{-10}$ | $0.92 \times 10^{-10}$ |
| CO | 0.5cc | $0.83 \times 10^{-10}$ | $0.87 \times 10^{-10}$ |
| $CO_2$ | 1cc | $0.76 \times 10^{-10}$ | $0.99 \times 10^{-10}$ |
| $CO_2$ | 10μL. | $0.63 \times 10^{-10}$ | $0.72 \times 10^{-10}$ |
| (1) Nitrogen Oxides | 1cc | $0.61 \times 10^{-10}$ | $0.64 \times 10^{-10}$ |
| (1) Nitrogen Oxides | 10μL | $0.57 \times 10^{-10}$ | $0.68 \times 10^{-10}$ |
| (1) Nitrogen Oxides | 1μL | $0.53 \times 10^{-10}$ | $0.60 \times 10^{-10}$ |
| HCN | 1cc | $0.28 \times 10^{-10}$ | $0.32 \times 10^{-10}$ |
| $SO_2$ | 10cc | $1.45 \times 10^{-10}$ | $1.60 \times 10^{-10}$ |
| (1) $CH_3CH=CH.CHO$ | 1cc | $1.40 \times 10^{-10}$ | $1.50 \times 10^{-10}$ |
| (1) $CH_3CH=CH.CHO$ | 0.2cc | $1.25 \times 10^{-10}$ | $1.50 \times 10^{-10}$ |
| $C_2H_2$ | 10cc | $0.43 \times 10^{-10}$ | $0.62 \times 10^{-10}$ |
| (1) Water | 10cc | $1.25 \times 10^{-10}$ | $1.25 \times 10^{-10}$ |

(1) Air saturated with vapor above liquid

Note: Relative humidity for all measurements was 50%

*Maximum deviation obtained after about 30 sec.

TABLE VII (Cont'd)

| GAS | VOLUME | INITIAL CURRENT (amp) | MAX. CURRENT (amp) |
|-----|--------|-----------------------|--------------------|
| Smoldering Cotton | - | $0.89 \times 10^{-10}$ | $1.05 \times 10^{-10}$ |
| Burning Cotton | - | $0.89 \times 10^{-10}$ | $3.10 \times 10^{-10}$ |
| Cigarette | - | $3.80 \times 10^{-10}$ | $8.40 \times 10^{-10}$ |

## TABLE VIII

SENSITIVITY OF POLY(IMIDAZOLE) FROM 1,4-BIS(PHENYLGLYOXYLOYL) BENZENE AND FERROCENE -1, 1'-DICARBOXALDEHYDE

| GAS | VOLUME | INITIAL CURRENT (amp) | MAX. CURRENT (amp)* |
|---|---|---|---|
| $NH_3$ | 10cc | $4.8 \times 10^{-10}$ | $48 \times 10^{-10}$ |
| $CH_3CH:CH.CHO$ | 1cc ① | $6.0 \times 10^{-10}$ | $10.0 \times 10^{-10}$ |
| CO | 10cc | $5.0 \times 10^{-10}$ | $5.0 \times 10^{-10}$ |
| $CO_2$ | 100cc | $7.0 \times 10^{-10}$ | $7.0 \times 10^{-10}$ |
| $H_2O$ | 10cc ① | $7.3 \times 10^{-10}$ | $7.3 \times 10^{-10}$ |
| $SO_2$ | 10cc | $5.5 \times 10^{-10}$ | $5.5 \times 10^{-10}$ |
| Nitrogen Oxides | 5cc | $6.5 \times 10^{-10}$ | $19.0 \times 10^{-10}$ |
| Nitrogen Oxides | 1cc | $7.0 \times 10^{-10}$ | $9.0 \times 10^{-10}$ |
| HCN | 10cc | $5.5 \times 10^{-10}$ | $5.5 \times 10^{-10}$ |
| $C_2H_2$ | 10cc | $4.7 \times 10^{-10}$ | $4.7 \times 10^{-10}$ |
| Cigarette Smoke | 5 secs ② | $6.0 \times 10^{-10}$ | $8.5 \times 10^{-10}$ |
| Cigarette Smoke | 30 secs ② | $5.5 \times 10^{-10}$ | $10.5 \times 10^{-10}$ |
| Burning Cotton | - | $4.7 \times 10^{-10}$ | $6.0 \times 10^{-10}$ |

① Air saturated with vapor above liquid

② Smoldering cigarette held in front of fan for indicated length of time

Note: Relative humidity for all measurements was 50%

*Maximum deviation obtained after about 30 sec.

## TABLE IX

### POLYMER RESPONSES IN DRY AIR*

| CONTAMINANT | AMOUNT ADDED | POLYMER I | | POLYMER II | | POLYMER III | |
|---|---|---|---|---|---|---|---|
| | | $I_0$** | $I$ | $I_0$ | $I$ | $I_0$ | $I$ |
| Ammonia | 10 cc | 0.091 | 0.105 | 0.011 | 0.020 | 0.097 | 0.109 |
| Carbon Monoxide | 10 cc | 0.091 | 0.091 | 0.011 | 0.011 | 0.097 | 0.097 |
| Acetylene | 10 cc | 0.091 | 0.091 | 0.011 | 0.011 | 0.103 | 0.103 |
| Sulphur Dioxide | 10 cc | - | - | - | - | - | - |
| Nitrogen Oxides | 10 cc | - | - | - | - | - | - |
| Crotonaldehyde (Saturated Vapor) | 10 cc | 0.097 | 0.097 | 0.011 | 0.011 | 0.103 | 0.103 |
| Cotton Smoke | 100 mg ignites | 0.091 | 0.106 | 0.011 | 0.014 | 0.097 | 0.111 |
| Cigarette Smoke | 30 sec in front of blower | 0.094 | 0.106 | 0.011 | 0.022 | 0.103 | 0.140 |

* These data were obtained using the setup of Figures 70 and 71 with calcium sulfite in the air stream.

** $I$ = value shown x $10^{-10}$ amp

TABLE X

POLYMER RESPONSES AT 25% RELATIVE HUMIDITY

| CONTAMINANT | AMOUNT ADDED | POLYMER I | | POLYMER II | | POLYMER III | | POLYMER IV | | POLYMER V | | POLYMER VI | |
|---|---|---|---|---|---|---|---|---|---|---|---|---|---|
| | | $I_0$* | I | $I_0$ | I | $I_0$ | I | $I_0$ | I | $I_0$ | I | $I_0$ | I |
| Ammonia | 10 cc | 0.14 | 0.63 | 0.02 | 0.03 | 0.69 | 1.26 | 9.14 | 16.6 | 0.71 | 1.26 | 0.33 | 1.20 |
| Carbon Monoxide | 40 cc | 0.14 | 0.14 | 0.02 | 0.02 | 0.70 | 0.70 | 5.71 | 5.71 | 0.80 | 0.86 | 0.47 | 0.47 |
| Acetylene | 20 cc | 0.20 | 0.20 | 0.02 | 0.02 | 0.69 | 0.69 | 5.43 | 5.43 | 1.26 | 1.26 | 0.43 | 0.43 |
| Sulphur Dioxide | 10 cc | 0.15 | 2.21 | 0.03 | 0.42 | 0.57 | 71.4 | 3.14 | 4.29 | 0.49 | 0.60 | 0.66 | 1.99 |
| Nitrogen Oxides | 10 cc | 0.14 | 1.86 | 0.03 | 0.30 | 0.69 | 5.71 | 3.43 | 35.0 | 0.69 | 5.29 | 0.03 | 2.14 |
| Hydrogen Cyanide | 10 cc | 0.14 | 0.30 | 0.03 | 0.04 | 0.69 | 0.69 | 5.14 | 5.29 | 0.14 | 0.14 | 0.60 | 0.80 |
| Crotonaldehyde (Saturated Vapor) | 50 cc | 0.15 | 0.15 | 0.03 | 0.03 | 0.69 | 0.69 | 5.00 | 5.00 | 1.34 | 1.34 | 0.53 | 0.55 |
| Cotton Smoke | 100 mg Cotton | 0.16 | 0.20 | 0.02 | 0.06 | 0.71 | 1.83 | 4.86 | 5.14 | 0.80 | 0.80 | 0.41 | 0.50 |
| Cigarette Smoke | ? | 0.16 | 0.18 | 0.02 | 0.03 | 0.63 | 1.94 | 4.86 | 5.71 | 0.97 | 0.97 | 0.40 | 0.53 |

POLYMER I   = THIOPHENE IMIDAZOLE        POLYMER III  = FERROCENE IMIDAZOLE       POLYMER V   = PHTHALOCYANINE + IRON

POLYMER II  = THIOPHENE SCHIFF'S BASE    POLYMER IV   = PHTHALOCYANINE          POLYMER VI  = POLY (DIMETHYLAMINO PHENYLACETYLENE)

*I = value shown x $10^{-10}$ amp

TABLE XI

POLYMER RESPONSES AT 50% RELATIVE HUMIDITY

| CONTAMINANT | AMOUNT ADDED | POLYMER I | | POLYMER II | | POLYMER III | | POLYMER IV | | POLYMER V | | POLYMER VI | |
|---|---|---|---|---|---|---|---|---|---|---|---|---|---|
| | | $I_0$* | I | $I_0$ | I | $I_0$ | I | $I_0$ | I | $I_0$ | I | $I_0$ | I |
| Ammonia | 10 cc | 0.21 | 1.58 | 0.08 | 0.89 | 5.29 | 6.43 | 3.43 | 4.71 | 1.43 | 2.00 | 0.21 | 0.89 |
| Carbon Monoxide | 50 cc | 0.34 | 0.34 | 0.09 | 0.09 | 4.00 | 4.00 | 3.00 | 3.00 | 0.94 | 1.00 | 0.49 | 0.49 |
| Acetylene | 50 cc | 0.33 | 0.33 | 0.09 | 0.09 | 3.86 | 3.81 | 3.00 | 3.00 | 0.91 | 0.77 | 0.49 | 0.49 |
| Sulphur Dioxide | 10 cc | 0.31 | 3.43 | 0.19 | 85.7 | 1.86 | 85.7 | 4.14 | 4.57 | 0.71 | 0.91 | 0.49 | 7.14 |
| Nitrogen Oxides | 10 cc | 0.24 | 2.66 | 0.16 | 3.19 | 2.86 | 18.6 | 3.71 | 6.00 | 0.54 | 6.29 | 0.47 | 65.7 |
| Hydrogen Cyanide | 10 cc | 0.29 | 0.61 | 0.16 | 0.17 | 3.26 | 3.26 | 3.14 | 3.14 | 0.77 | 0.77 | 0.49 | 0.81 |
| Crotonaldehyde (Saturated Vapor) | 50 cc | 0.35 | 0.35 | 0.29 | 0.29 | 3.00 | 3.00 | 3.00 | 3.00 | 0.97 | 0.97 | 0.47 | 0.49 |
| Cotton Smoke | 100 mg Cotton | 0.21 | 0.26 | 0.08 | 0.15 | 3.71 | 10.3 | 3.00 | 3.14 | 0.74 | 0.74 | 0.47 | 0.54 |
| Cigarette Smoke | ? | 0.21 | 0.24 | 0.08 | 0.30 | 3.71 | 6.86 | 3.00 | 3.29 | 0.86 | 0.86 | 0.47 | 0.54 |

POLYMER I = THIOPHENE IMIDAZOLE          POLYMER III = FERROCENE IMIDAZOLE     POLYMER V = PHTHALOCYANINE + IRON

POLYMER II = THIOPHENE SCHIFF'S BASE     POLYMER IV = PHTHALOCYANINE          POLYMER VI = POLY (DIMETHYLAMINO PHENYLACETYLENE)

*I = value shown x $10^{-10}$ amp

TABLE XII

POLYMER RESPONSES AT 75% RELATIVE HUMIDITY

| CONTAMINANT | AMOUNT ADDED | POLYMER I | | POLYMER II | | POLYMER III | | POLYMER IV | | POLYMER V | | POLYMER VI | |
|---|---|---|---|---|---|---|---|---|---|---|---|---|---|
| | | $I_0$* | I | $I_0$ | I | $I_0$ | I | $I_0$ | I | $I_0$ | I | $I_0$ | I |
| Ammonia | 10 cc | 0.26 | 2.11 | 1.57 | 22.9 | 3.14 | 62.8 | 21.2 | 60.3 | 0.71 | 2.86 | 27.1 | 286 |
| Carbon Monoxide | 50 cc | 0.29 | 0.29 | 2.57 | 2.86 | 1.14 | 1.14 | 31.4 | 31.4 | 0.71 | 0.71 | 16.3 | 16.3 |
| Acetylene | 50 cc | 0.40 | 0.40 | 1.14 | 1.14 | 1.06 | 1.06 | 30.0 | 30.0 | 0.29 | 0.29 | 12.6 | 12.9 |
| Sulphur Dioxide | 10 cc | 0.35 | 71.4 | 0.86 | 71.4 | 0.49 | 85.7 | 34.2 | 62.9 | 1.86 | 42.9 | 3.29 | 54.3 |
| Nitrogen Oxides | 10 cc | 0.29 | 3.43 | 0.83 | 8.57 | 0.43 | 5.71 | 50.4 | 82.9 | 0.49 | 7.14 | 10.6 | 286 |
| Hydrogen Cyanide | 10 cc | 0.29 | 0.93 | 0.80 | 0.80 | 0.51 | 0.51 | 47.1 | 49.1 | 0.51 | 0.53 | 12.6 | 14.3 |
| Crotonaldehyde (Saturated Vapor) | 50 cc | 0.35 | 0.35 | 0.91 | 0.91 | 0.69 | 0.69 | 57.1 | 53.2 | 0.48 | 0.48 | 12.9 | 13.1 |
| Cotton Smoke | 100 mg Cotton | 0.23 | 0.25 | 0.66 | 0.67 | 0.69 | 1.20 | 29.0 | 29.0 | 0.37 | 0.48 | 8.86 | 9.14 |
| Cigarette Smoke | ? | 0.23 | 0.24 | 0.86 | 0.89 | 0.97 | 1.72 | 29.0 | 30.0 | 0.37 | 0.40 | 10.9 | 11.4 |

POLYMER I = THIOPHENE IMIDAZOLE    POLYMER III = FERROCENE IMIDAZOLE    POLYMER V = PHTHALOCYANINE + IRON

POLYMER II = THIOPHENE SCHIFF'S BASE    POLYMER IV = PHTHALOCYANINE    POLYMER VI = POLY (DIMETHYLAMINO PHENYLACETYLENE)

*I = value shown $\times$ $10^{-10}$ amp

## TABLE XIII

### POLYMER RESPONSES AT 100% RELATIVE HUMIDITY

| CONTAMINANT | AMOUNT ADDED | POLYMER I | | POLYMER II | | POLYMER III | | POLYMER IV | | POLYMER V | | POLYMER VI | |
|---|---|---|---|---|---|---|---|---|---|---|---|---|---|
| | | $I_0$* | I | $I_0$ | I | $I_0$ | I | $I_0$ | I | $I_0$ | I | $I_0$ | I |
| Ammonia | 10 cc | 1.00 | 27.5 | 3.86 | 137 | 8.29 | 85.7 | 514 | 3140 | 1.00 | 8.29 | (1)- | - |
| Carbon Monoxide | 50 cc | 1.14 | 1.14 | 5.14 | 5.29 | 6.43 | 6.43 | 743 | 743 | 1.00 | 1.00 | - | - |
| Acetylene | 50 cc | 1.14 | 1.14 | 4.86 | 4.86 | 7.71 | 7.71 | 486 | 486 | 1.91 | 1.83 | - | - |
| Sulphur Dioxide | 10 cc | 2.57 | 85.7 | 8.00 | 857 | 9.14 | 114 | 400 | 943 | 2.71 | 18.6 | - | - |
| Nitrogen Oxides | 10 cc | 2.00 | 17.1 | 5.00 | 57.1 | 5.71 | 9.71 | 443 | 766 | 1.43 | 24.9 | - | - |
| Hydrogen Cyanide | 10 cc | 2.14 | 4.43 | 4.86 | 4.86 | 9.71 | 9.71 | 471 | 471 | 2.43 | 2.43 | - | - |
| Crotonaldehyde (Saturated Vapor) | 50 cc | 1.71 | 1.71 | 5.14 | 5.29 | 6.86 | 6.86 | 500 | 486 | 2.14 | 2.14 | - | - |
| Cotton Smoke | 100 mg Cotton | 1.14 | 1.57 | 5.43 | 6.86 | 7.57 | 9.29 | 429 | 436 | 1.86 | 2.14 | - | - |
| Cigarette Smoke | ? | 1.00 | 1.71 | 4.00 | 4.43 | 7.14 | 8.57 | 428 | 457 | 1.71 | 2.00 | - | - |

POLYMER I    = THIOPHENE IMIDAZOLE      POLYMER III = FERROCENE IMIDAZOLE      POLYMER V    = PHTHALOCYANINE + IRON

POLYMER II   = THIOPHENE SCHIFF'S BASE     POLYMER IV   = PHTHALOCYANINE        POLYMER VI   = POLY (DIMETHYLAMINO PHENYLACETYLENE)

(1) Sensor too conductive at this humidity. Circuits become saturated.

*I = value shown x $10^{-10}$ amp

## TABLE XIV
### MINIMUM QUANTITY OF GAS REQUIRED TO CAUSE OBSERVABLE RESPONSE

| CONTAMINANT | RELATIVE HUMIDITY | | | | | | | | | | | | | | | | | | | | | | | |
|---|---|---|---|---|---|---|---|---|---|---|---|---|---|---|---|---|---|---|---|---|---|---|---|---|
| | POLYMER I | | | | POLYMER II | | | | POLYMER III | | | | POLYMER IV | | | | POLYMER V | | | | POLYMER VI | | | |
| | 25 | 50 | 75 | 100 | 25 | 50 | 75 | 100 | 25 | 50 | 75 | 100 | 25 | 50 | 75 | 100 | 25 | 50 | 75 | 100 | 25 | 50 | 75 | 100 |
| Ammonia | 10 µL | 10 µL | 10 µL | 10 µL | 10 cc | 1 cc | 10 µL | 10 µL | 0.1 cc | 0.1 cc | 10 µL | 10 µL | 1 cc | 1 cc | 1 cc | 10 µL | 1 cc | 1 cc | 0.1 cc | 0.1 cc | 1 cc | 0.1 cc | 10 µL | - |
| Carbon Monoxide | * | * | * | * | * | * | 10 cc | 10 cc | * | * | * | * | * | * | * | * | 10 cc | 10 cc | * | * | * | * | * | - |
| Acetylene | * | * | * | * | * | * | * | * | * | * | * | * | * | * | * | * | * | * | * | * | * | * | 10 cc | - |
| Sulfur Dioxide | 10 µL | 0.1 cc | 10 µL | 10 µL | 10 µL | 10 µL | 10 µL | 10 µL | 10 µL | 10 µL | 10 µL | 10 µL | 1 cc | 1 cc | 1 cc | 0.1 cc | 10 cc | 10 cc | 1 cc | 0.1 cc | 1 cc | 0.1 cc | 10 µL | - |
| Nitrogen Oxides | 5 µL | 10 µL | 10 µL | 10 µL | 10 µL | 10 µL | 0.1 cc | 10 µL | 10 µL | 0.1 cc | 0.1 cc | 0.1 cc | 10 µL | 0.1 cc | 0.1 cc | 0.1 cc | 0.1 cc | 0.1 cc | 1 cc | 0.1 cc | 0.1 cc | 0.1 cc | 10 µL | - |
| Hydrogen Cyanide | 0.1 cc | 0.1 cc | 0.1 cc | 0.1 cc | * | * | * | * | * | * | * | * | 10 cc | * | 10 cc | * | * | * | 10 cc | * | 10 cc | 1 cc | 1 cc | - |
| Crotonaldehyde (Saturated Vapor) | 10 cc | 10 cc | * | * | * | 10 cc | * | 10 cc | * | * | * | * | * | * | 10 cc | * | * | * | * | * | 10 cc | 10 cc | 10 cc | - |

* No response up to 100 cc
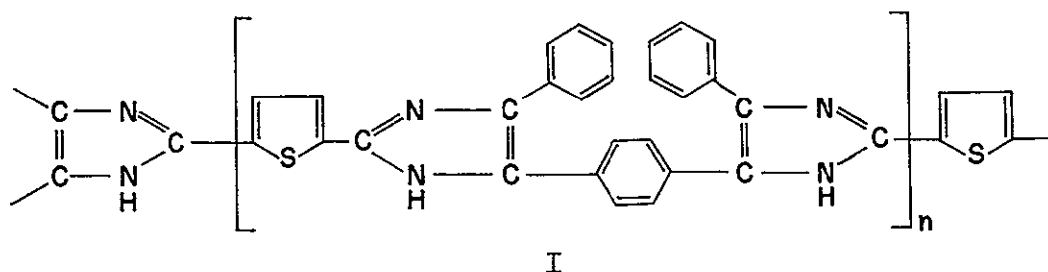
FIGURE 1. POLY(IMIDAZOLE) FROM THIOPHENE-2,5-DIALDEHYDE AND
1,4-BIS(PHENYLGLYOXYLOYL)BENZENE (I)
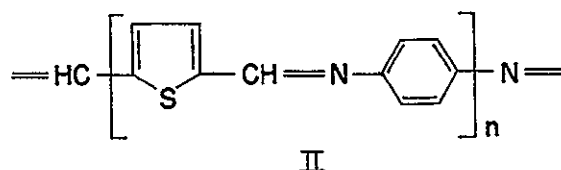


FIGURE 2. POLY(SCHIFF'S BASE) FROM THIOPHENE-2,5-DIALDEHYDE AND
1,4-PHENYLENEDIAMINE (II)
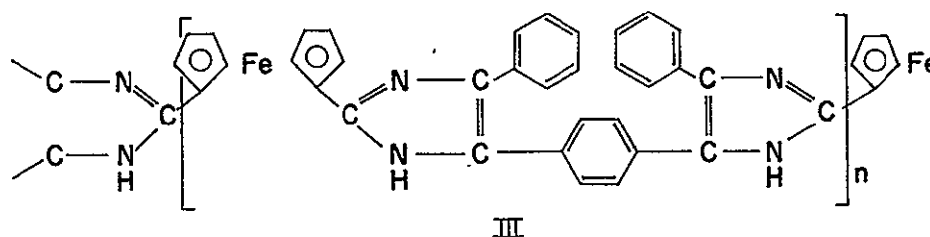


FIGURE 3. POLY(IMIDAZOLE) FROM FERROCENE-1,1'-DIALDEHYDE (III)
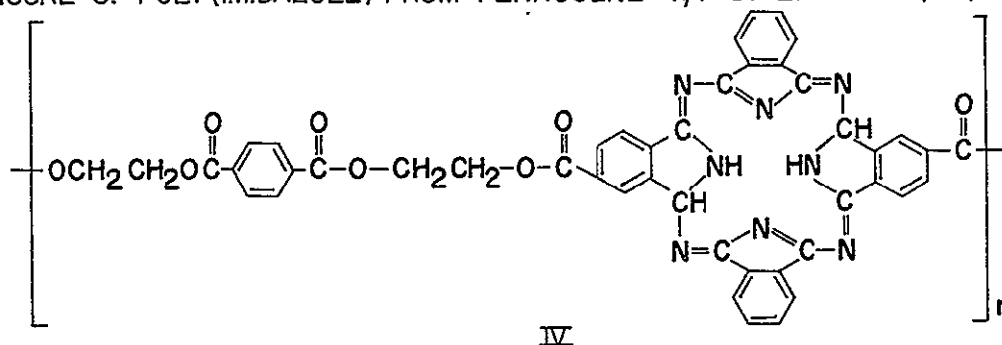


FIGURE 4. POLYESTER COPOLYMER WITH METAL-FREE PHTHALOCYANINE (IV)
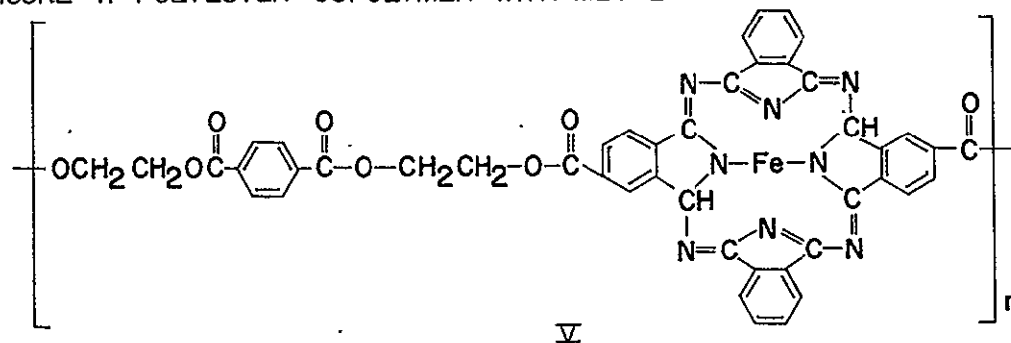


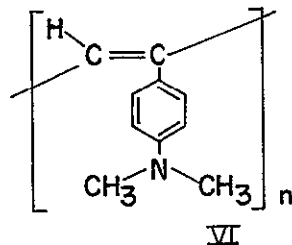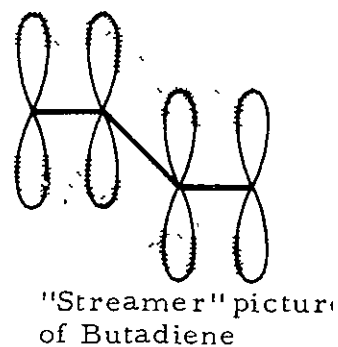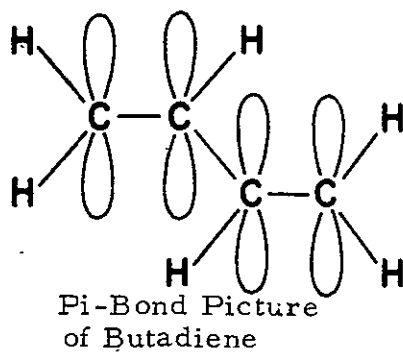FIGURE 5. POLYESTER COPOLYMER WITH IRON PHTHALOCYANINE (V)



FIGURE 6. POLY(p-DIMETHYLAMINOPHENYLACETYLENE)(VI)

63

Classical Formula
of Butadiene

Pi-Bond Picture
of Butadiene

"Streamer" picture
of Butadiene
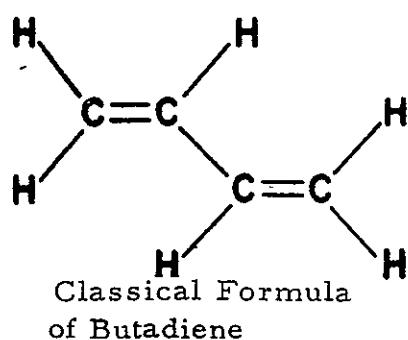
*CO341*

FIGURE 7.  BONDS IN BUTADIENE SHOWING ELECTRON CLOUD



(a)

(b)
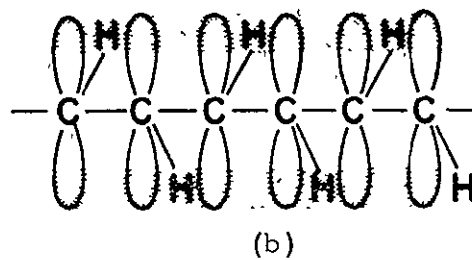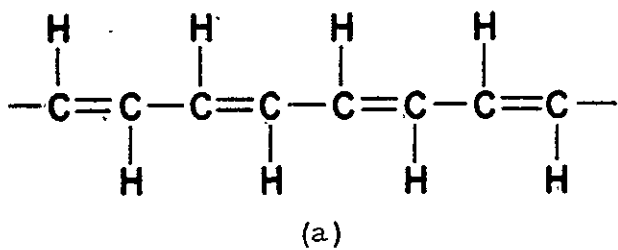
*CO342*

FIGURE 8.  (a)  STRUCTURAL CLASSICAL FORMULA OF A POLYACETYLENE
           (b)  "STREAMER" PICTURE SHOWING SMEARING OUT OF
                ELECTRON CLOUD
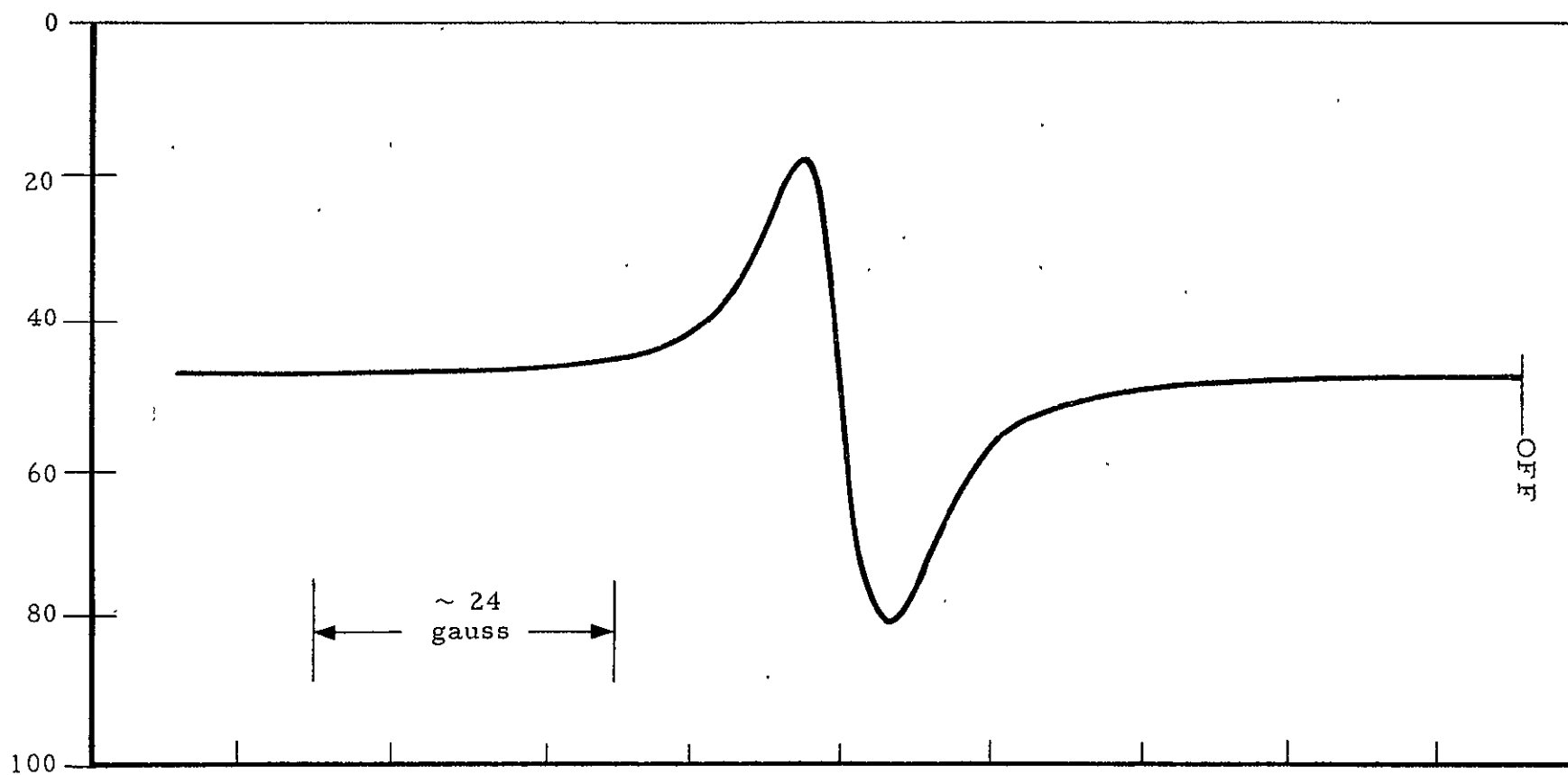
FIGURE 9. EPR SPECTRUM OF POLYPHENYLACETYLENE

FIGURE 10. EPR SPECTRUM OF POLY-4-NITROPHENYLACETYLENE

Si(OEt)₄ → 

n – BuLi →

CHO → thiophene-CHO → $C(OEt)_2$ (H)

DMF ←  Li—[thiophene]—$C(OEt)_2$ (H)

OC(H)—[thiophene]—$C(OEt)_2$ (H)

HCL
(EtOH)

OHC—[thiophene]—CHO

THIOPHENE –2,5– DIALDEHYDE (IA)

—CH₂Cl + Mg  →  —CH₂ MgCl

OCH—[benzene]—CHO

CrO₃
Acetic Acid
(cold)

—CH₂CHOH—[benzene]—CHOHCH₂—

—CH₂CO—[benzene]—COCH₂—

SeO₂
(refluxing acetic acid)

—COCO—[benzene]—COCO—

1, 4 – BIS(PHENYLGLYOXYLOYL)BENZENE (IB)

IA + IB + 2NH₃ —→

POLYMER I

FIGURE 11. REACTION SEQUENCE FOR PREPARATION OF POLY(IMIDAZOLE) STARTING WITH THIOPHENE –2 ALDEHYDE
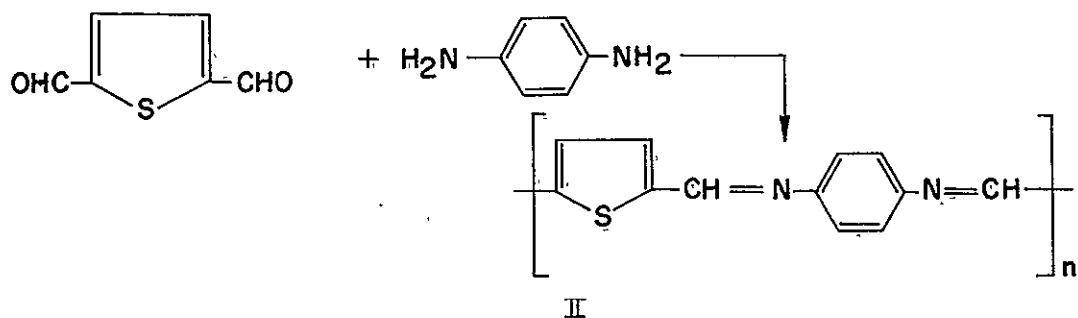
FIGURE 12. REACTION SEQUENCE FOR PREPARATION OF POLY(SCHIFF'S BASE)(II) FROM THIOPHENE-2,5-DIALDEHYDE



Ferrocene-1,1'-dialdehyde IIIA

IIIA + IB (See Figure 11) + 2 NH₃ ⟶
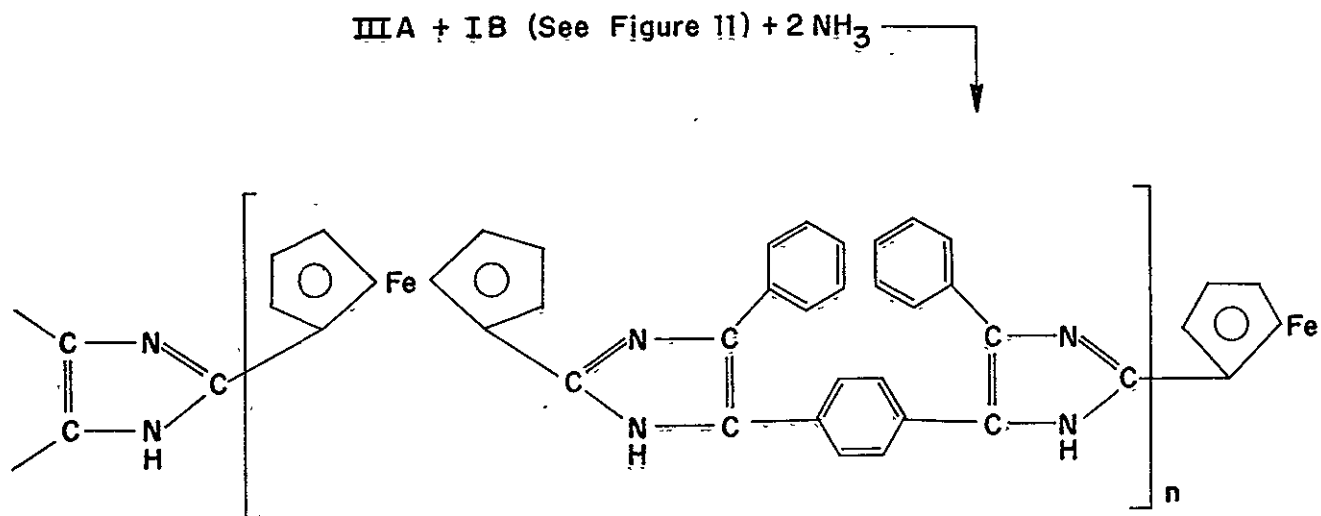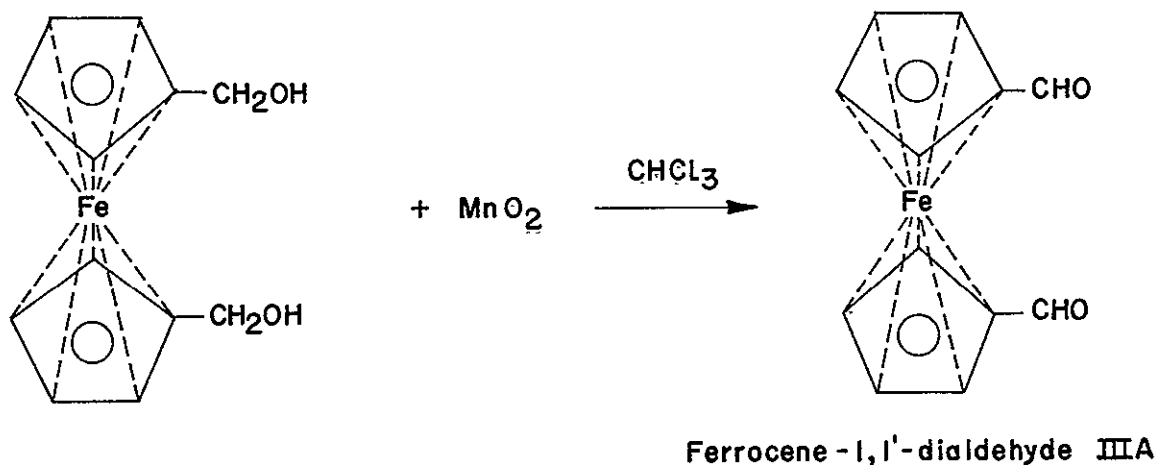


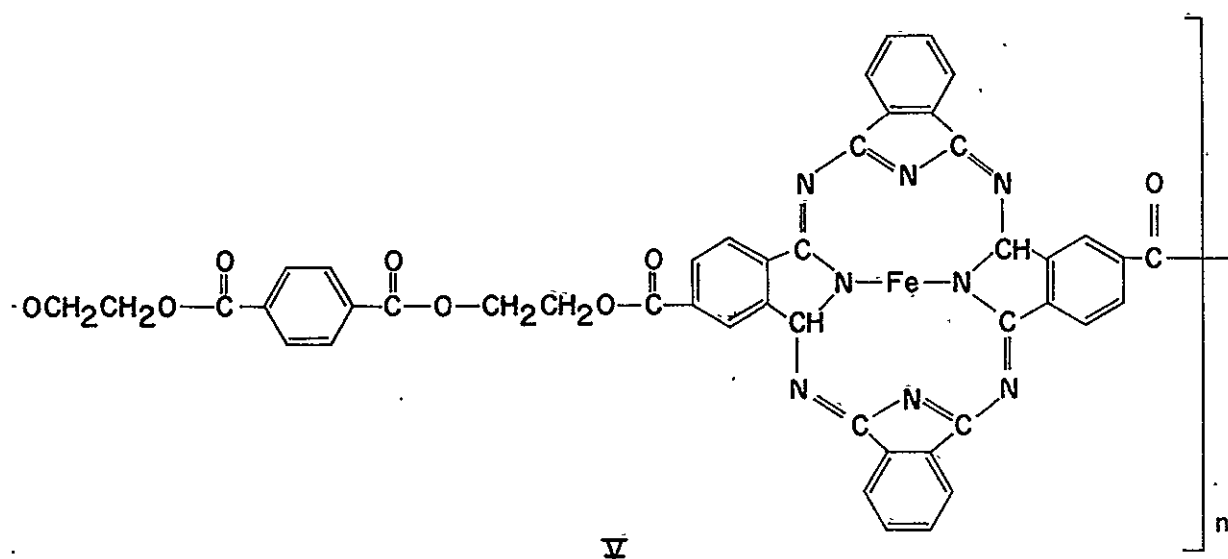FIGURE 13. REACTION SEQUENCE FOR PREPARATION OF POLY(IMIDAZOLE) FROM FERROCENE-1,1'-DIALDEHYDE
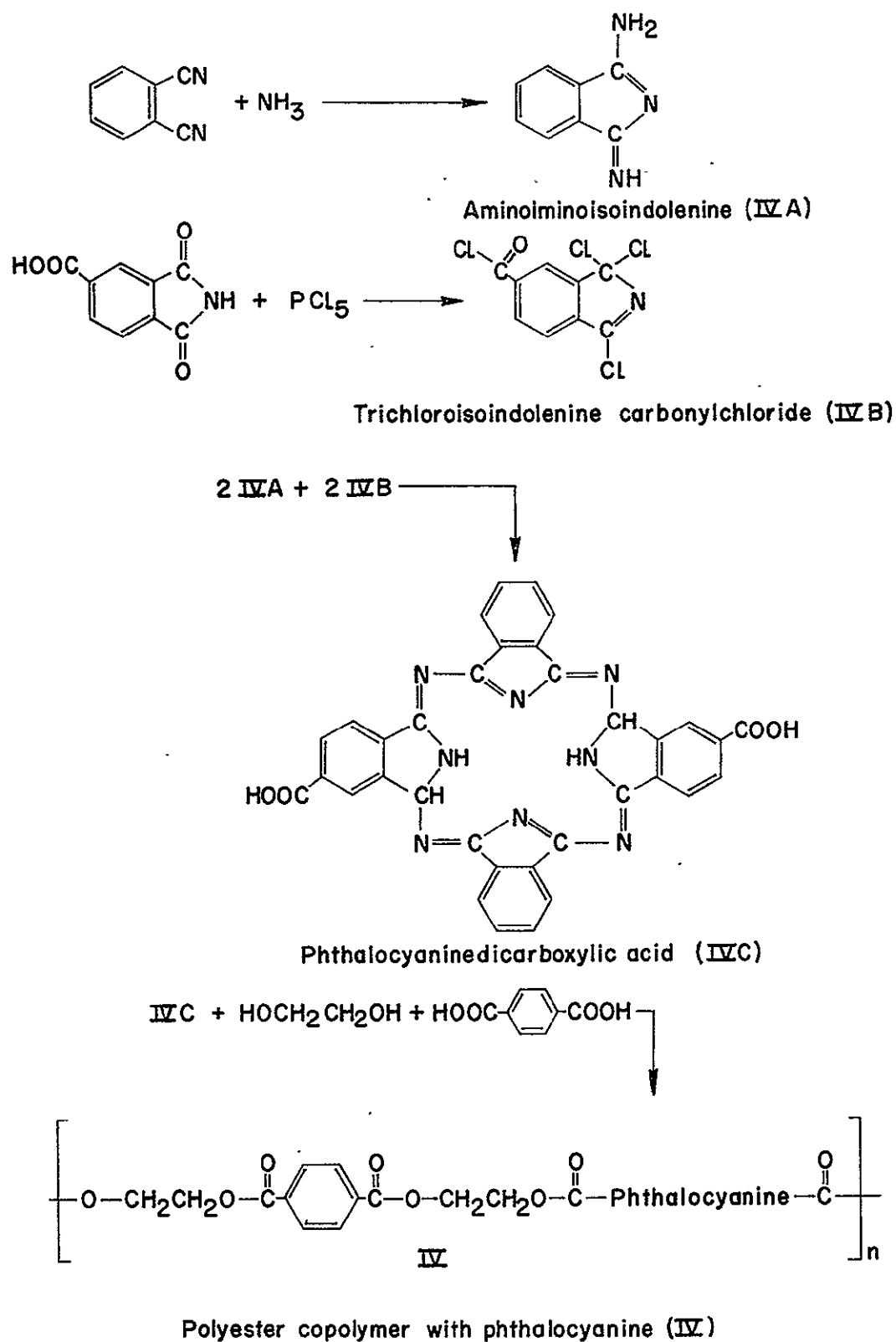
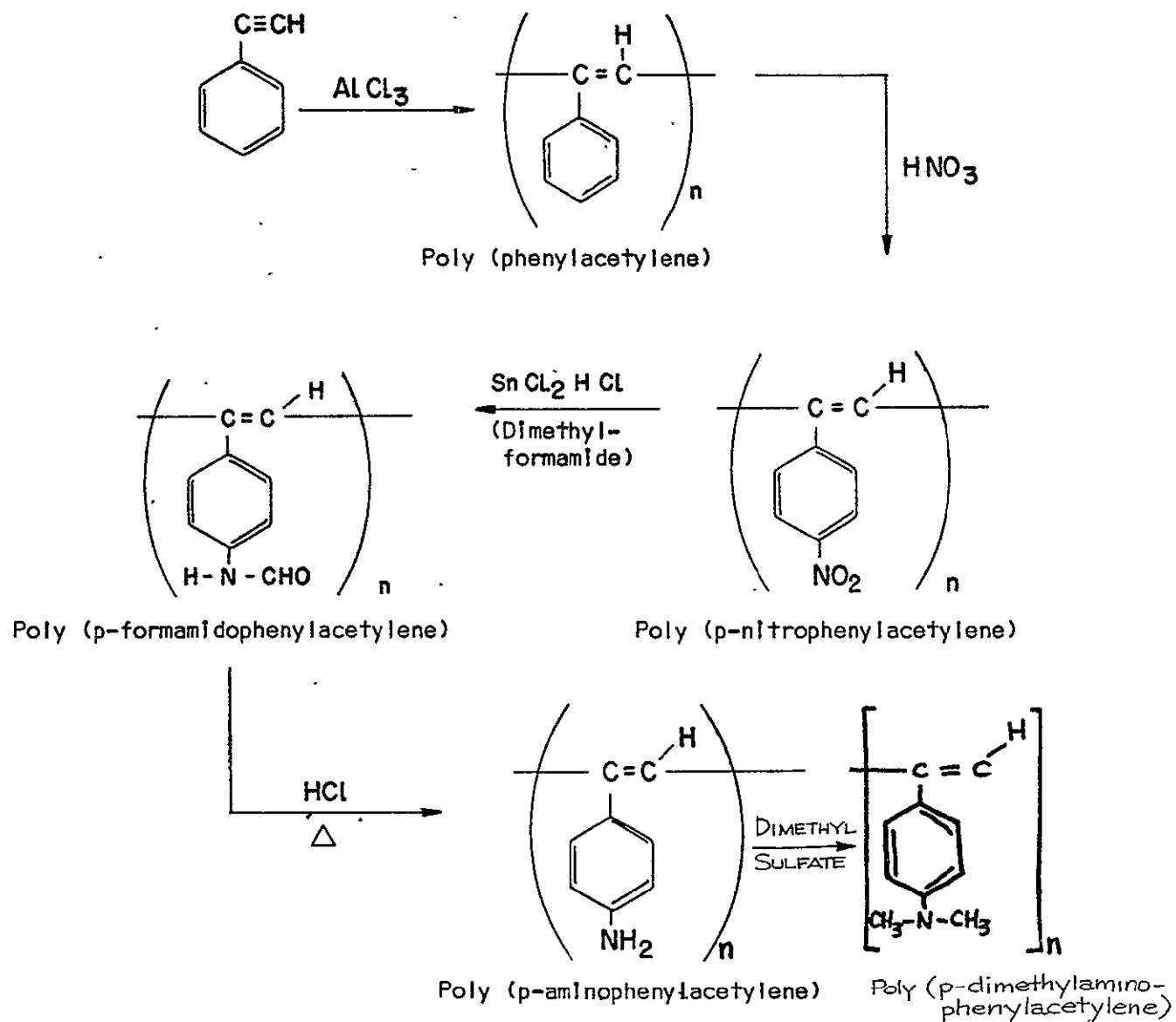FIGURE 14. PREPARATIVE SEQUENCE TO PHTHALOCYANINE (METAL-FREE)
POLYESTER COPOLYMER (IV)

FIGURE 15. REACTION SEQUENCE FOR PREPARATION OF POLYESTER COPOLYMER WITH IRON PHTHALOCYANINE (V)
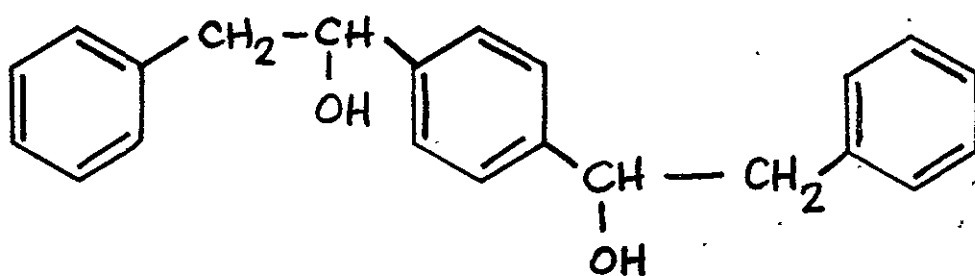
70

C≡CH

$AlCl_3$ →

Poly (phenylacetylene)

$HNO_3$

Poly (p-formamidophenylacetylene)

$SnCl_2$ H Cl ← (Dimethyl-formamide)

Poly (p-nitrophenylacetylene)

$NO_2$

HCl
△

$NH_2$

Poly (p-aminophenylacetylene)

DIMETHYL SULFATE →

$CH_3-N-CH_3$

Poly (p-dimethylamino-phenylacetylene)

FIGURE 16. REACTION SEQUENCE USED IN PREPARATION OF SOME POLY(PHENYLACETYLENES)

71

FIGURE 17. STRUCTURE OF $\alpha,\alpha'$ (PARA-PHENYLENE) BIS ($\beta$-PHENYLETHANOL)
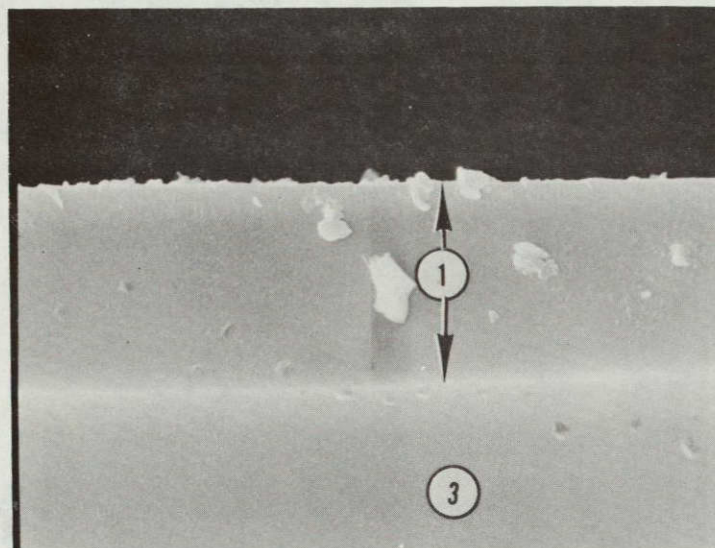
FIGURE 18.  EDGE VIEW (90°) OF POLY(IMIDAZOLE)/THIOPHENE (I) AT 2000X
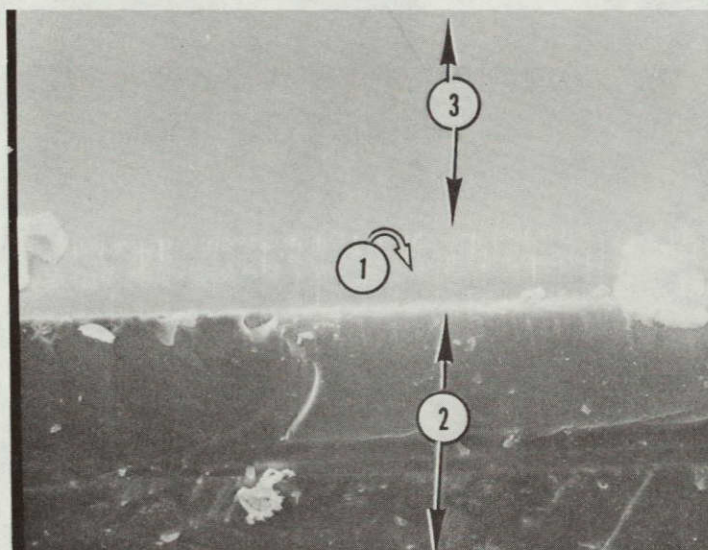


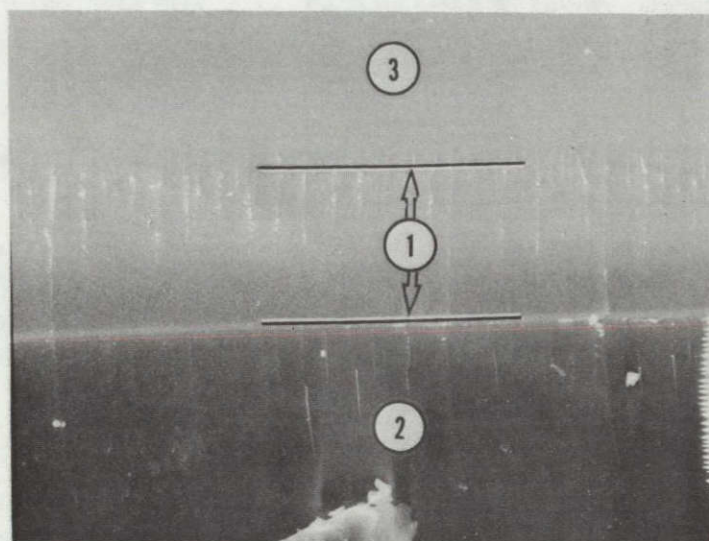FIGURE 19.  45° VIEW OF POLYMER I AT 400X
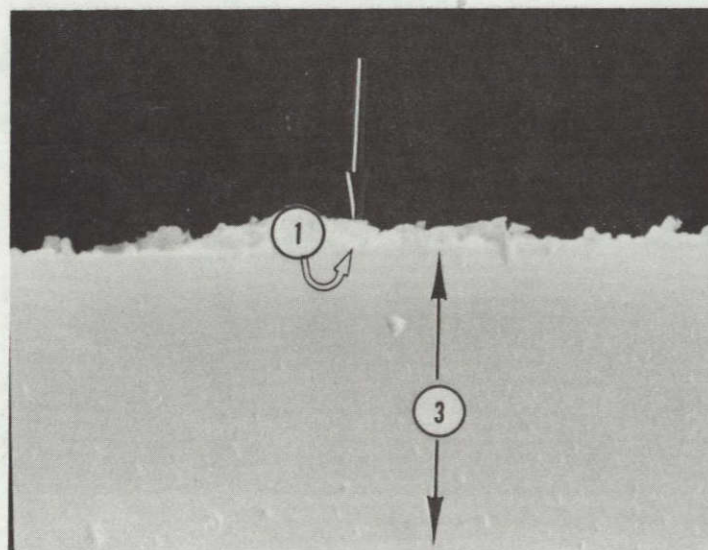
FIGURE 20.    45° VIEW OF POLYMER I AT 800X



FIGURE 21.    EDGE VIEW (90°) OF POLY(SCHIFF'S BASE)/THIOPHENE (II)
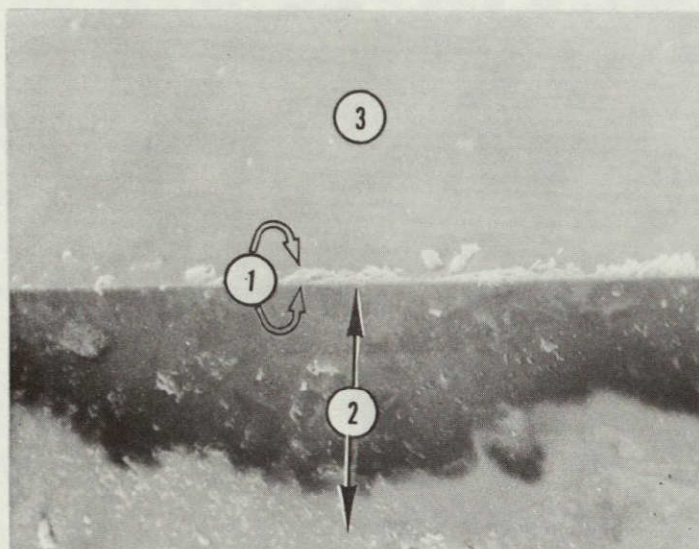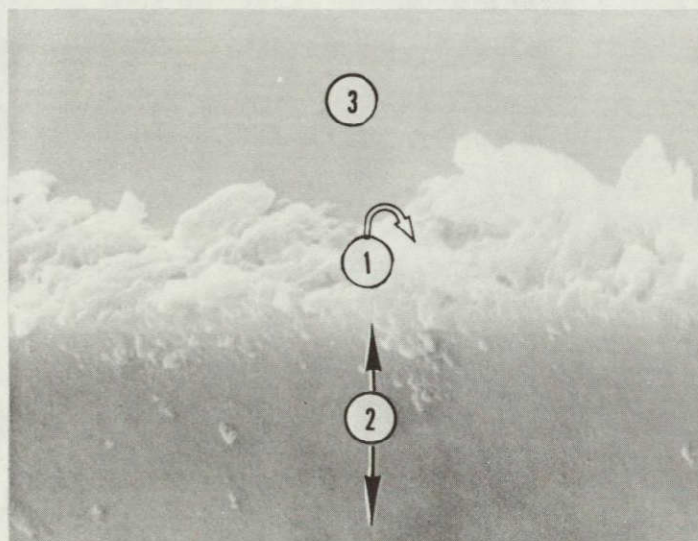AT 4000X

FIGURE 22. 45° VIEW OF POLYMER II AT 400X



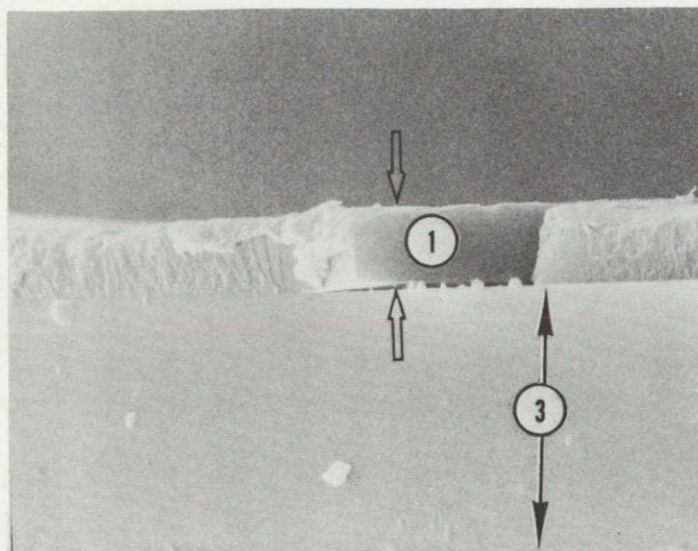FIGURE 23. 45° VIEW OF POLYMER II AT 4000X

FIGURE 24. EDGE VIEW (90°) OF POLY(IMIDAZOLE)/FERROCENE (III) AT 4000X
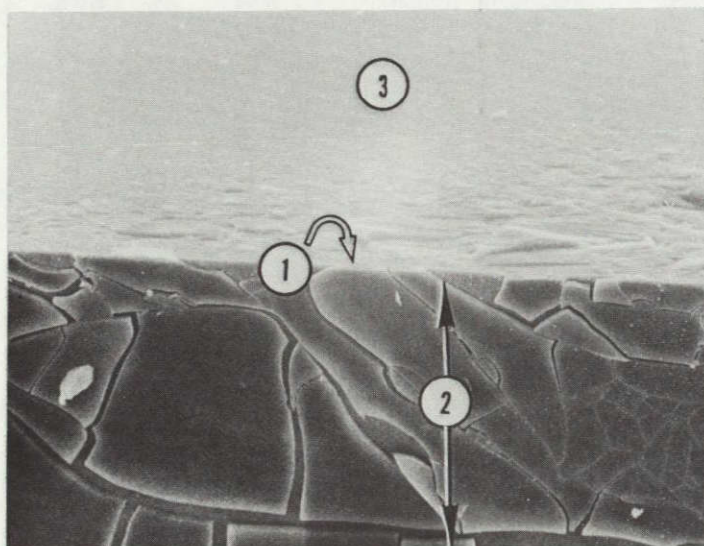


FIGURE 25. 45° VIEW OF POLYMER III AT 400X

FIGURE 26.   45° VIEW OF POLYMER III AT 4000X
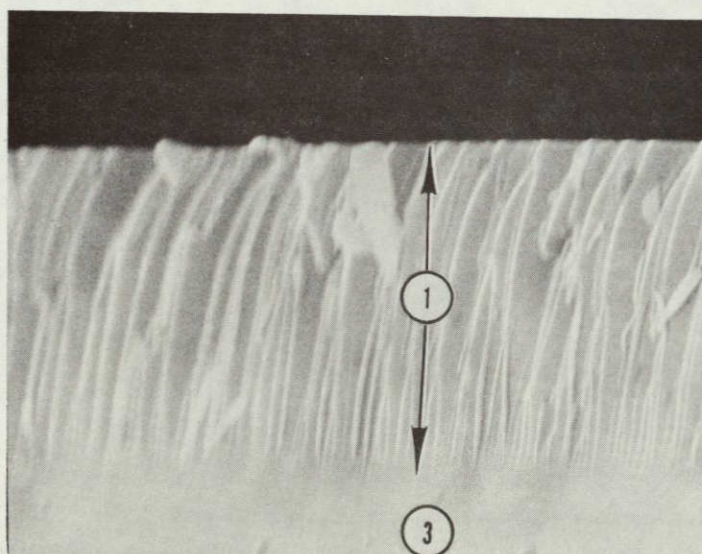


FIGURE 27.   EDGE VIEW (90°) OF POLYESTER/PHTHALOCYANINE (IV) AT 4000X
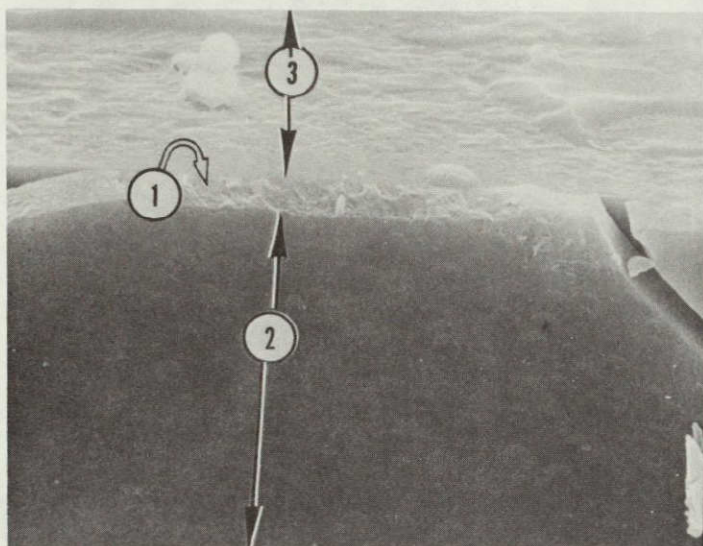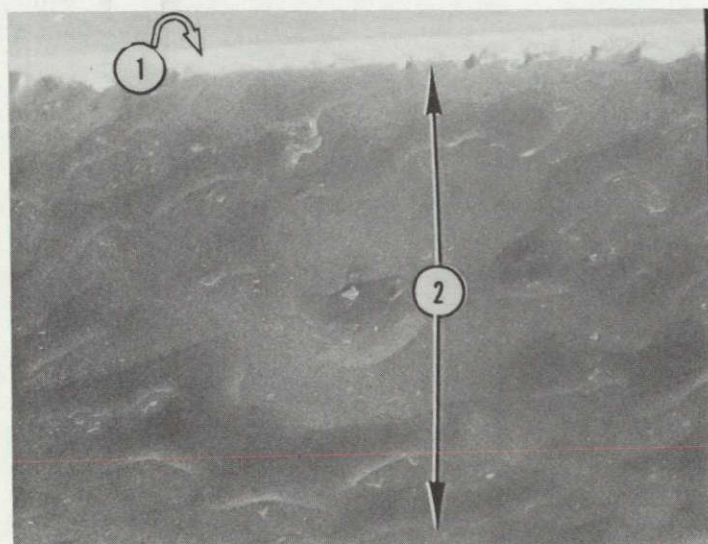
FIGURE 28. 45° VIEW OF POLYMER IV AT 400X
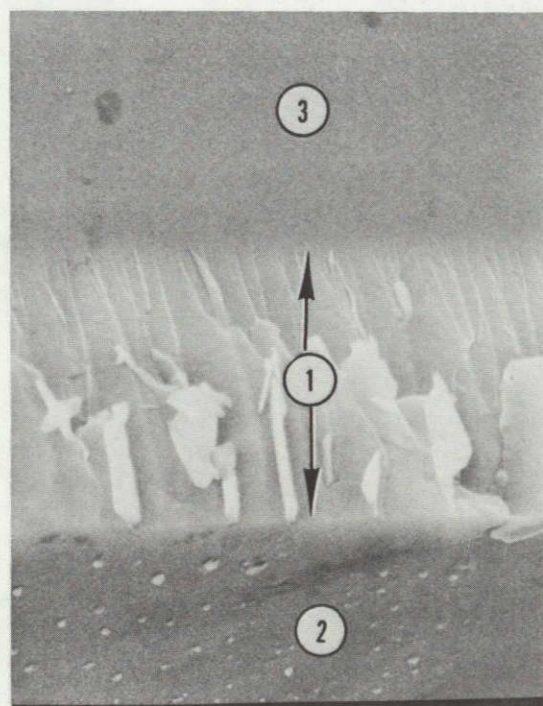


FIGURE 29. 45° VIEW OF POLYMER IV AT 4000X
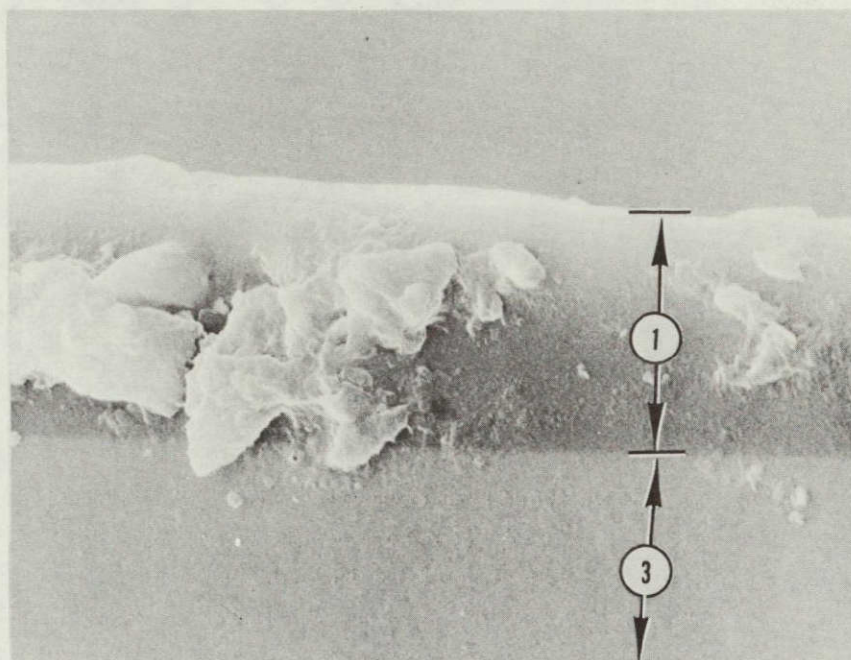
FIGURE 30.   EDGE VIEW (90°) OF POLYESTER/PHTHALOCYANINE (IRON) (Ⅴ) AT 4500X
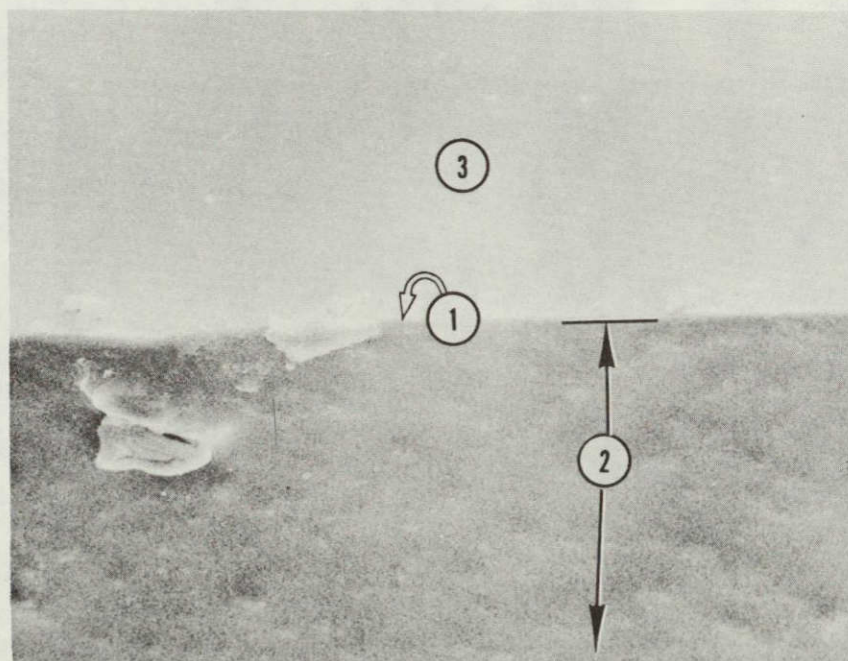
FIGURE 31.   45° VIEW OF POLYMER Ⅴ AT 450X
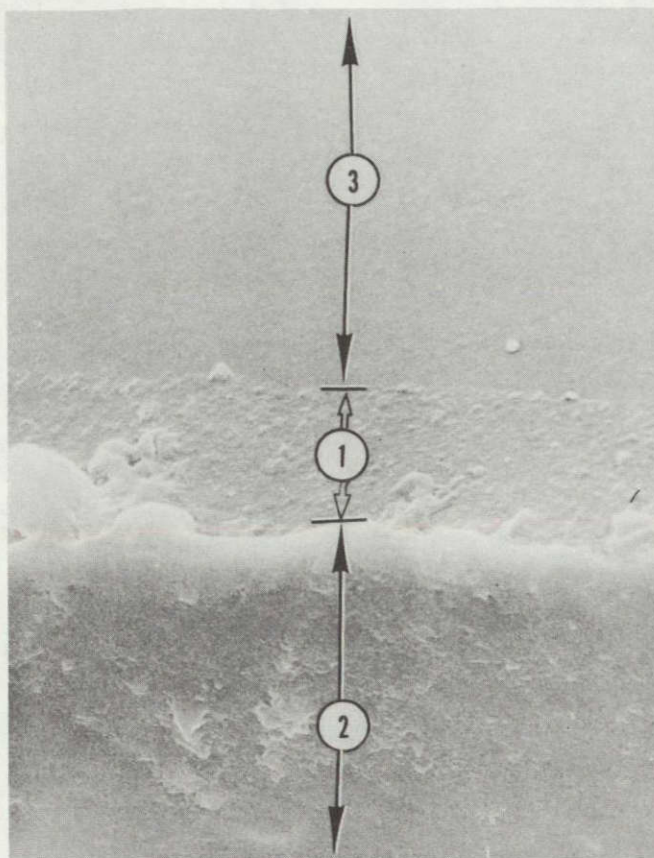
FIGURE 32. 45° VIEW OF POLYMER $\underline{V}$ AT 4500X
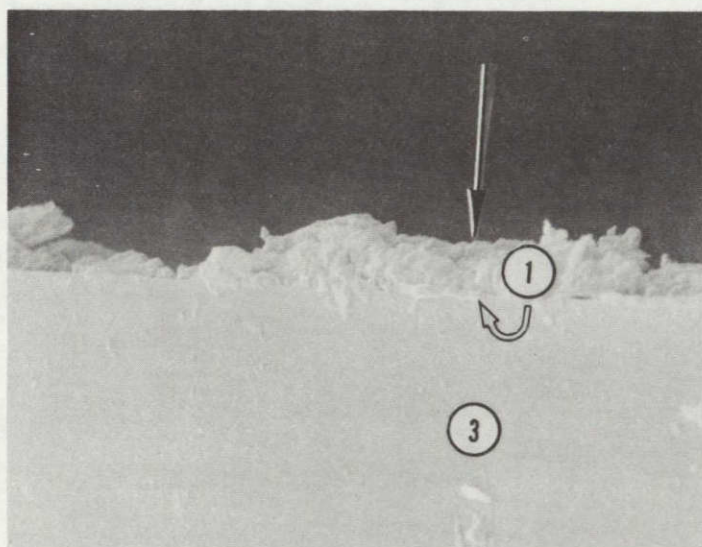


FIGURE 33. EDGE VIEW (90°) OF POLY(P-DIMETHYLAMINOPHENYLACETYLENE) ($\underline{VI}$) AT 4000X
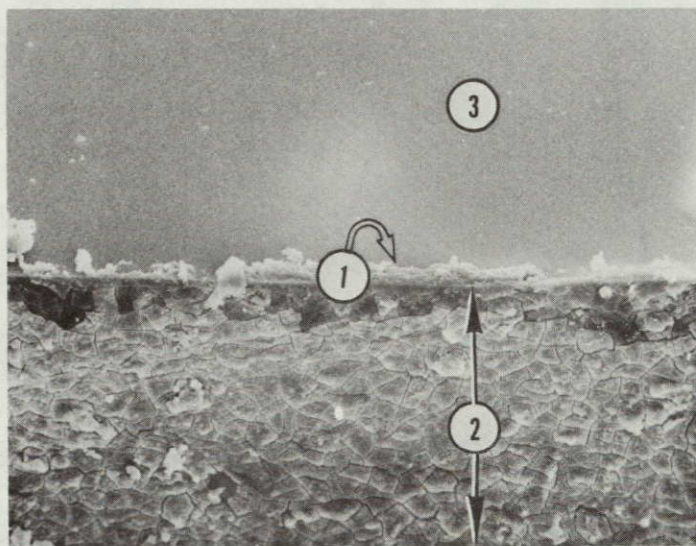
FIGURE 34.  45° VIEW OF POLYMER $\overline{VI}$ AT 400X
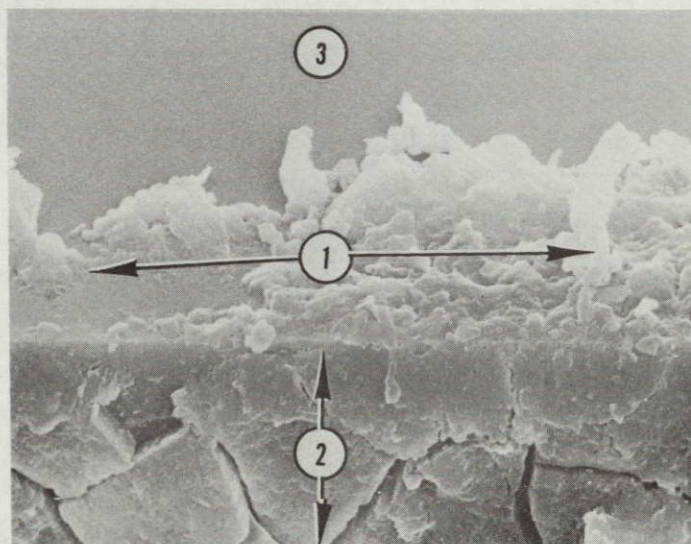


FIGURE 35.  45° VIEW OF POLYMER $\overline{VI}$ AT 4000X

Molecular Size (Angstroms)
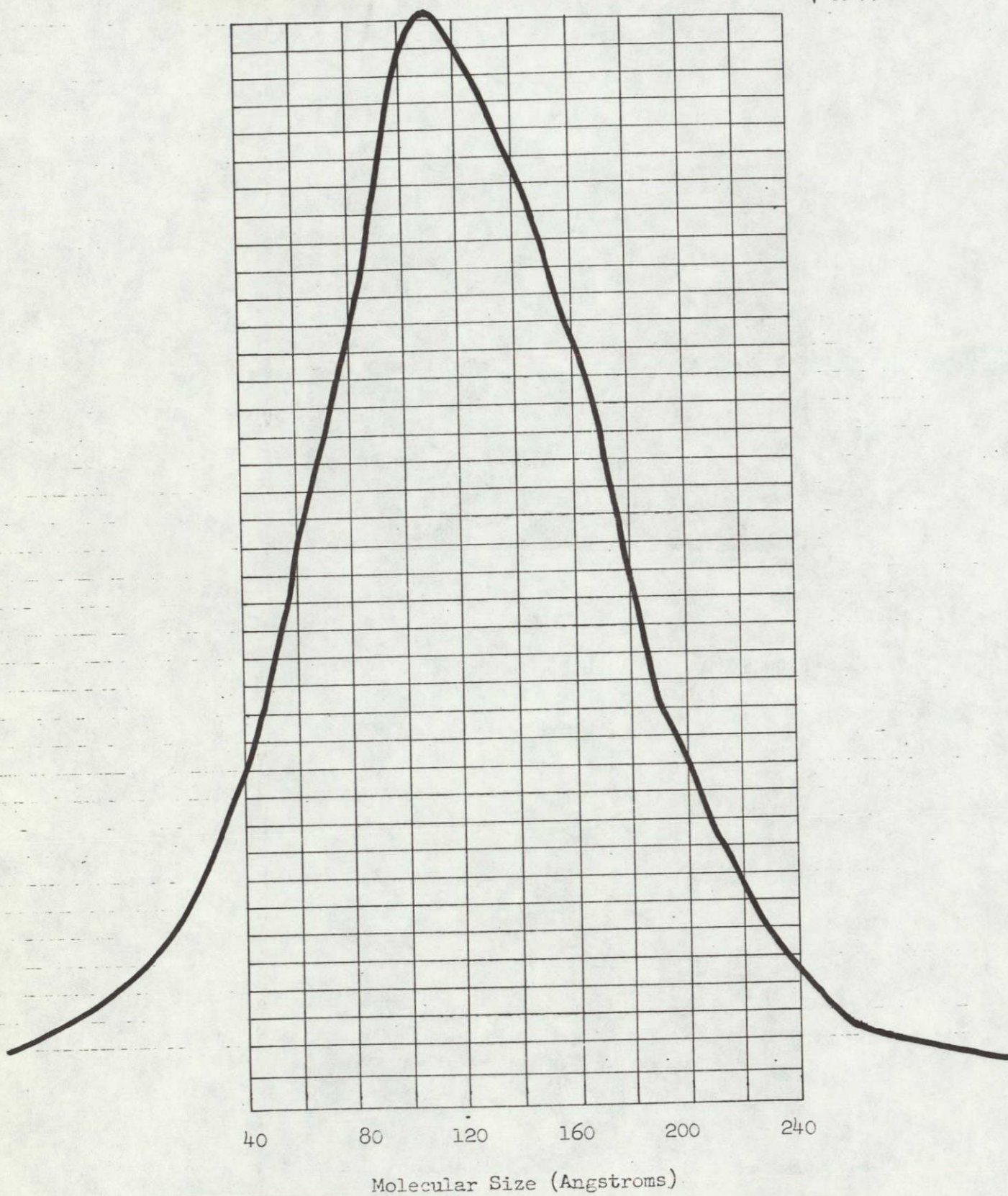
FIGURE 36. MOLECULAR SIZE DISTRIBUTION OF POLY(IMIDAZOLE)/THIOPHENE (I)

Molecular Size (Angstroms)
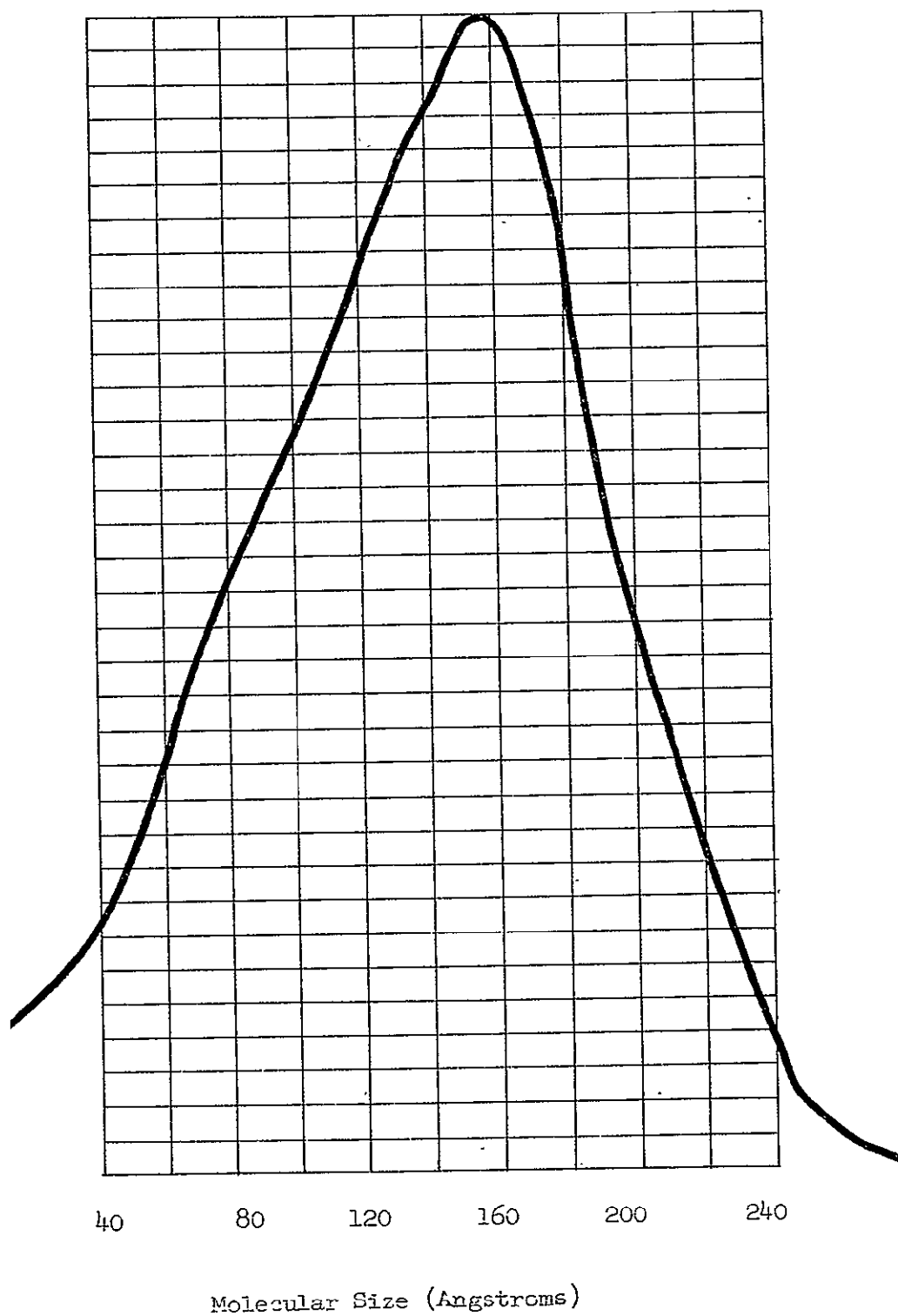
FIGURE 37. MOLECULAR SIZE DISTRIBUTION OF POLYESTER/PHTHALOCYANINE (IV)

Molecular Size (Angstroms)
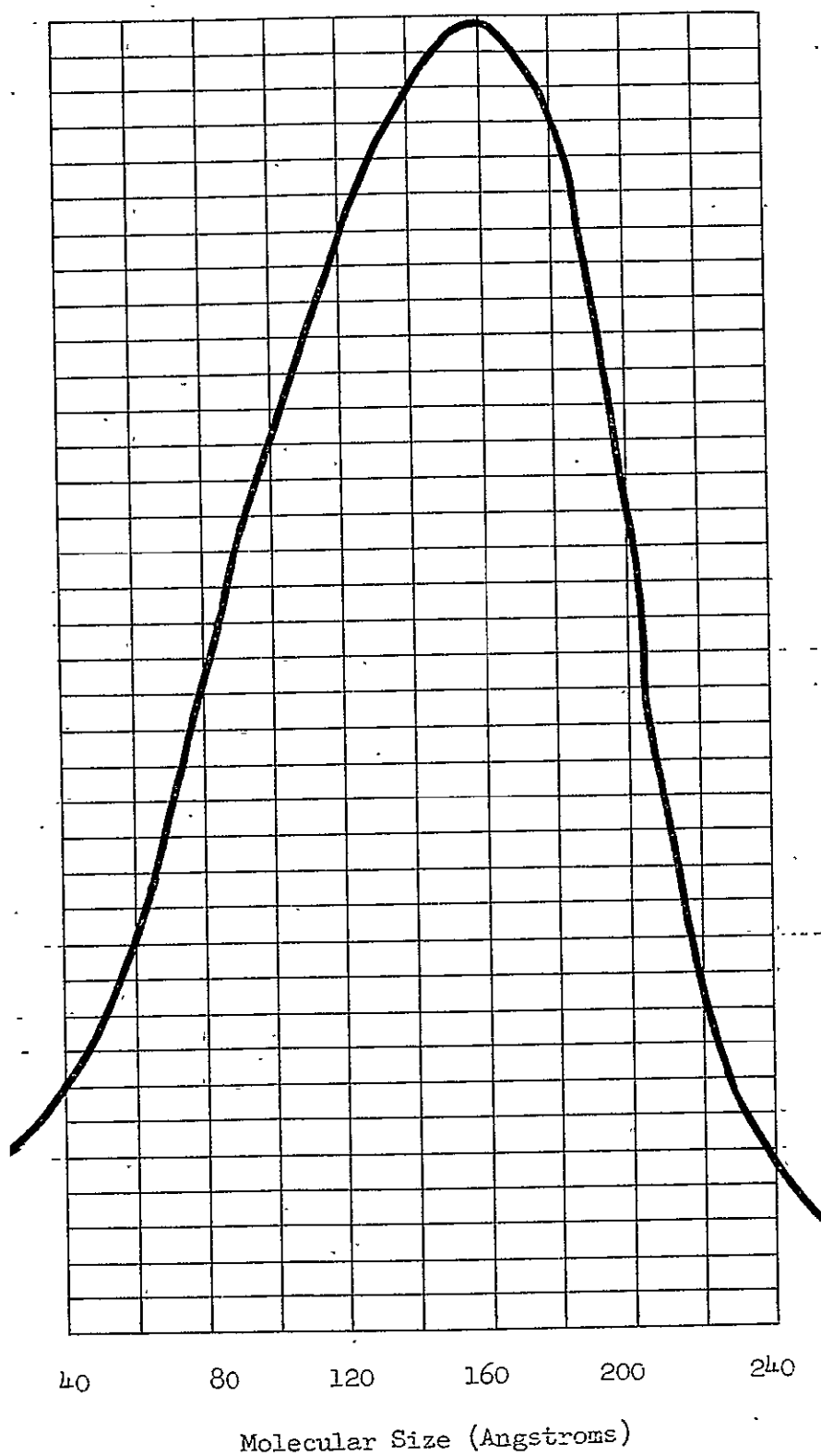
FIGURE 38. MOLECULAR SIZE DISTRIBUTION OF
POLYESTER/PHTHALOCYANINE (IRON) (V)
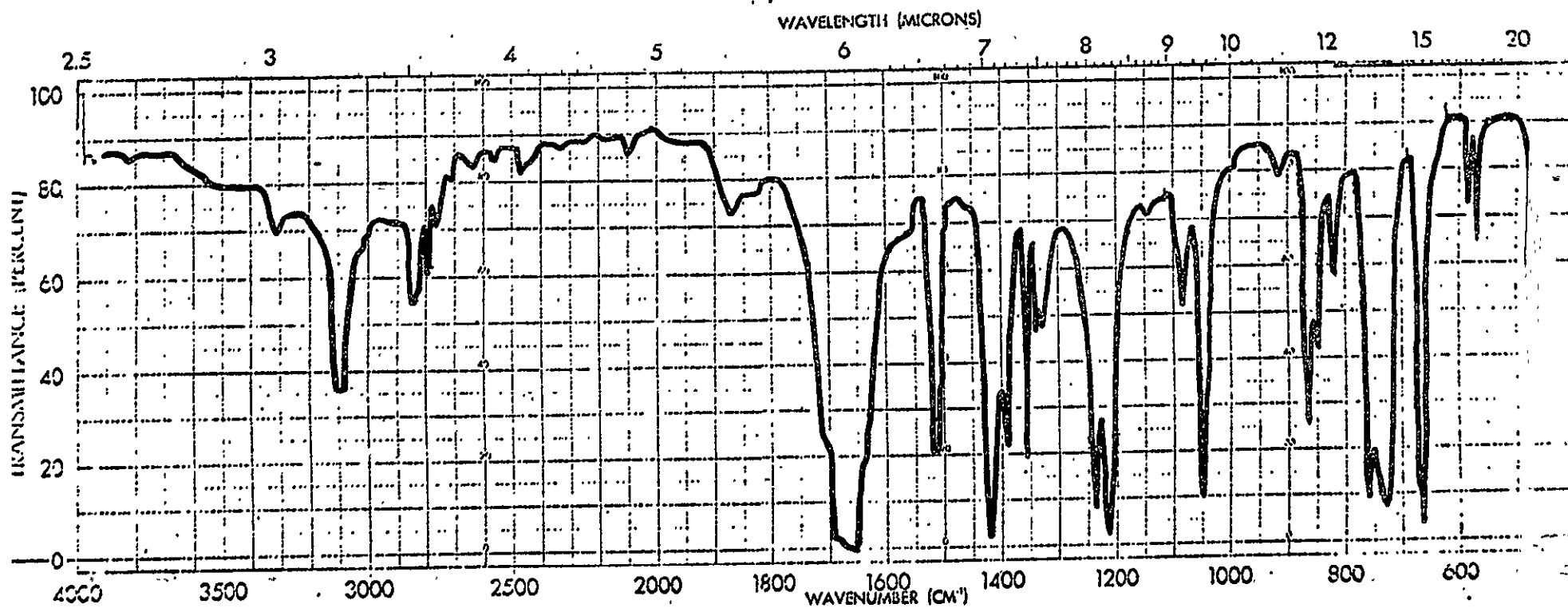
FIGURE 39. INFRARED SPECTRUM OF THIOPHENE-2-CARBOXALDEHYDE
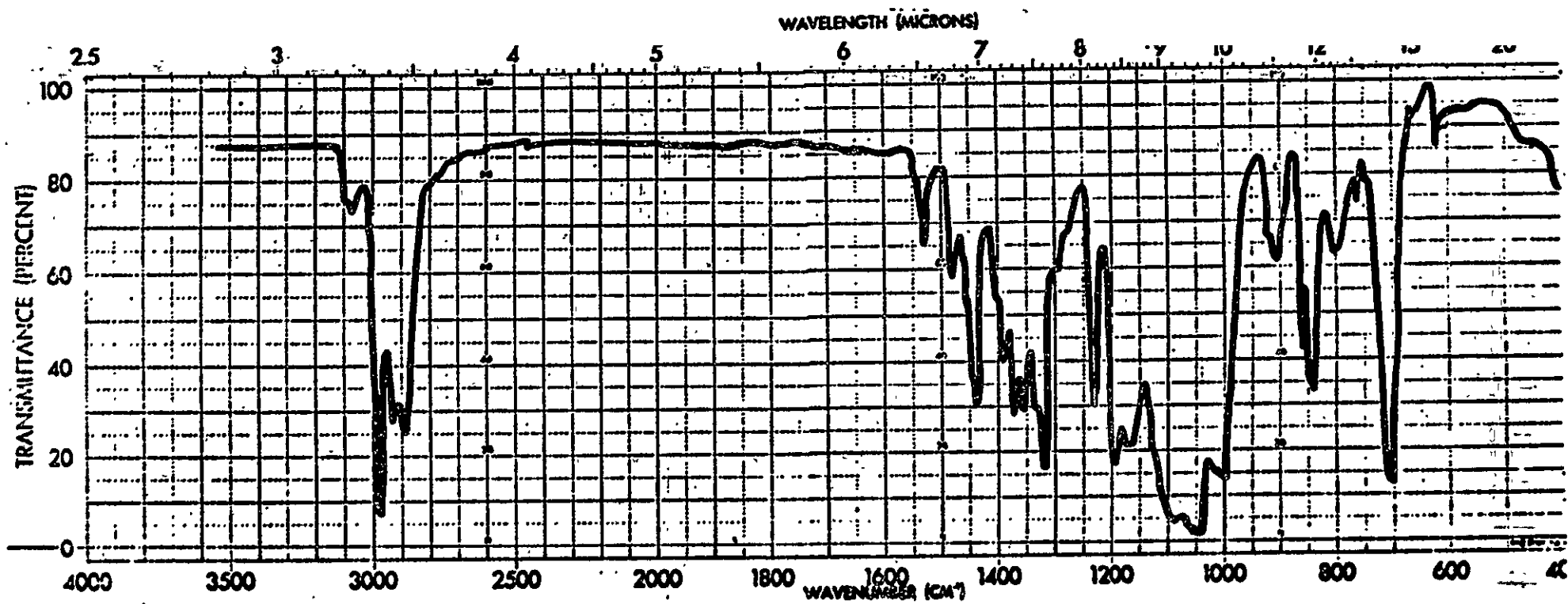
FIGURE 40. INFRARED SPECTRUM OF THIOPHENE-2-CARBOXALDEHYDE DIETHYL ACETAL
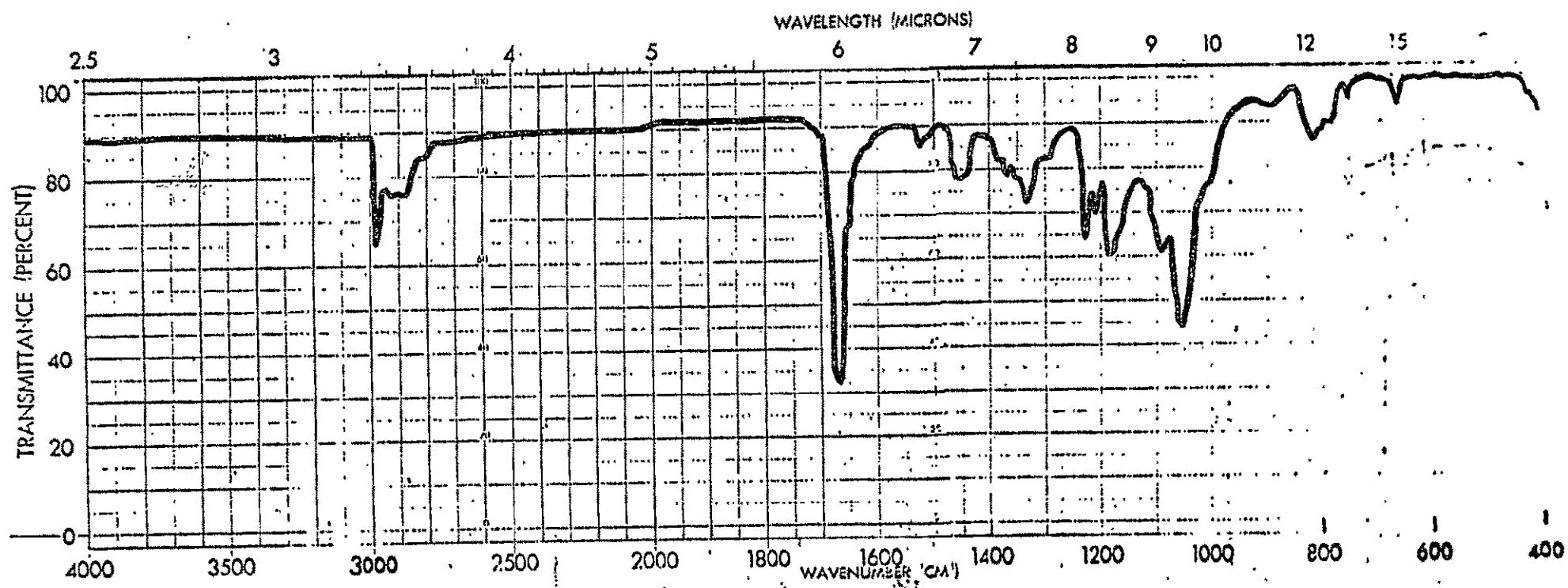
FIGURE 41. INFRARED SPECTRUM OF THIOPHENE-2,5-DICARBOXALDEHYDE DIETHYL ACETAL
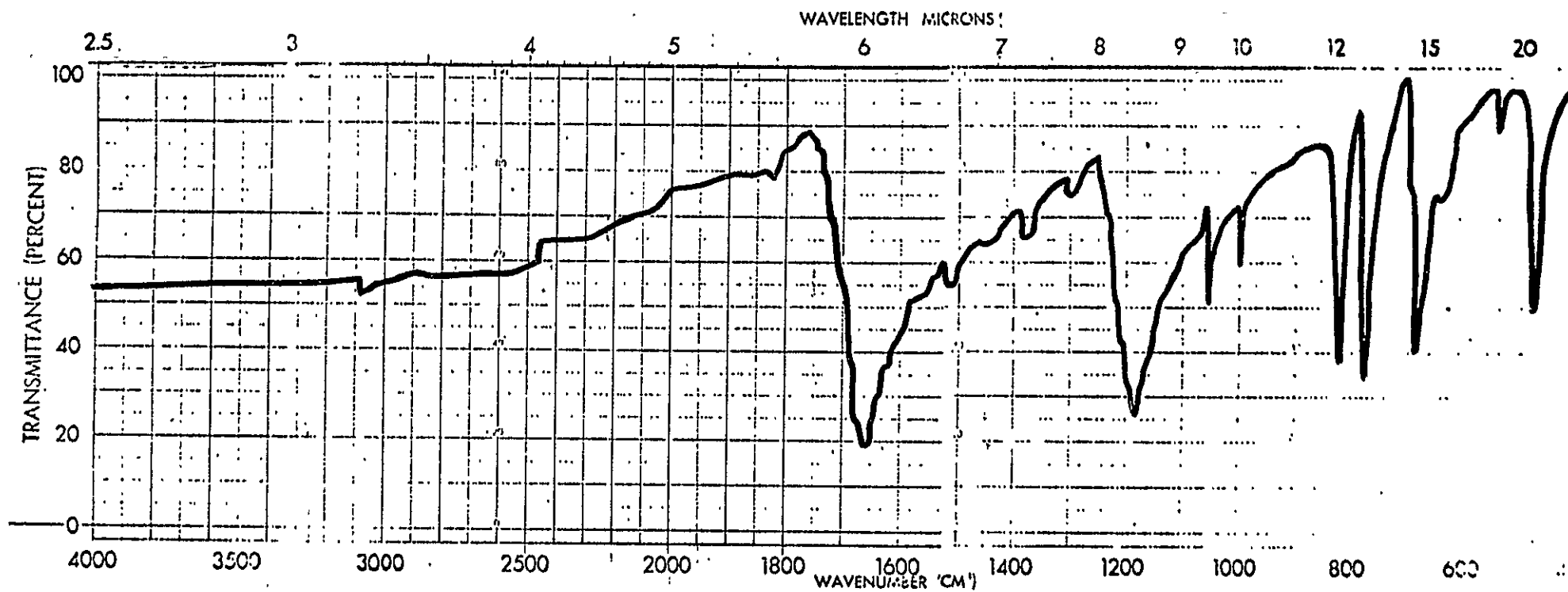
FIGURE 42. INFRARED SPECTRUM OF THIOPHENE-2,5-DICARBOXALDEHYDE
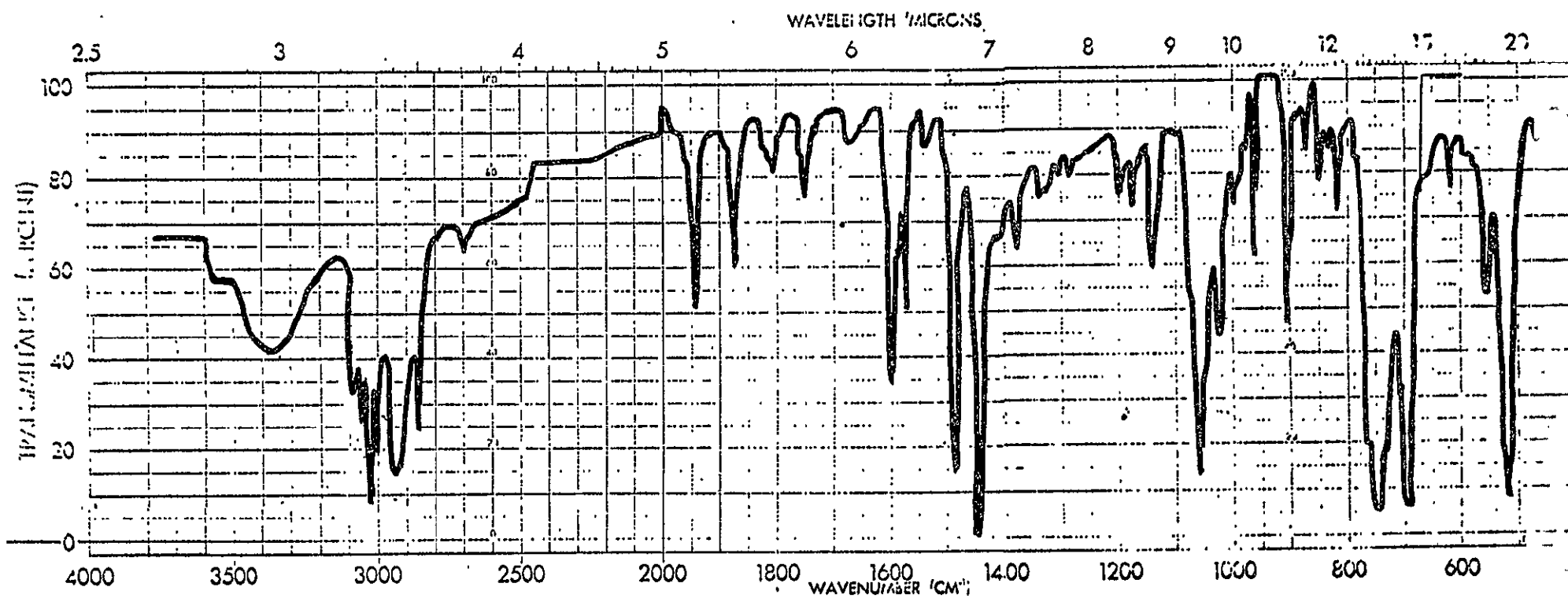
FIGURE 43. INFRARED SPECTRUM OF $\alpha,\alpha'$ - (PARA-PHENYLENE)BIS($\beta$ -PHENYLETHANOL)
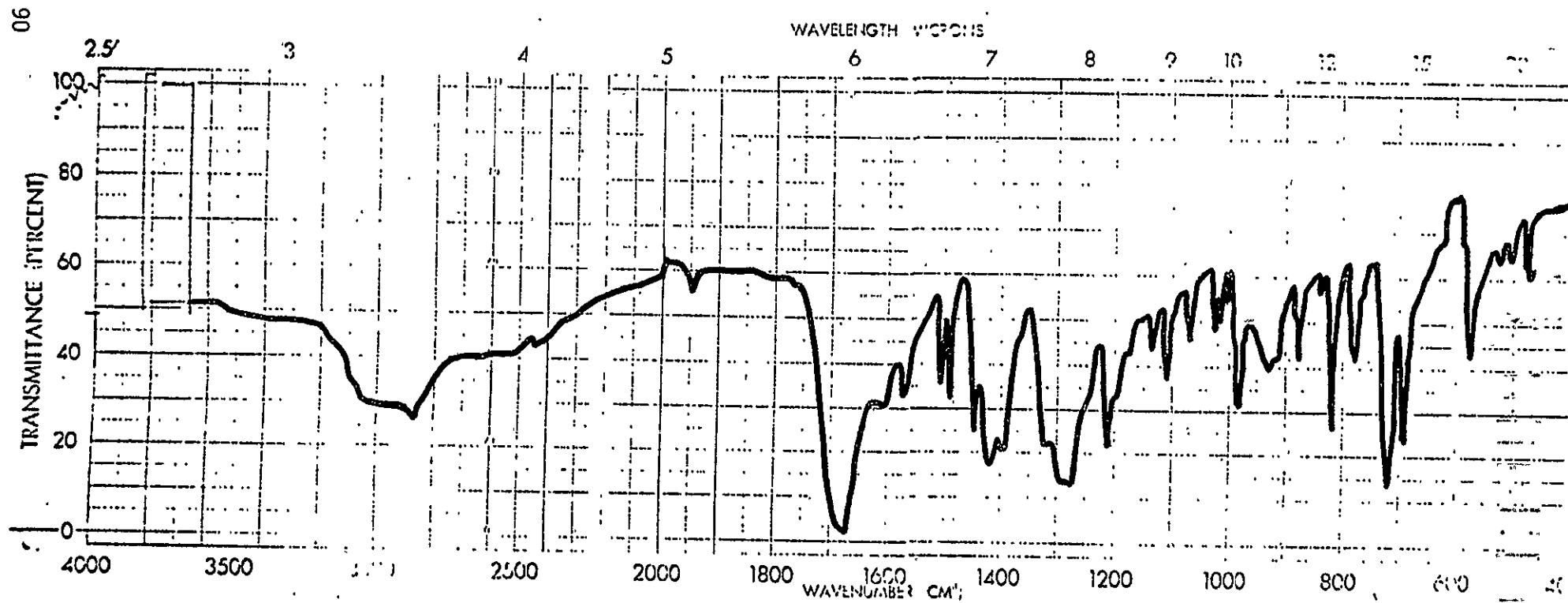
FIGURE 44. INFRARED SPECTRUM OF 1,4-BIS(PHENYLACETYL)BENZENE
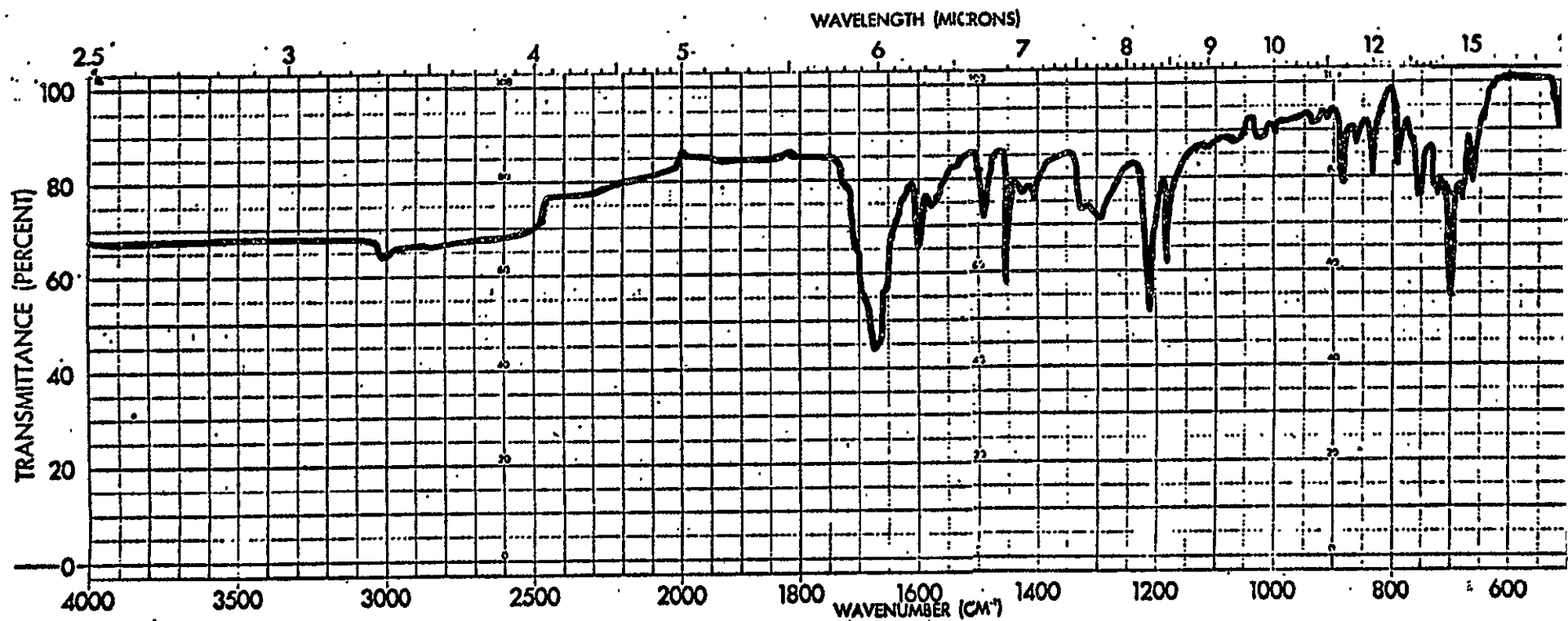
FIGURE 45. INFRARED SPECTRUM OF 1,4-BIS(PHENYLGLYOXYLOYL)BENZENE
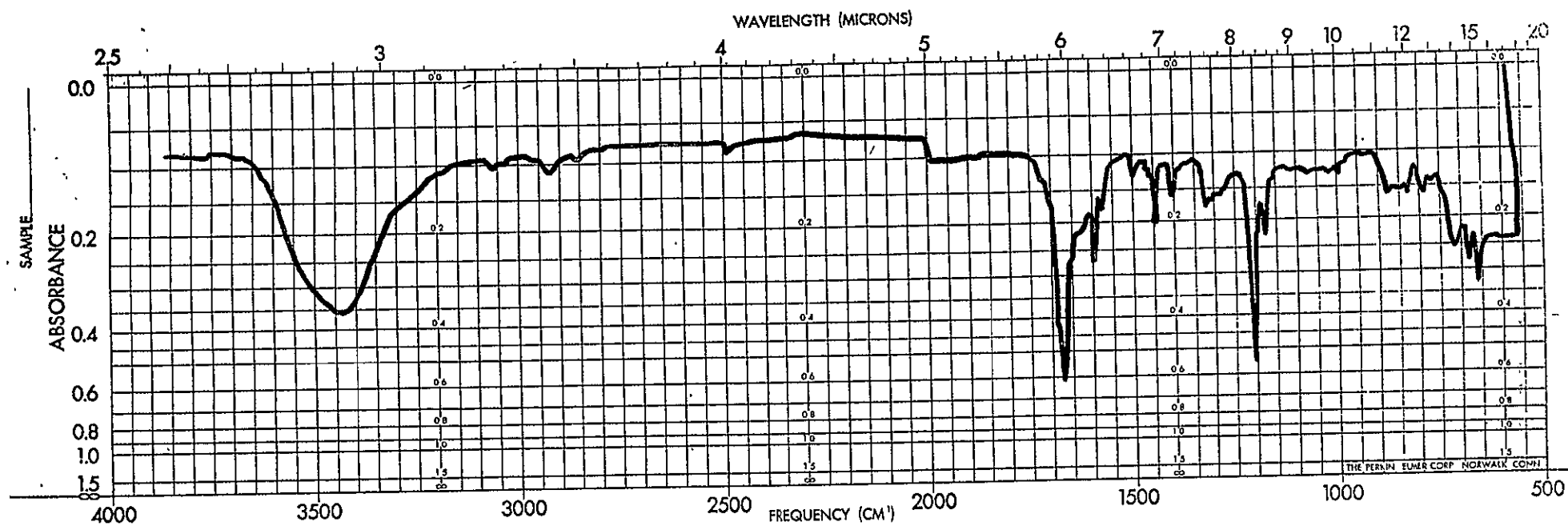
FIGURE 46. 1,4-BIS(PHENYLGLYOXYLOYL) BENZENE, INFRARED SPECTRUM IN KBR (REFERENCE 26)
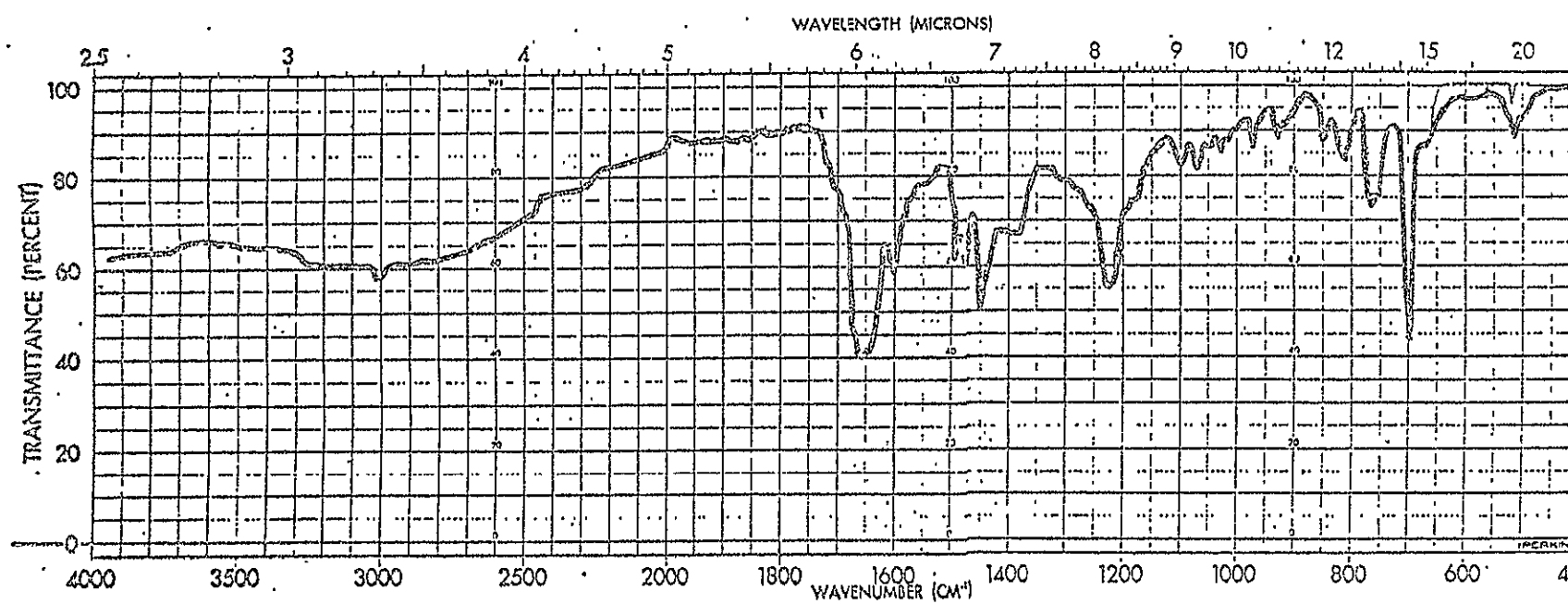
FIGURE 47.    INFRARED SPECTRUM OF POLYIMIDAZOLE FROM 1,4-BIS(PHENYLGLYOXYLOYL)
BENZENE AND THIOPHENE-2,5-DICARBOXALDEHYDE
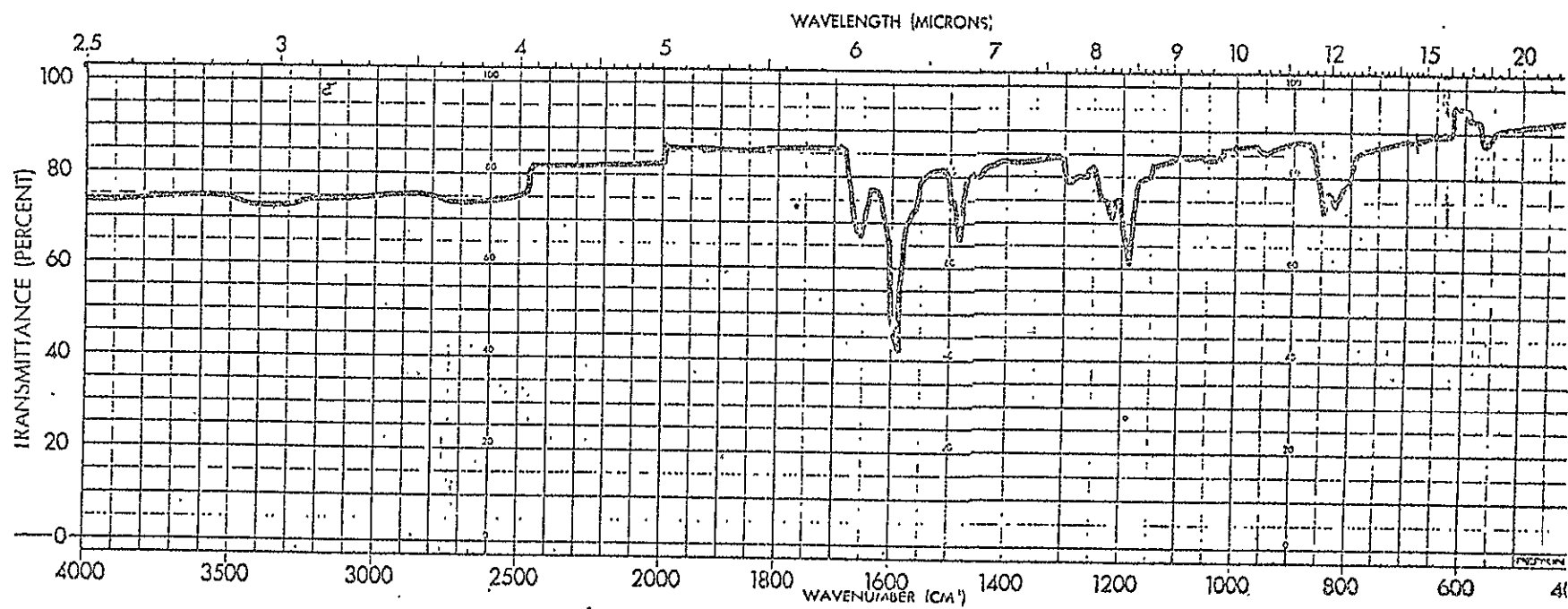
FIGURE 48. INFRARED SPECTRUM OF POLY(SCHIFF'S BASE) FROM p - PHENYLENEDIAMINE
AND THIOPHENE-2,5-DICARBOXALDEHYDE
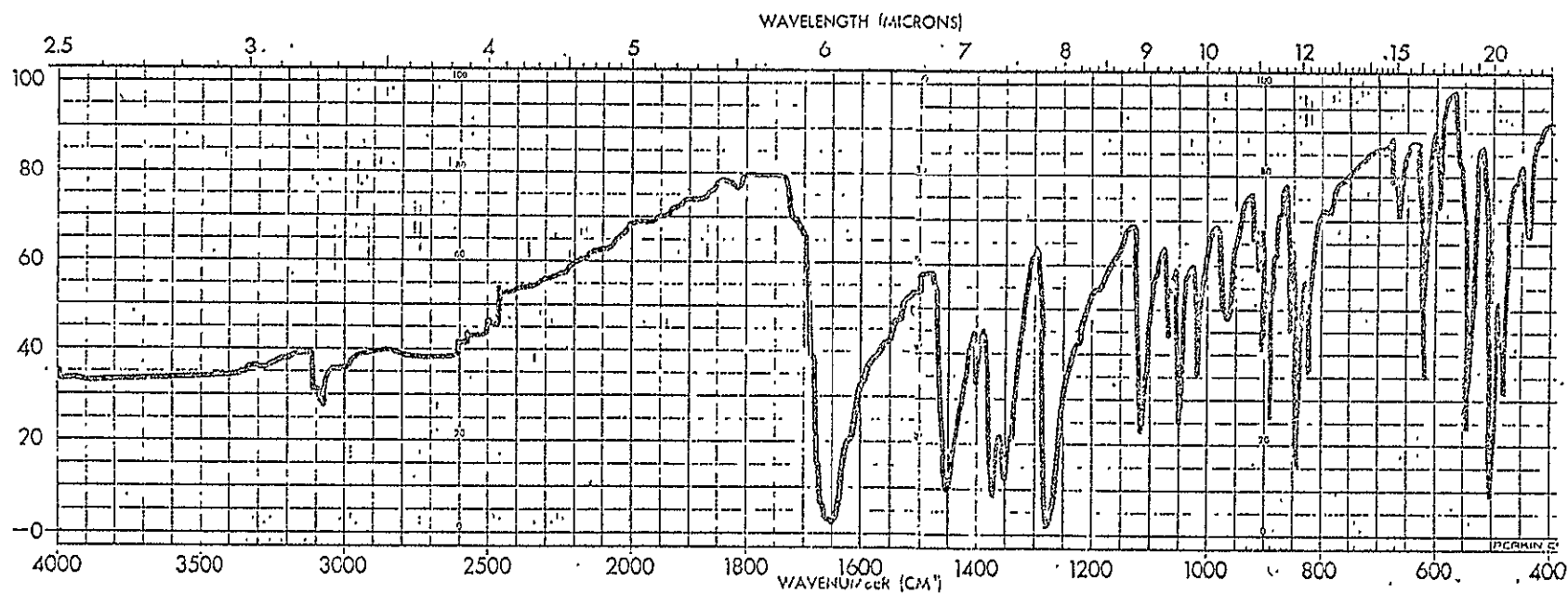
FIGURE 49. INFRARED SPECTRUM OF FERROCENE-1,1'-DICARBOXALDEHYDE
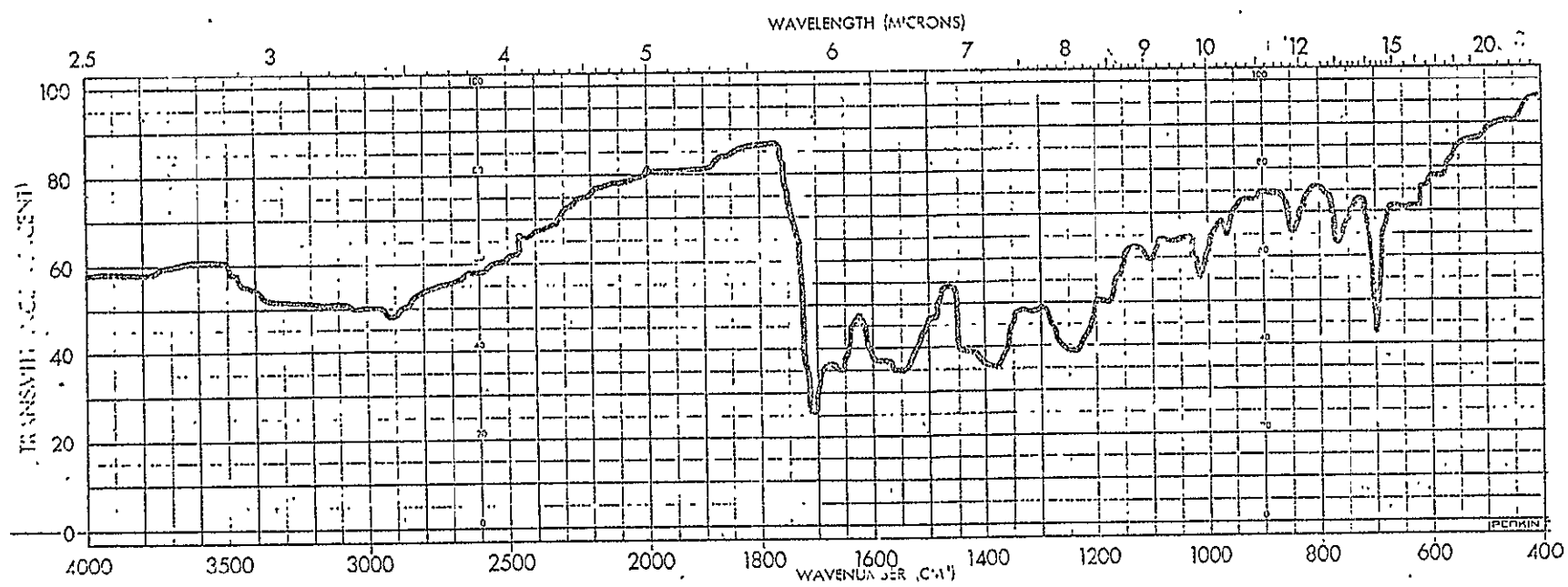
FIGURE 50. INFRARED SPECTRUM OF FERROCENE/IMIDAZOLE POLYMER
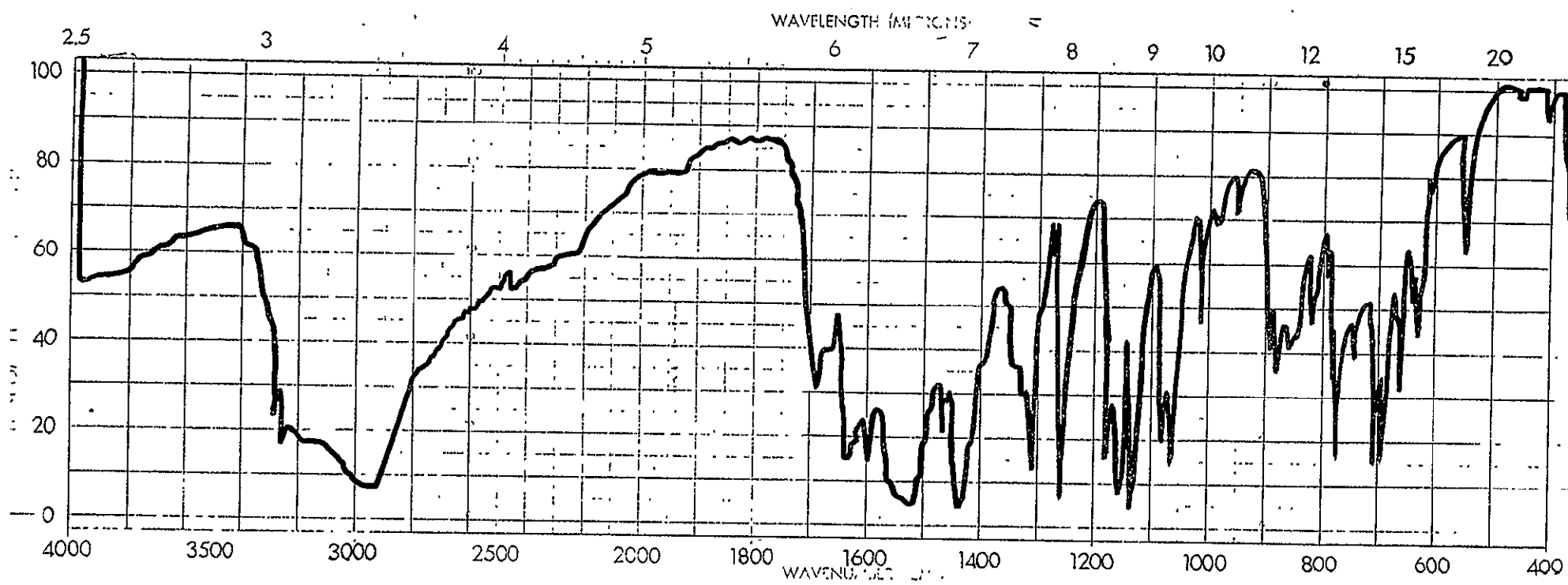
FIGURE 51. INFRARED SPECTRUM OF AMINOIMINOISOINDOLENINE
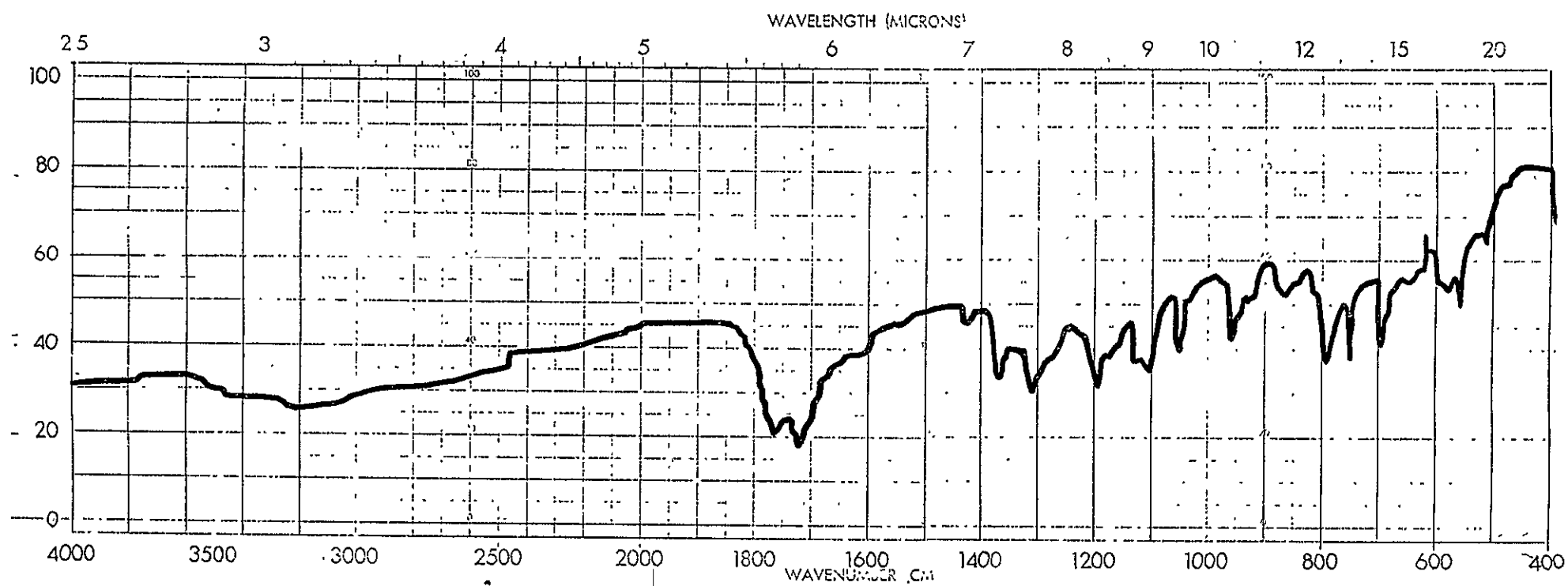
FIGURE 52.   INFRARED SPECTRUM OF TRICHLOROISOINDOLENINE CARBONYLCHLORIDE
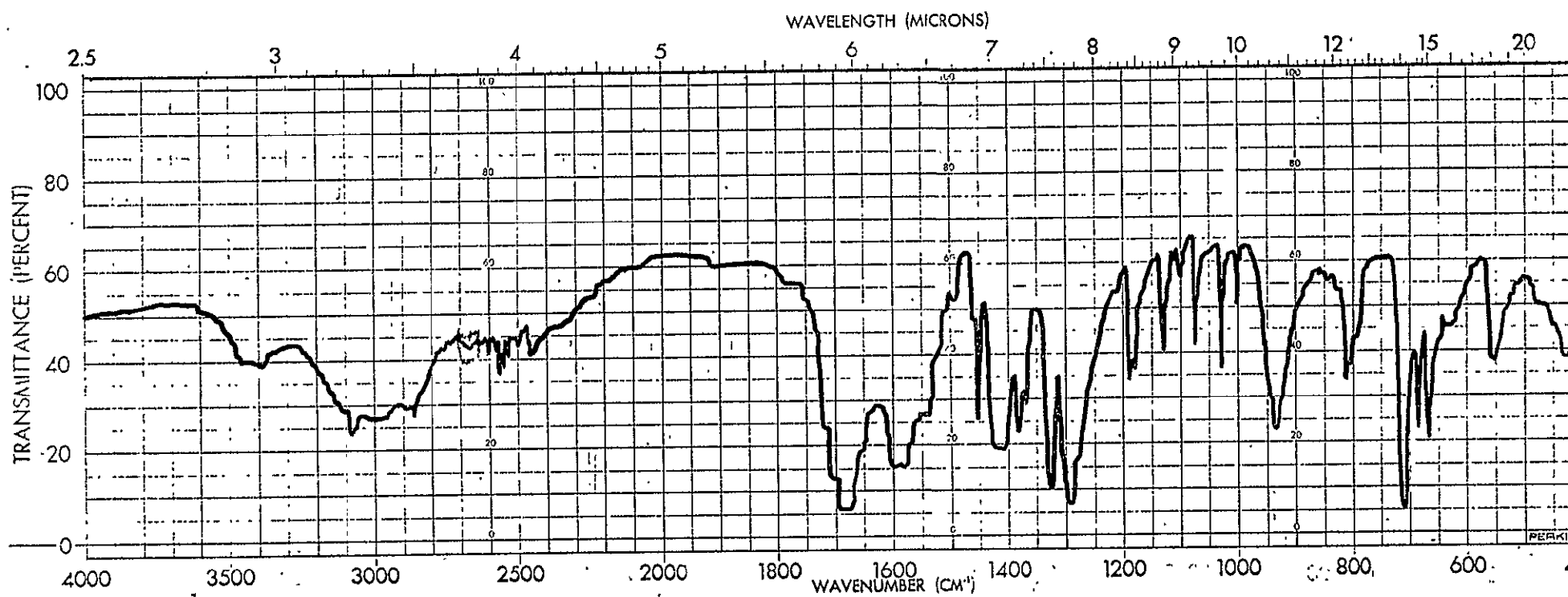
FIGURE 53. INFRARED SPECTRUM OF PHTHALOCYANINE DICARBOXYLIC ACID

WAVELENGTH (MICRONS)
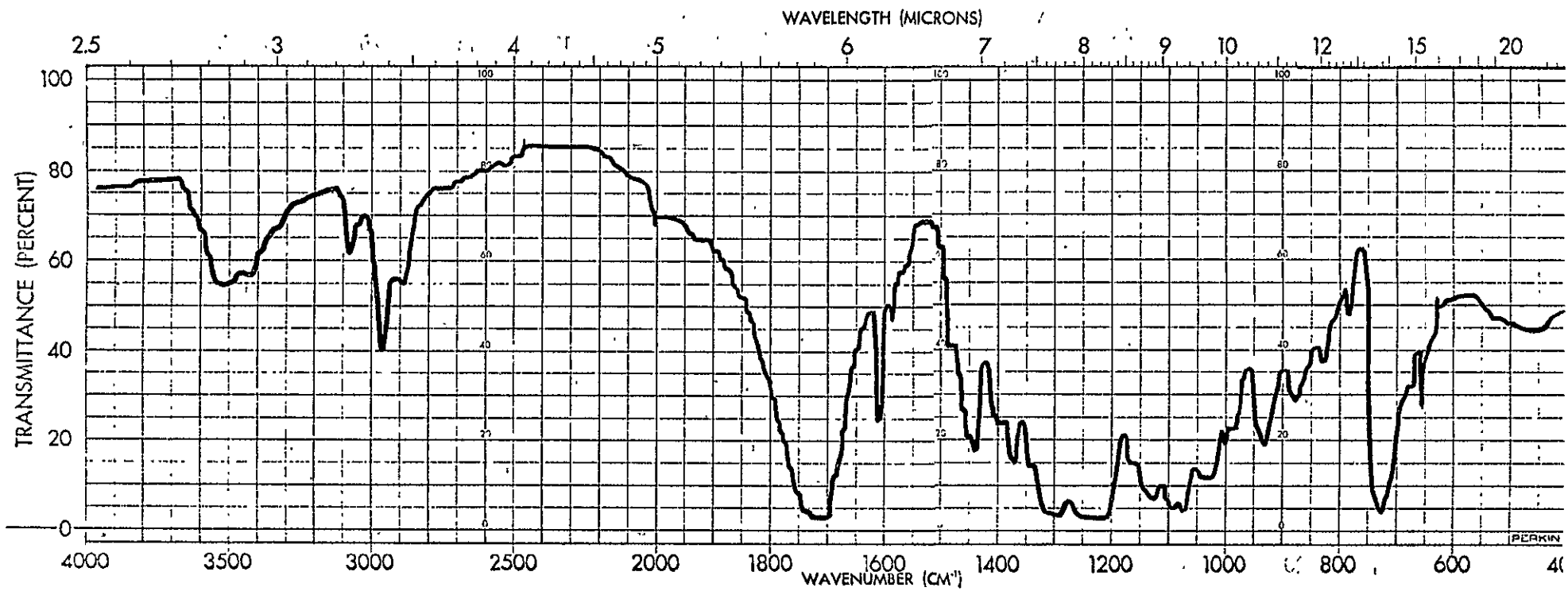


FIGURE 54.    INFRARED SPECTRUM OF POLYESTER/PHTHALOCYANINE (IV)
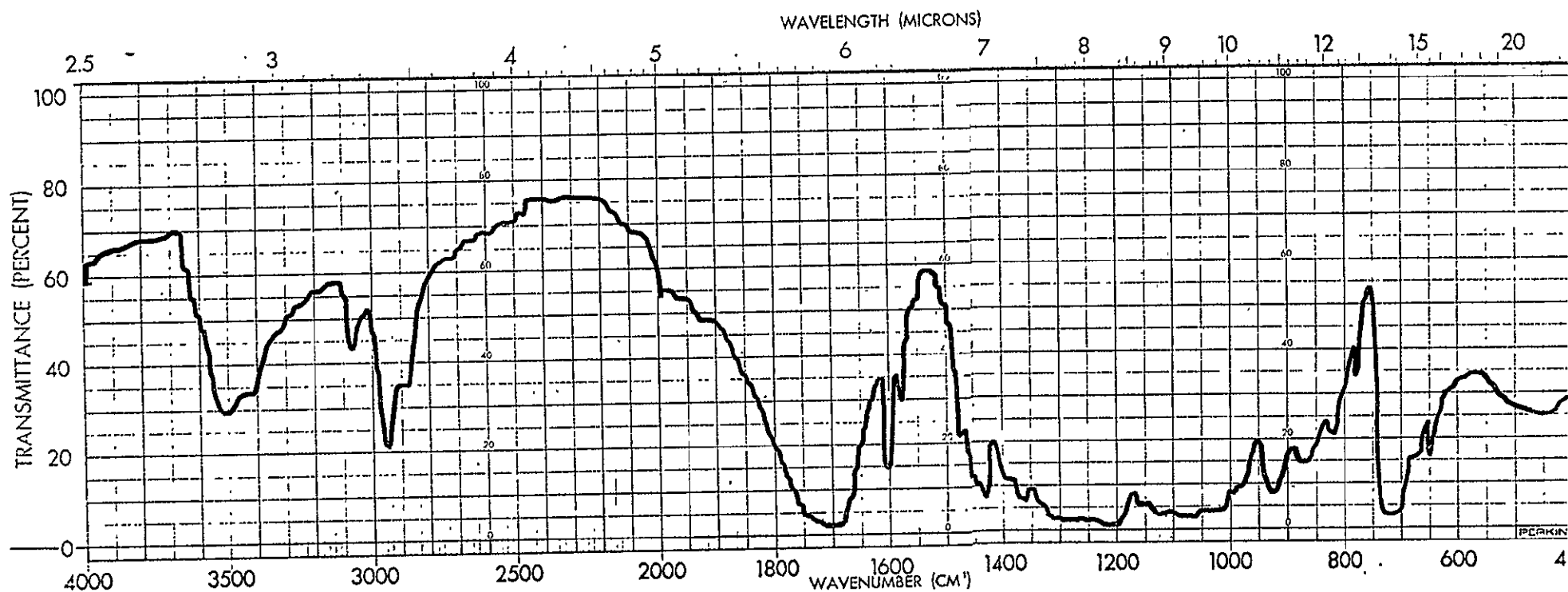
FIGURE 55. INFRARED SPECTRUM OF POLYESTER/PHTHALOCYANINE (IRON) (V)
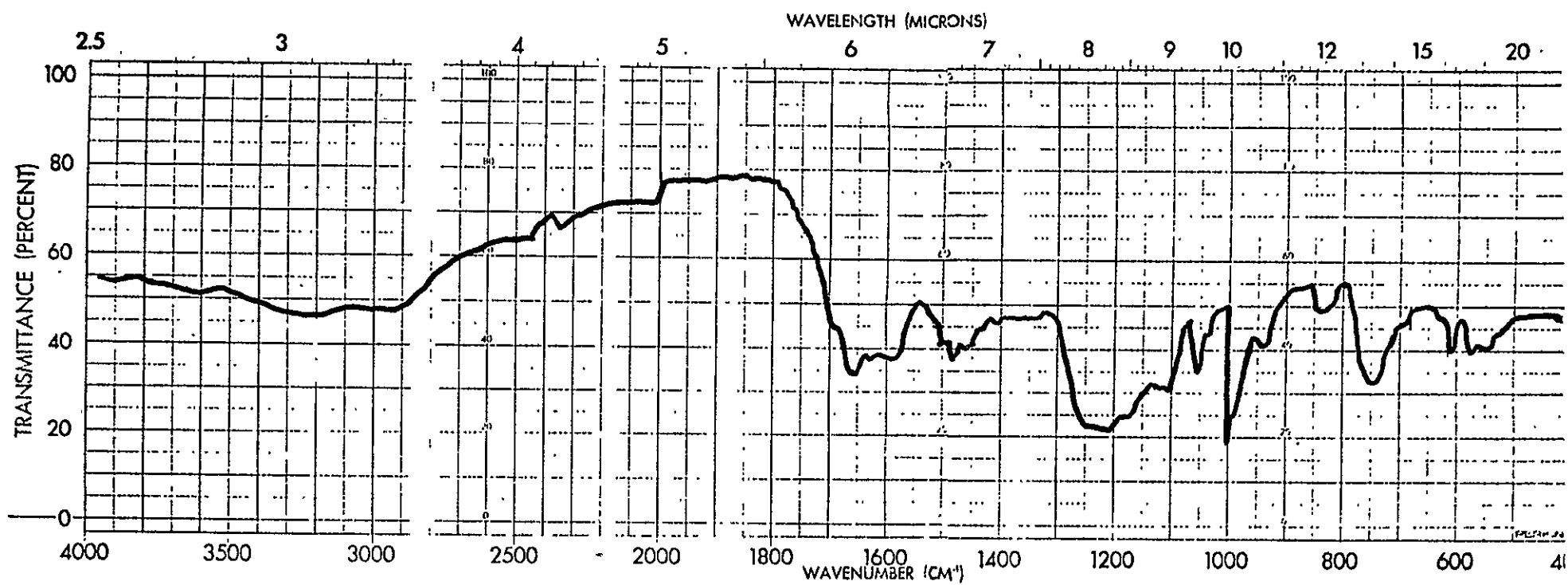
FIGURE 56. INFRARED SPECTRUM OF POLY(P-DIMETHYLAMINOPHENYLACETYLENE)
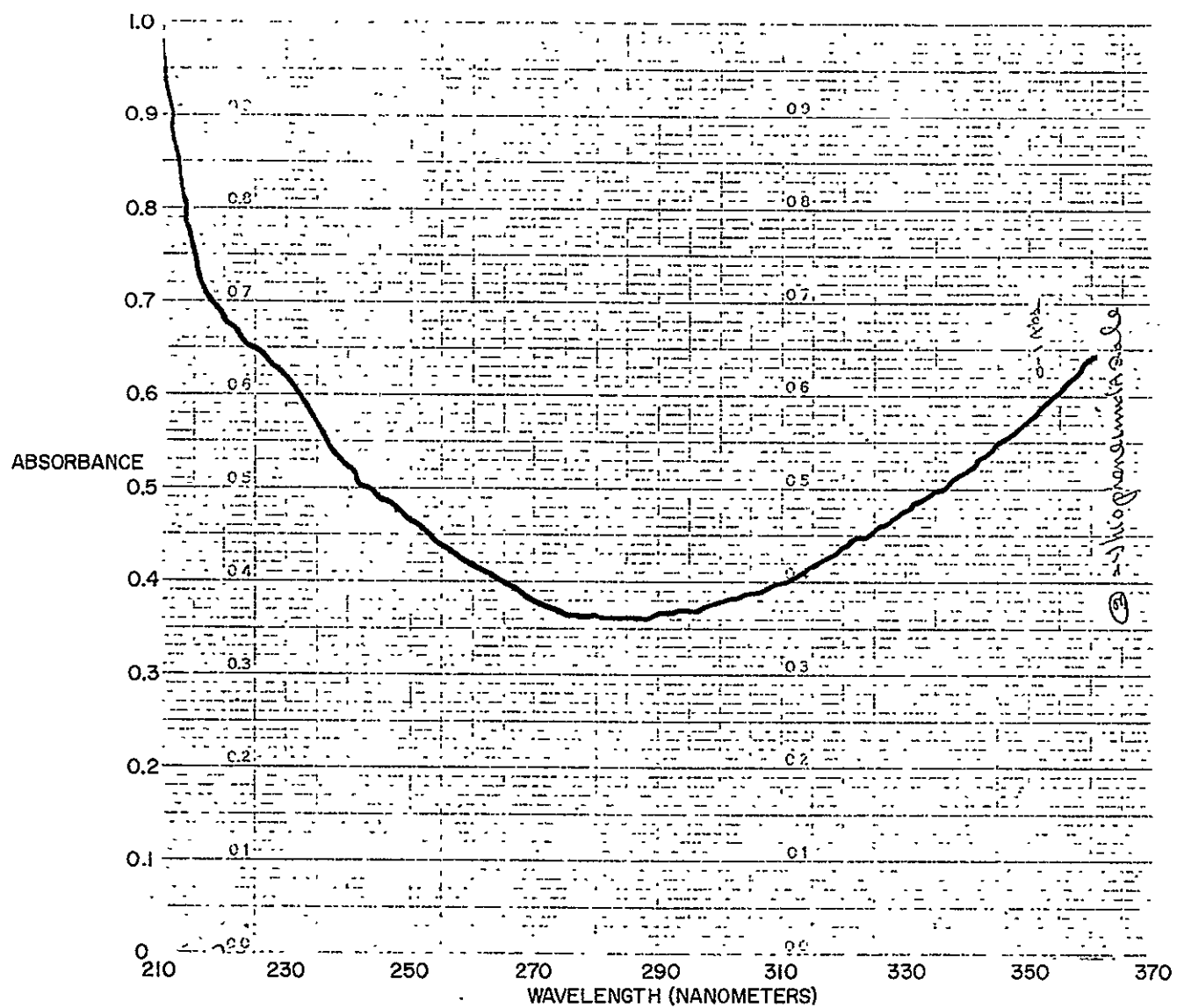
FIGURE 57.   ULTRAVIOLET ABSORPTION SPECTRUM OF
POLY(IMIDAZOLE)/THIOPHENE (I)

103
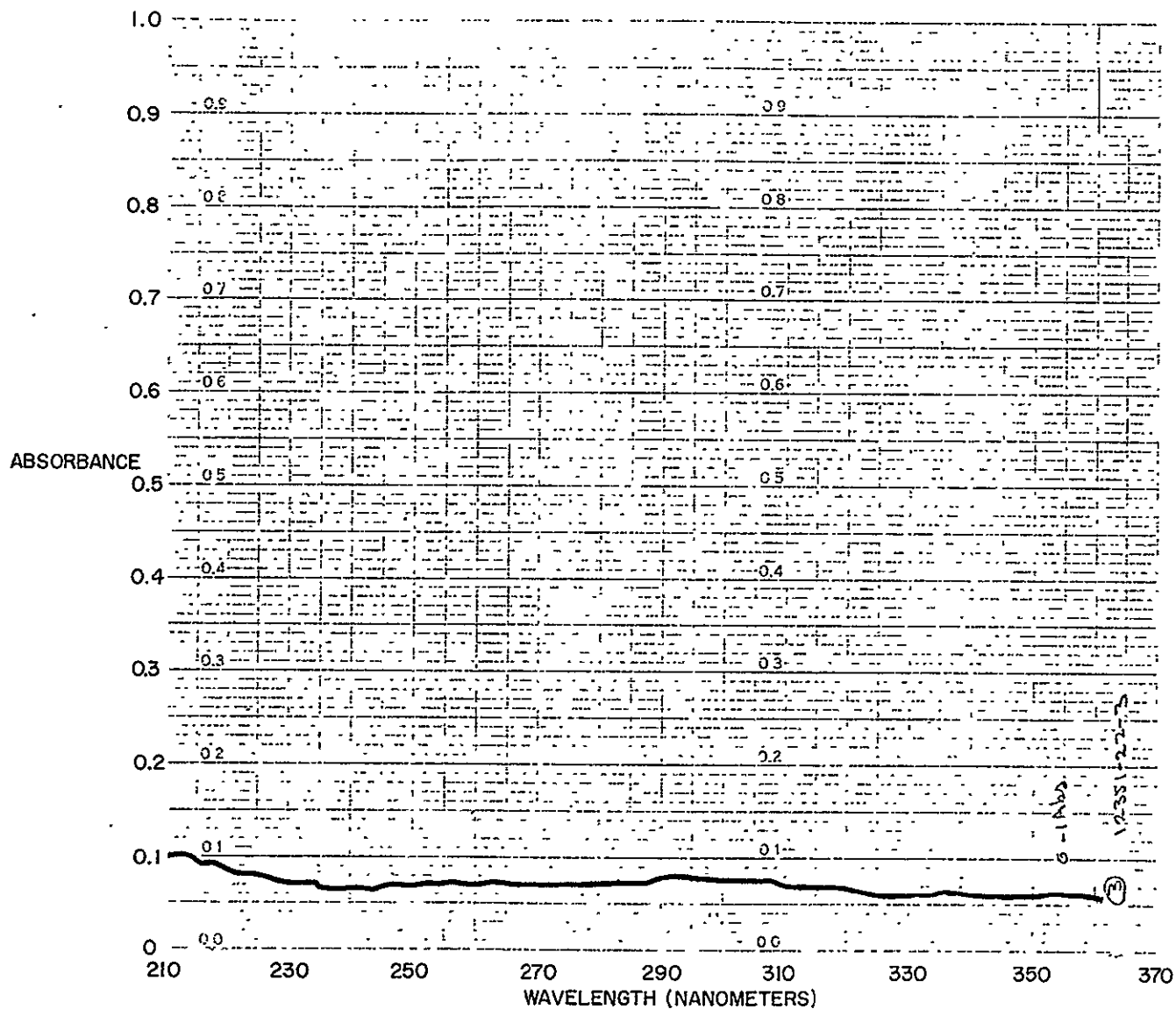
FIGURE 58. ULTRAVIOLET ABSORPTION SPECTRUM OF POLY(SCHIFF'S BASE)/THIOPHENE (II)
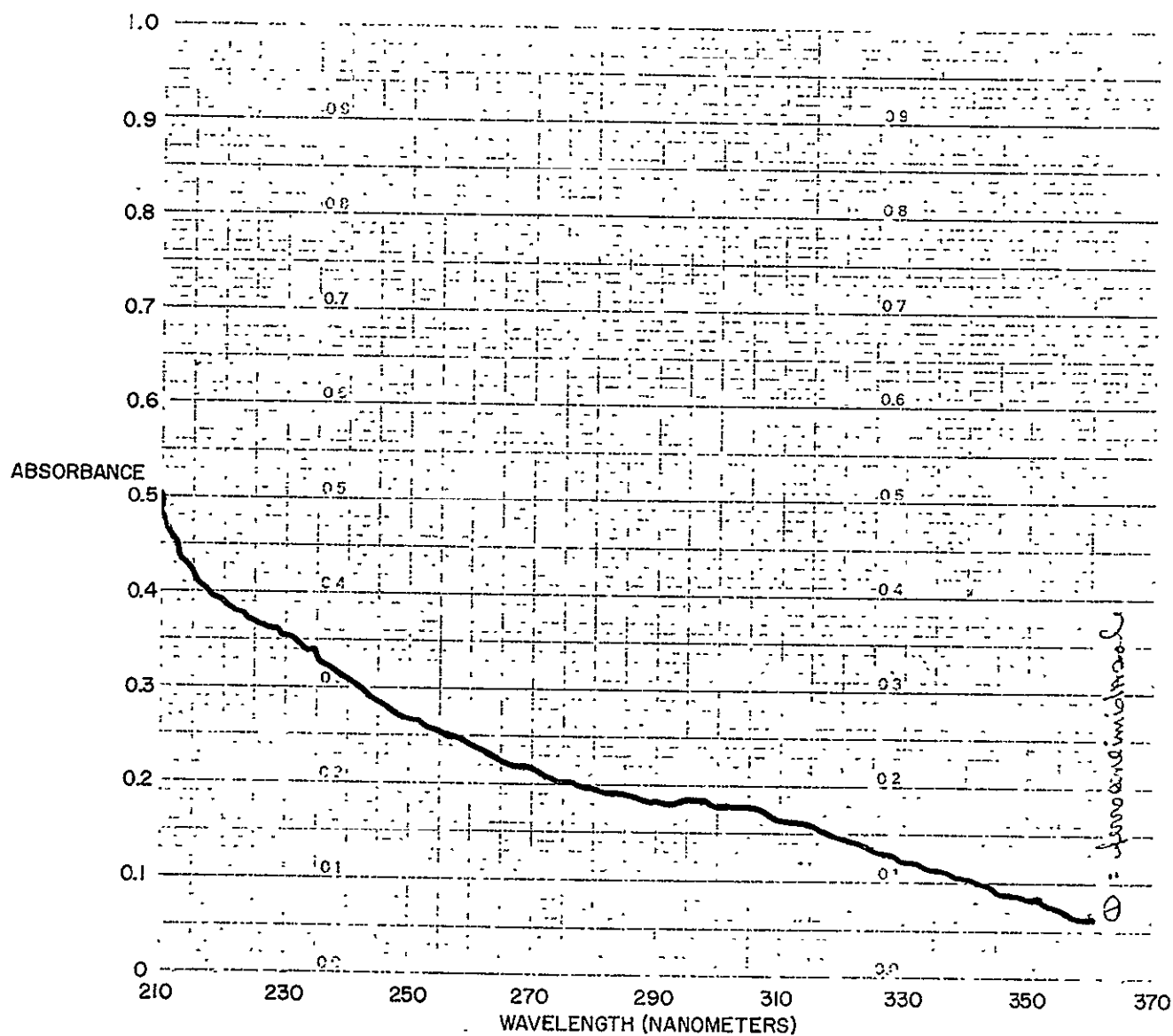
FIGURE 59.   ULTRAVIOLET ABSORPTION SPECTRUM OF
POLY(IMIDAZOLE)/FERROCENE (III)
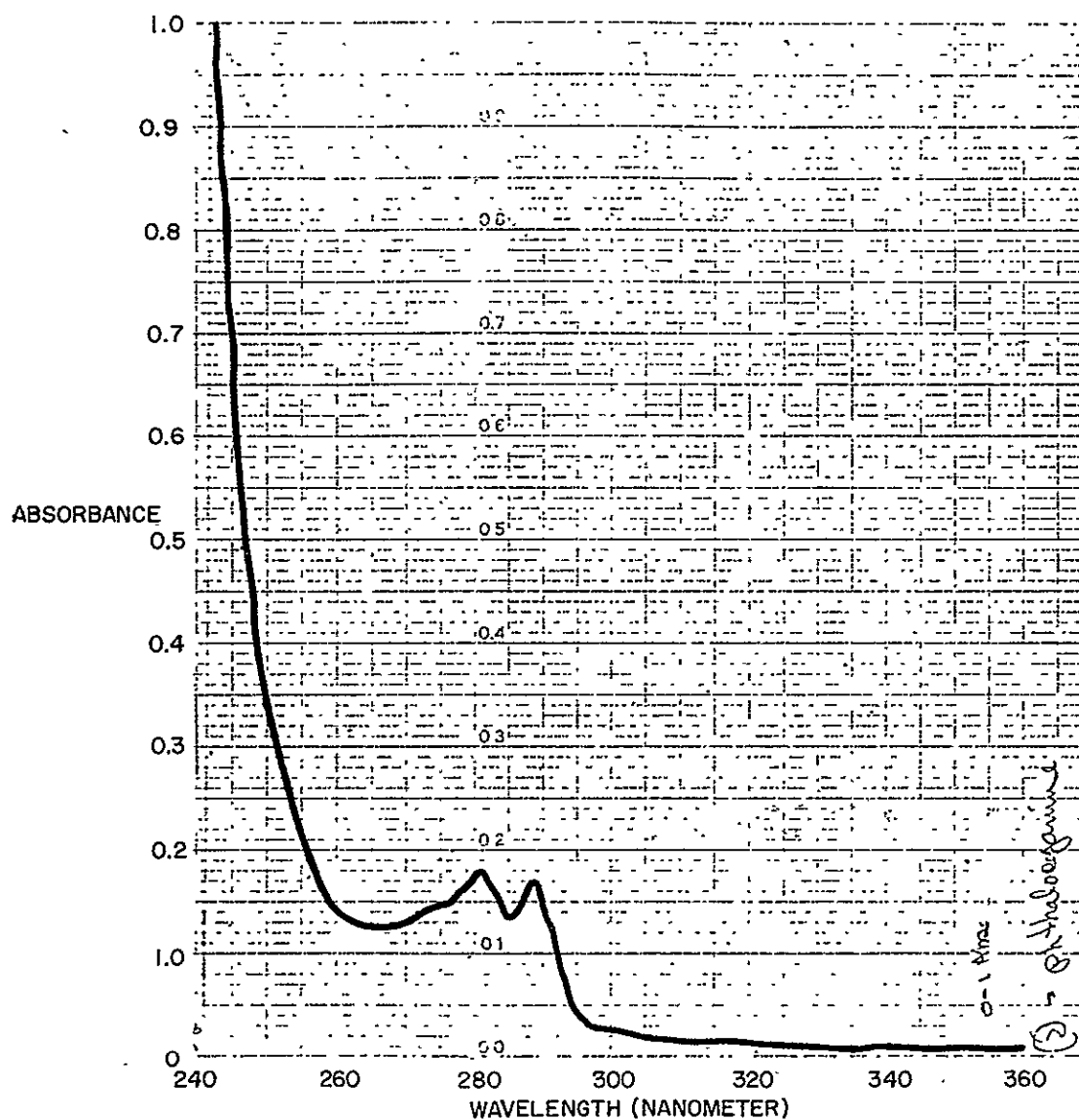
FIGURE 60. ULTRAVIOLET ABSORPTION SPECTRUM OF
POLYESTER/PHTHALOCYANINE (IV)

106
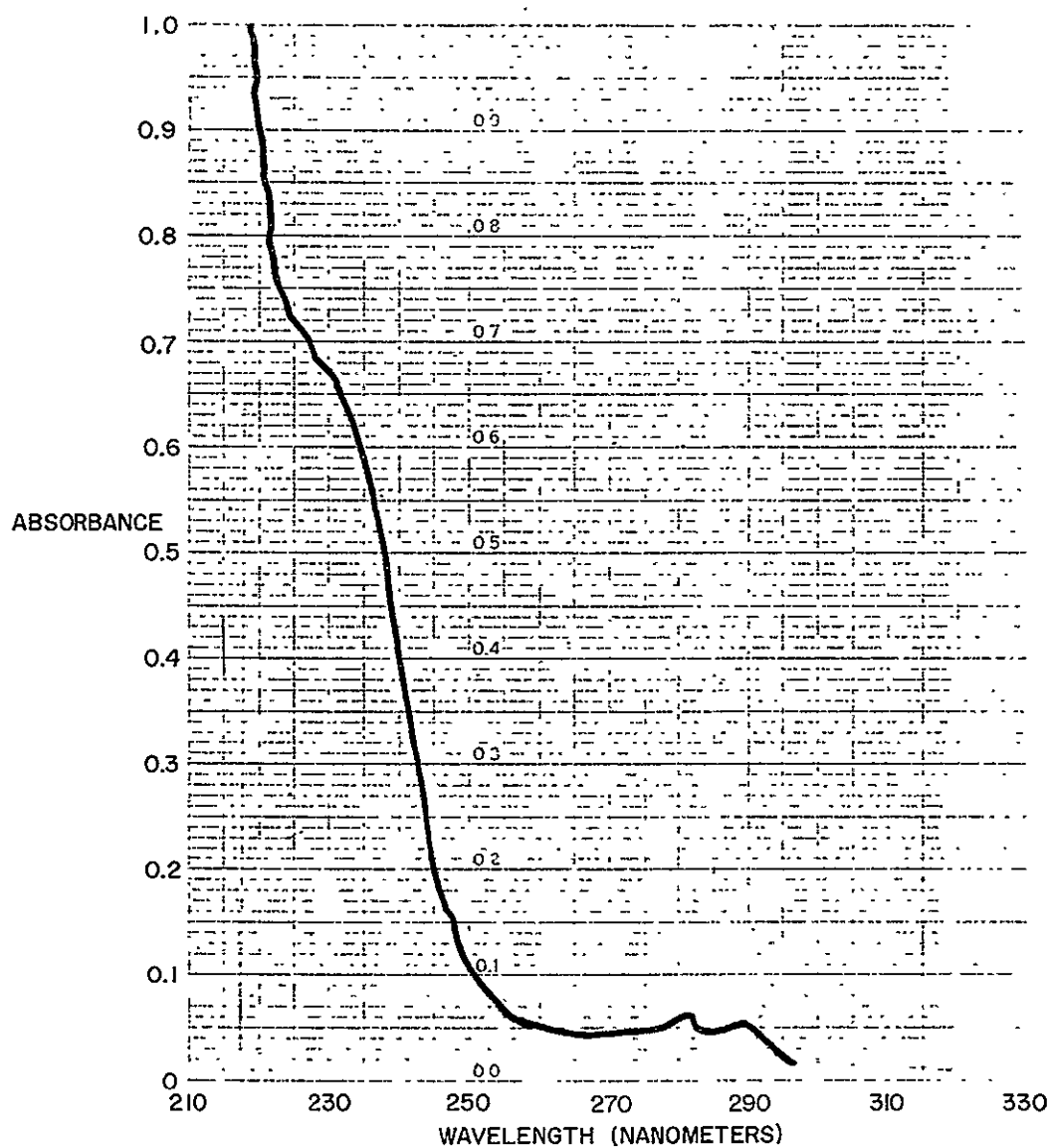
FIGURE 61.   ULTRAVIOLET ABSORPTION SPECTRUM OF
POLYESTER/PHTHALOCYANINE (IRON) (V)
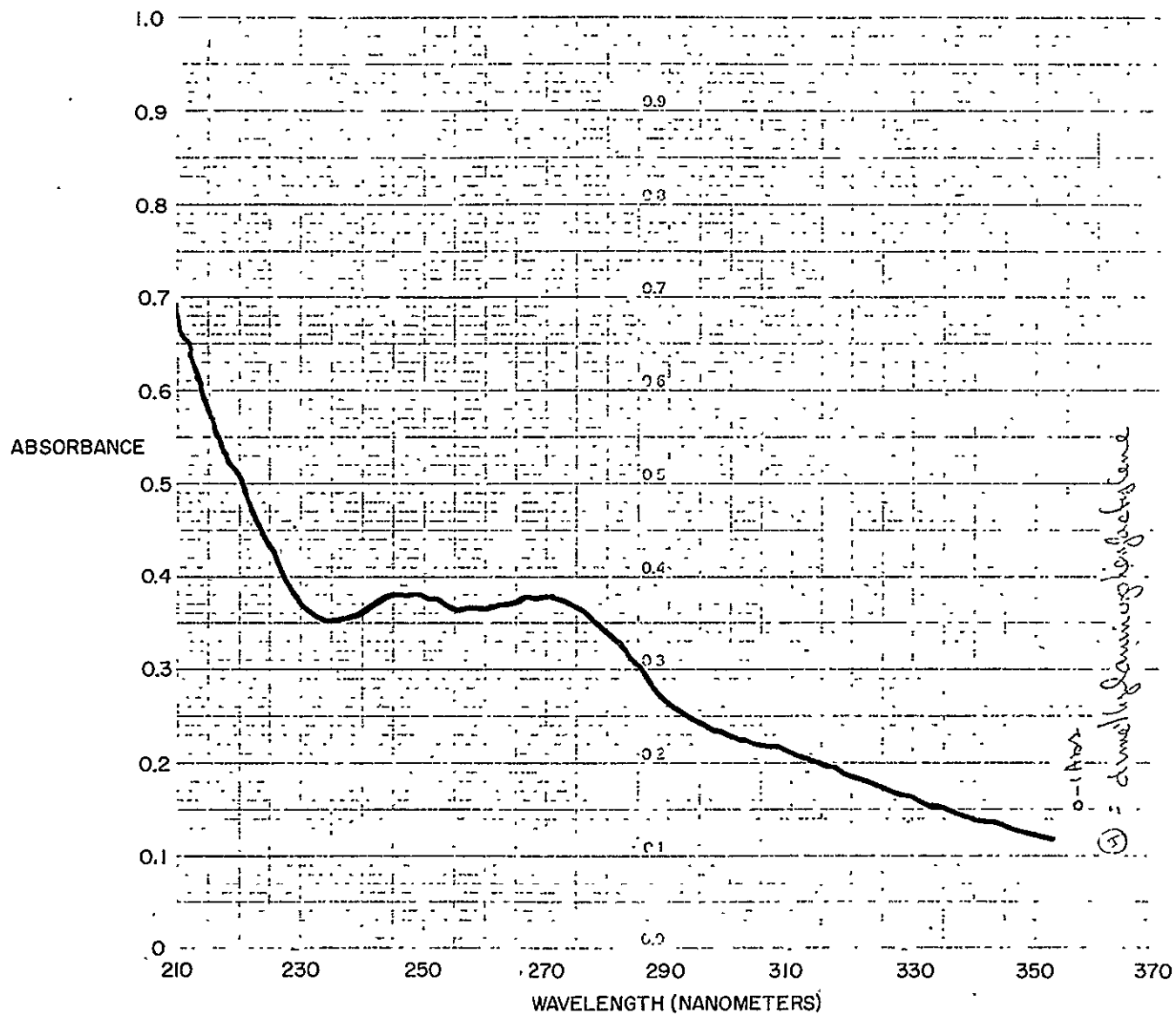
FIGURE 62. ULTRAVIOLET ABSORPTION SPECTRUM OF
POLY(P-DIMETHYLAMINOPHENYLACETYLENE) (VI)
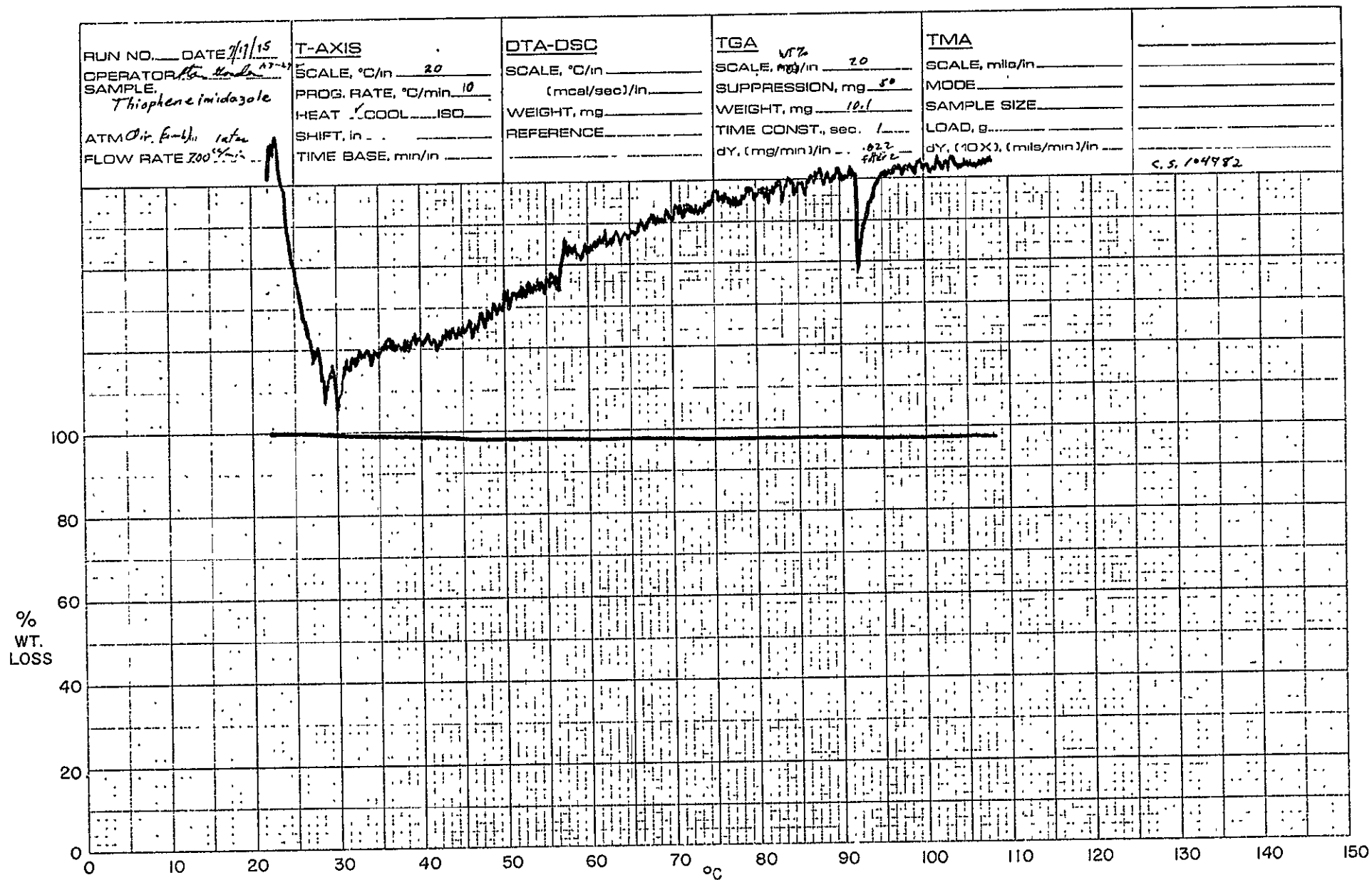
FIGURE 63. THERMOGRAVIMETRIC ANALYSIS CURVE FOR POLY(IMIDAZOLE)/THIOPHENE (I)

RUN NO.____ DATE 7/17/75

OPERATOR: _____ A3-77

SAMPLE:
Thiophene Schiff's
12357-22-3 Base

ATM Air (wet) lot

FLOW RATE 200 cc/min

**T-AXIS**
SCALE, °C/in ____ 20
PROG. RATE, °C/min __ 10
HEAT __ COOL ___ ISO ___
SHIFT, in _____
TIME BASE, min/in _____

**DTA-DSC**
SCALE, °C/in _____
(mcal/sec)/in _____
WEIGHT, mg _____
REFERENCE _____

**TGA**
SCALE, mg/in __ 20
SUPPRESSION, mg __ 50
WEIGHT, mg __ 10.1
TIME CONST., sec __ 1
dY, (mg/min)/in __ .022

**TMA**
SCALE, mils/in _____
MODE _____
SAMPLE SIZE _____
LOAD, g _____
dY, (10X), (mils/min)/in ____

C.S. 104702



FIGURE 64.   THERMOGRAVIMETRIC ANALYSIS CURVE FOR POLY(SCHIFF'S BASE)/THIOPHENE (Ⅱ)

RUN NO._____ DATE _____  
OPERATOR _____  
SAMPLE:  
    *ferrocene*  
    *Imidazole*  
ATM _____  
FLOW RATE _____

**T-AXIS**  
SCALE, °C/in ___20___  
PROG. RATE, °C/min ___10___  
HEAT___ COOL___ ISO___  
SHIFT, in._____  
TIME BASE, min/in _____

**DTA-DSC**  
SCALE, °C/in _____  
(mcal/sec)/in _____  
WEIGHT, mg _____  
REFERENCE _____  

**TGA**  
SCALE, mg/in ___20___  
SUPPRESSION, mg ___50___  
WEIGHT, mg ___10.2___  
TIME CONST., sec ___1___  
dY, (mg/min)/in ___.022___  
*filter 2*

**TMA**  
SCALE, mils/in _____  
MODE _____  
SAMPLE SIZE _____  
LOAD, g _____  
dY, (10X), (mils/min)/in ___

*C.S. 104782*
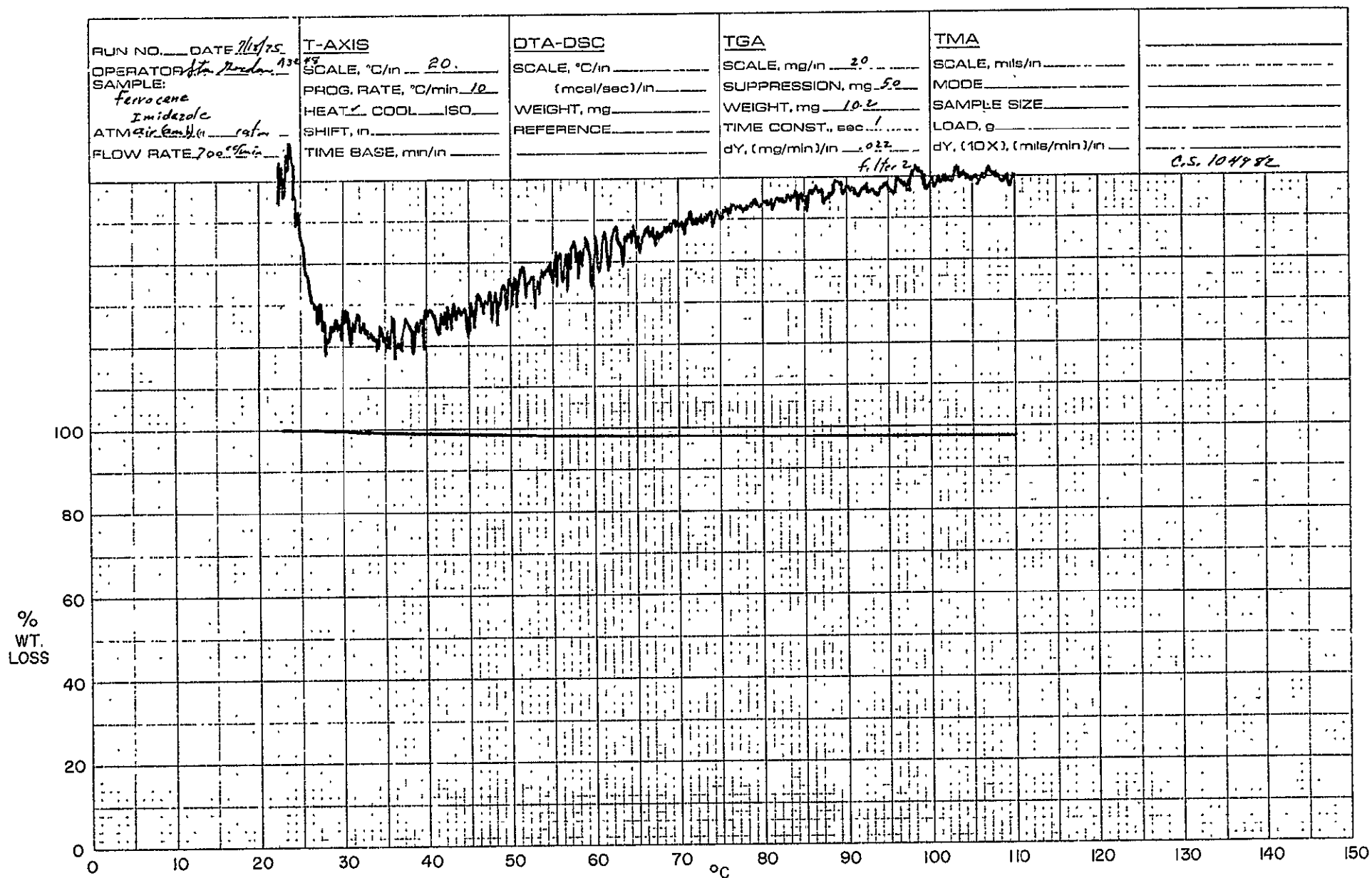
FIGURE 65.  THERMOGRAVIMETRIC ANALYSIS CURVE FOR POLY(IMIDAZOLE)/FERROCENE (Ⅲ)

FIGURE 66.  THERMOGRAVIMETRIC ANALYSIS CURVE FOR POLYESTER/PHTHALOCYANINE (IV)
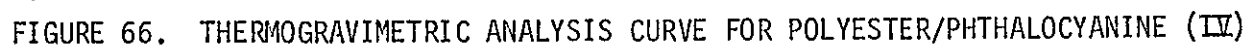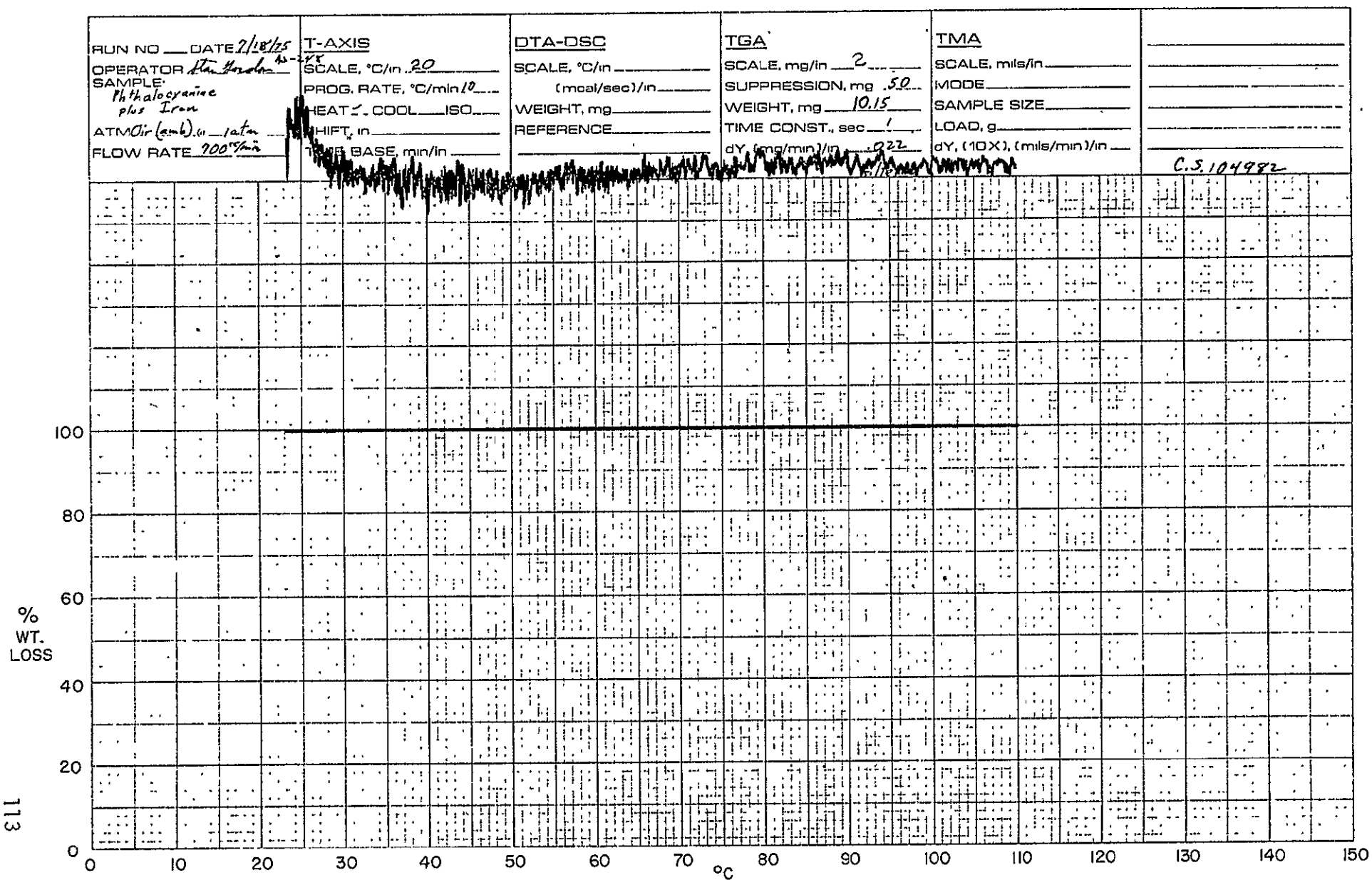
FIGURE 67. THERMOGRAVIMETRIC ANALYSIS CURVE FOR POLYESTER/PHTHALOCYANINE (IRON) (Ⅴ)

RUN NO. __ DATE 7/16/75

OPERATOR __ *Stan Hardan* A3

SAMPLE
*Dimethyl amino*
*p phenylacetylene*

ATM *Air (emb)* or _ *1 atm*

FLOW RATE. *700 cc/min*

**T-AXIS** 24V

SCALE, °C/in __ 20

PROG. RATE, °C/min 10

HEAT __ COOL __ ISO __

SHIFT, in __

TIME BASE, min/in __

**DTA-DSC**

SCALE, °C/in __

(mcal/sec)/in __

WEIGHT, mg __

REFERENCE __

**TGA** WT%

SCALE, mg/in __ 20

SUPPRESSION, mg __ 50

WEIGHT, mg __ 1025

TIME CONST., sec __ 1

dY, (mg/min)/in . 022

*filter 2*

**TMA**

SCALE, mils/in __

MODE __

SAMPLE SIZE __

LOAD, g __

dY, (10X), (mils/min)/in __

*C.S. 104982*
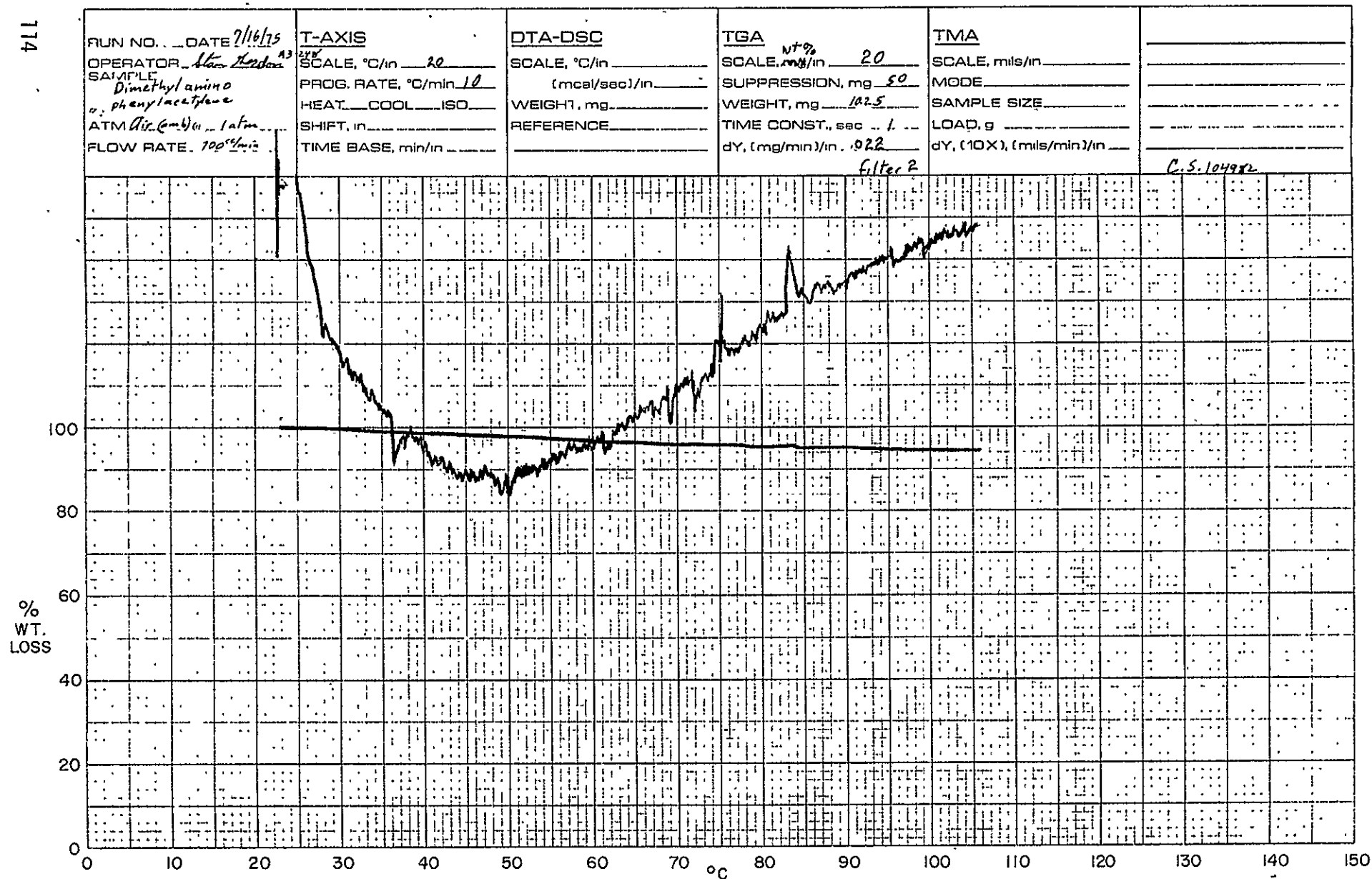


FIGURE 68. THERMOGRAVIMETRIC ANALYSIS CURVE FOR POLY(P-DIMETHYLAMINOPHENYLACETYLENE) (VI)
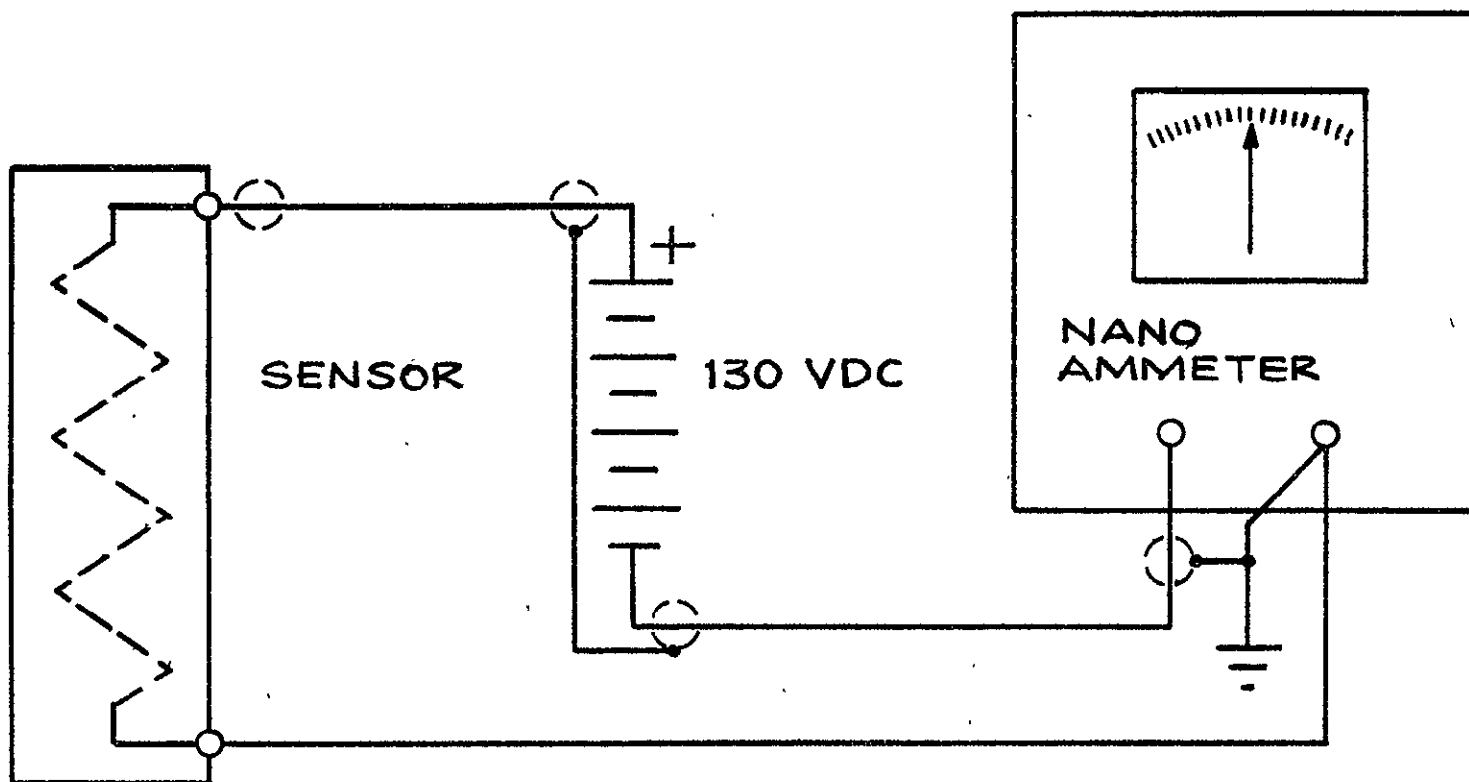
FIGURE 69.   SCHEMATIC DIAGRAM OF TEST CIRCUITRY
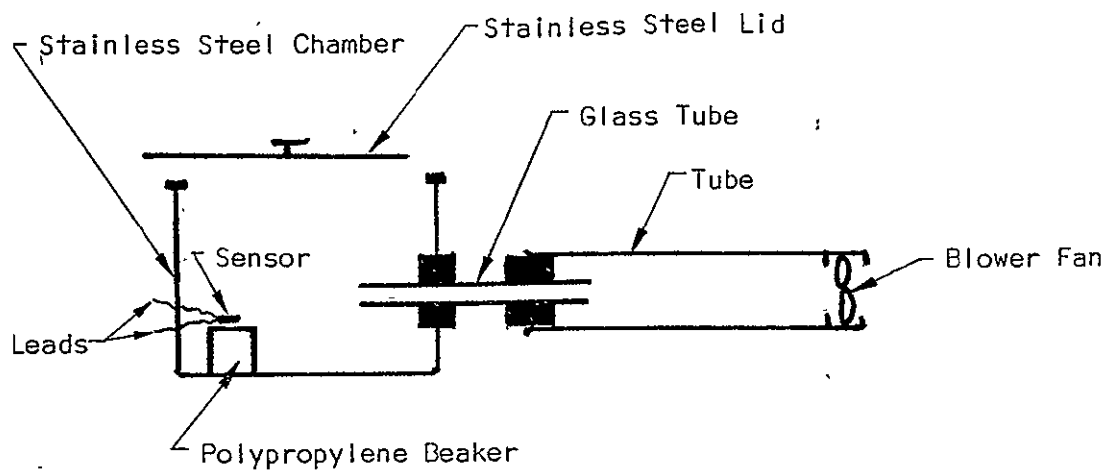
FIGURE 70. - SCHEMATIC DIAGRAM OF CHAMBER AND SENSOR USED IN GAS
MEASUREMENTS.
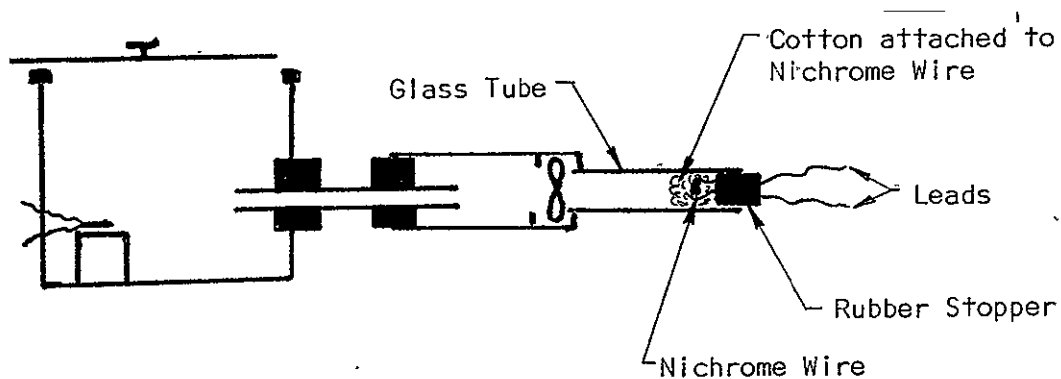


FIGURE 71. - SCHEMATIC DIAGRAM OF CHAMBER, SENSOR AND COIL USED TO GET
SMOLDERING COTTON FIRE.
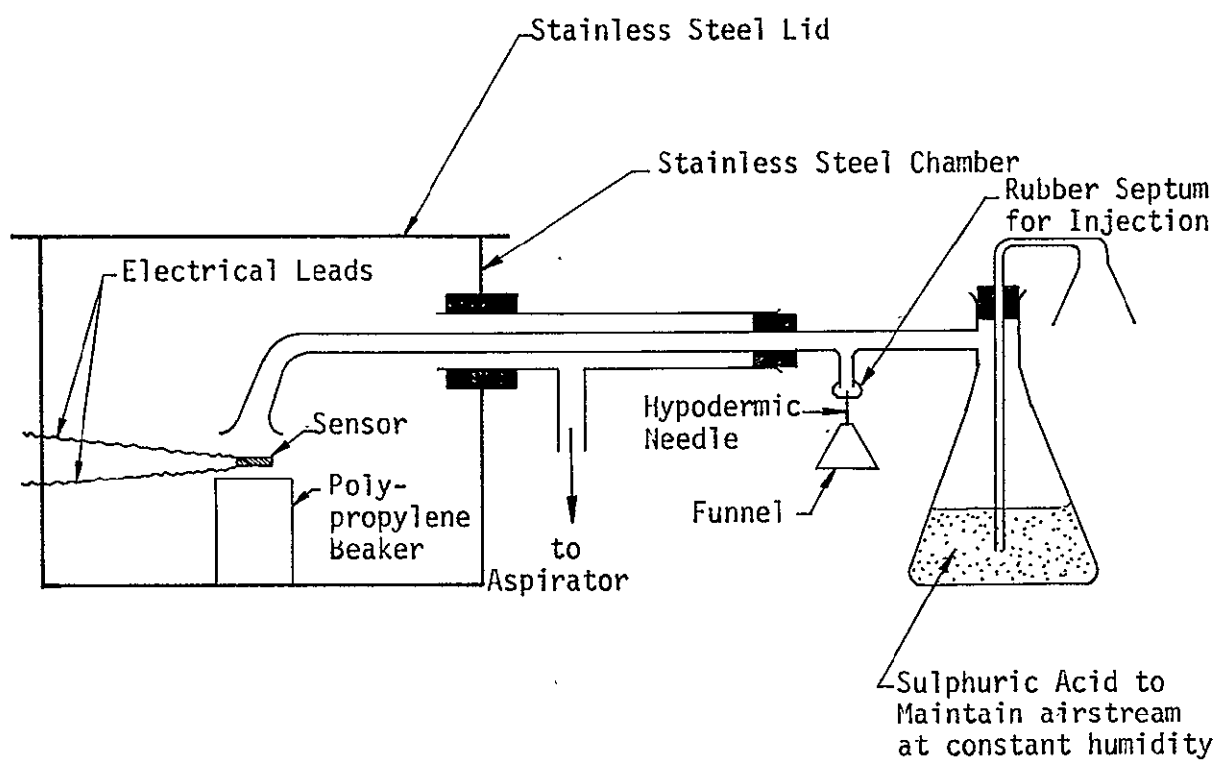
FIGURE 72. MODIFIED SET-UP FOR OBTAINING GAS RESPONSE
DATA UNDER VARIOUS RELATIVE HUMIDITIES    .

Chart Movement ⟶
6"/MIN.

Remove Cigarette

Current
Decrease

Current
Increase

Apply Cigarette

Ignite
Cotton

Extinguish
Cotton

0    10    20    30    40
Time (seconds)

0    10    20
Time (seconds)
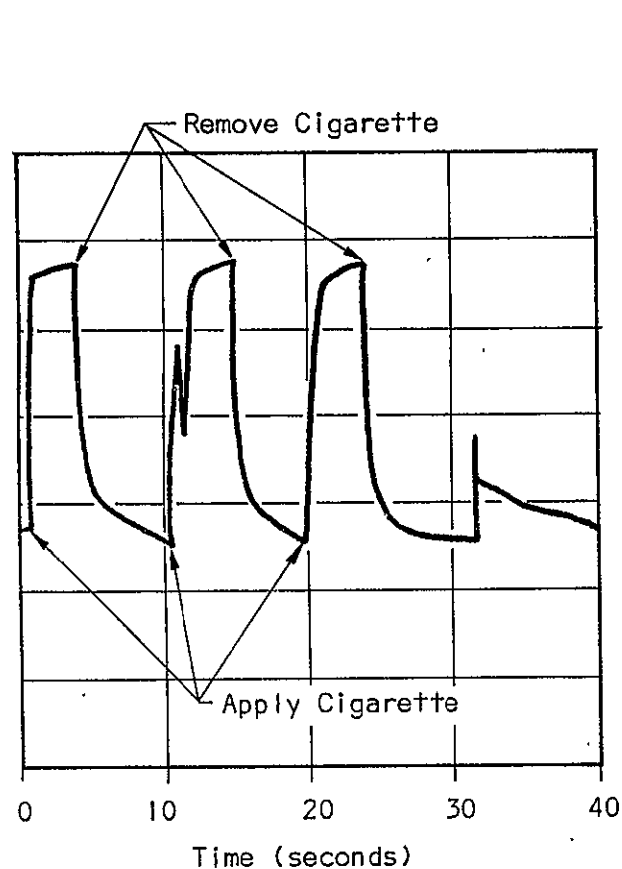
73a CIGARETTE SMOKE CAUSES CURRENT TO DECREASE
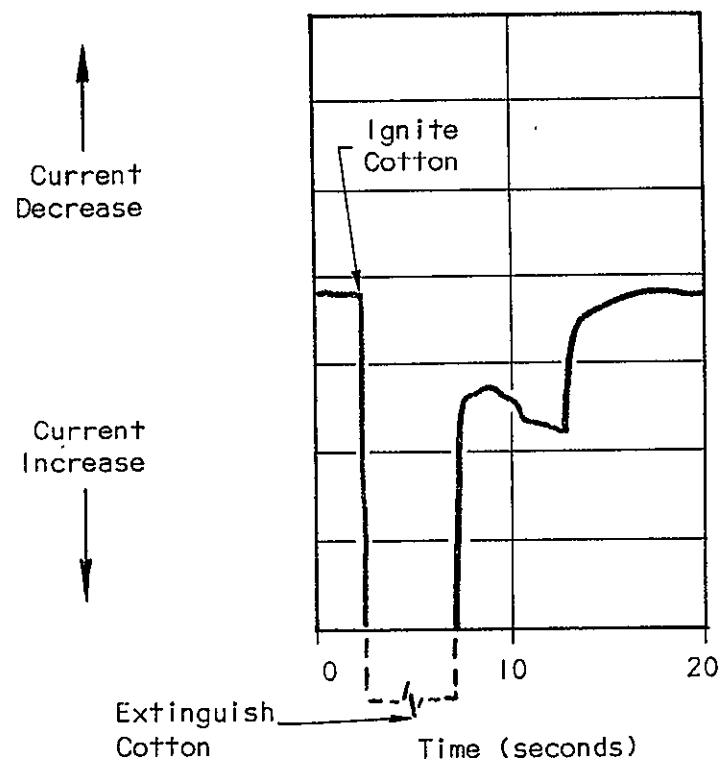
73b COTTON SMOKE CAUSES CURRENT TO INCREASE

FIGURE 73. - STRIP CHART RECORDING OF RESPONSES OF THIOPHENE/IMIDAZOLE POLYMER TO CIGARETTE SMOKE AND
SMOLDERING (BURNING) COTTON.
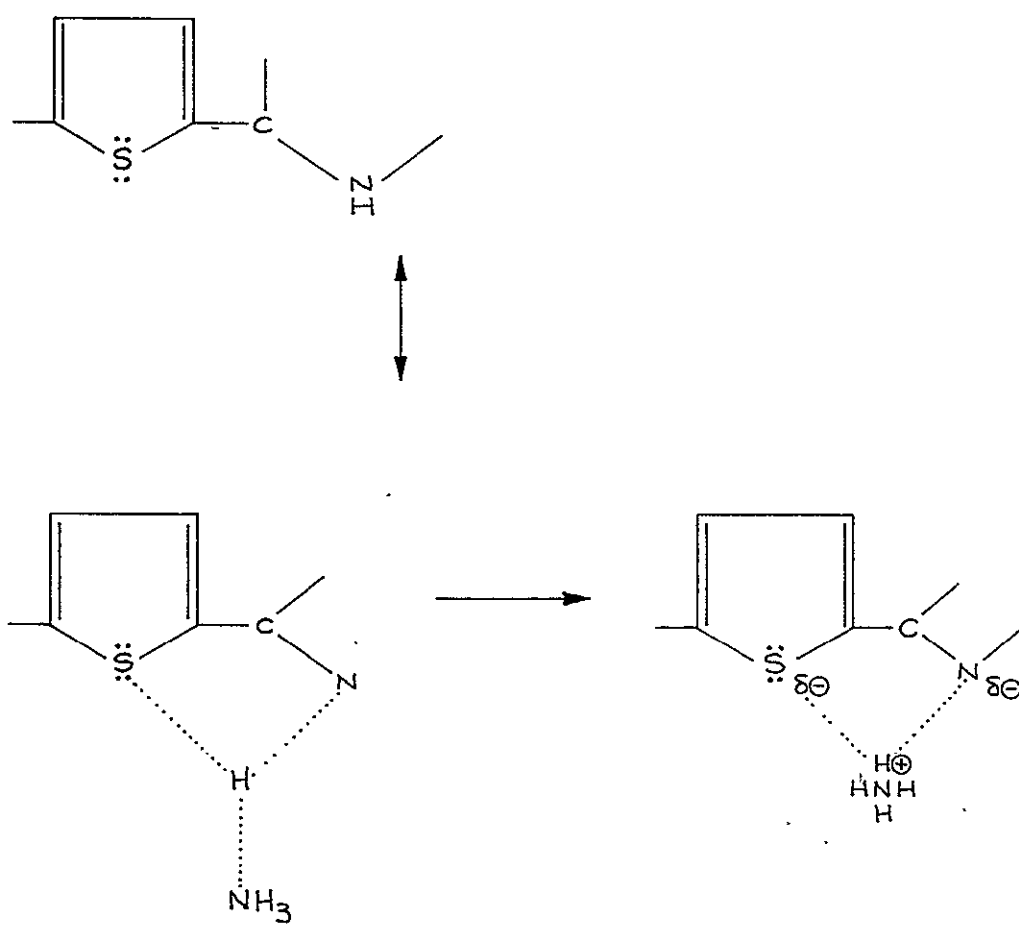
FIGURE 74. INTERACTION OF NH$_3$ WITH DELOCALIZED HYDROGEN IN POLY(IMIDAZOLE)/THIOPHENE

BLANK PAGE

ELECTROMETER

VACUUM
CHAMBER

BATTERY
130 V

TO VACUUM RACK AND GAS INJECTION PORT
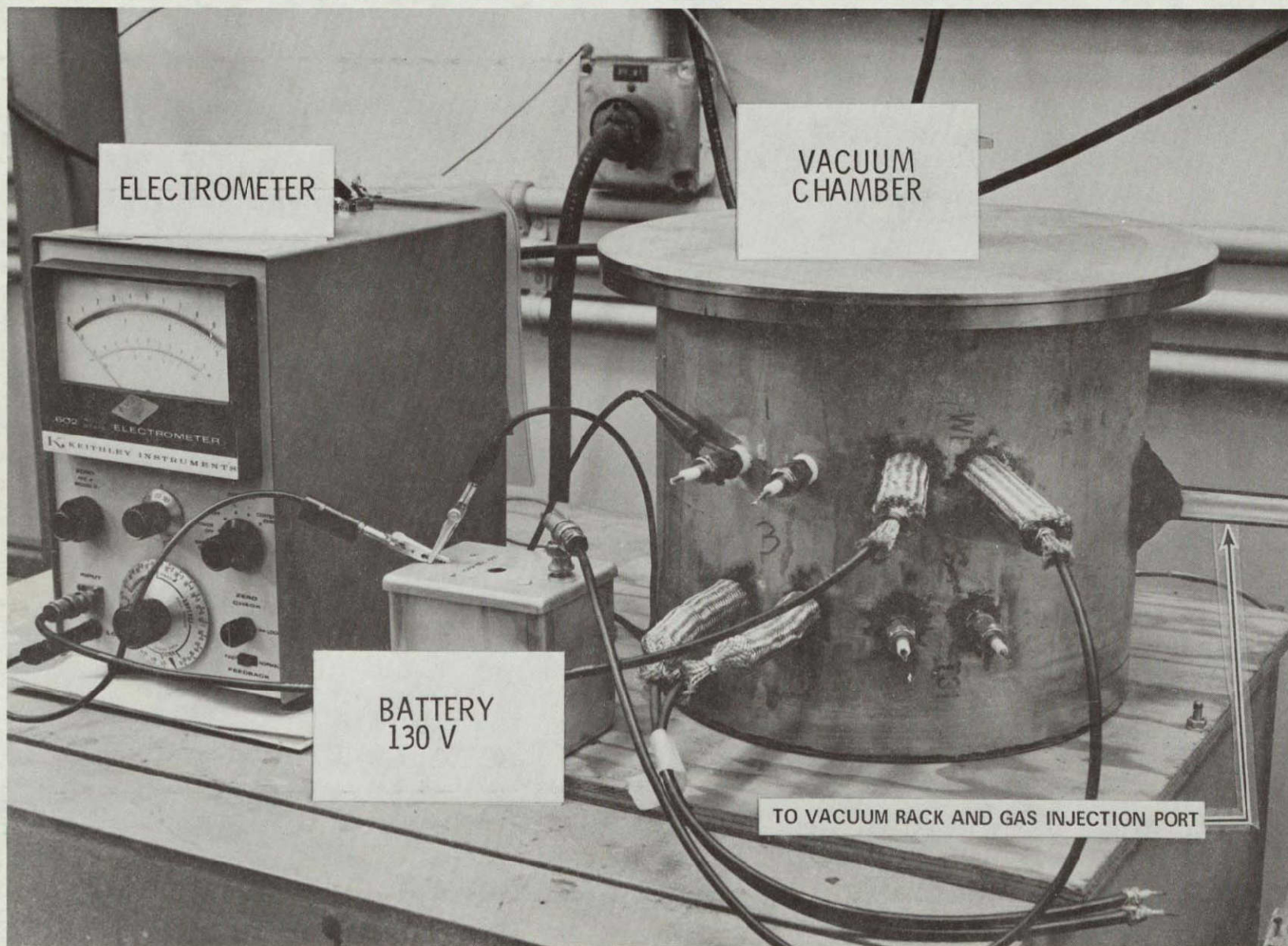
Plate 1.  Vacuum Chamber and Associated Electrical Equipment

**TEFLON SUPPORT SHEET**

**LEADS THROUGH CHAMBER WALL**
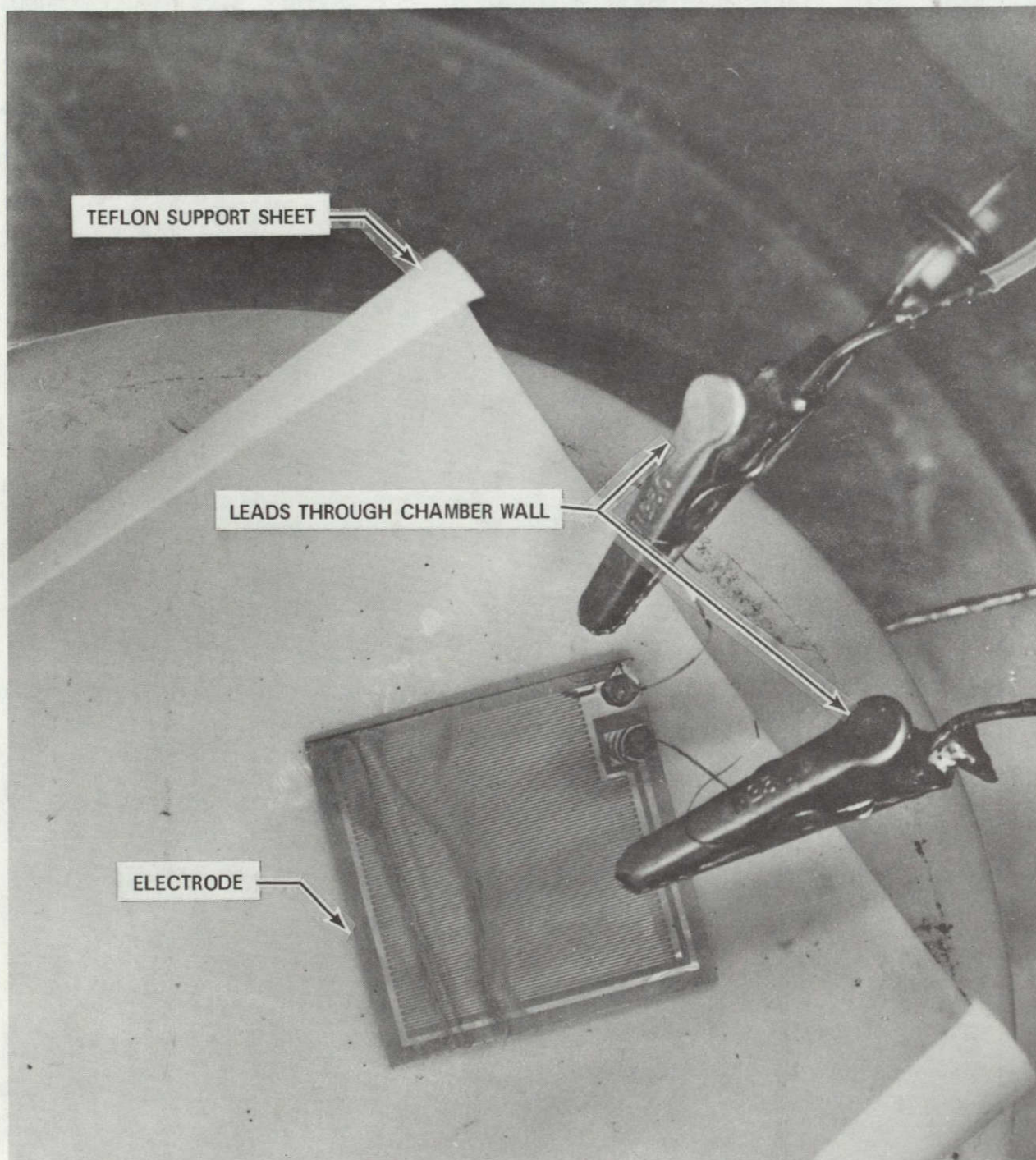
**ELECTRODE**

Plate 2. Interior of Chamber Showing Sensing Electrode (Polymer Coated) Attached to Electrical Leads

GOLD ELECTRODE    GLASS SUPPORT
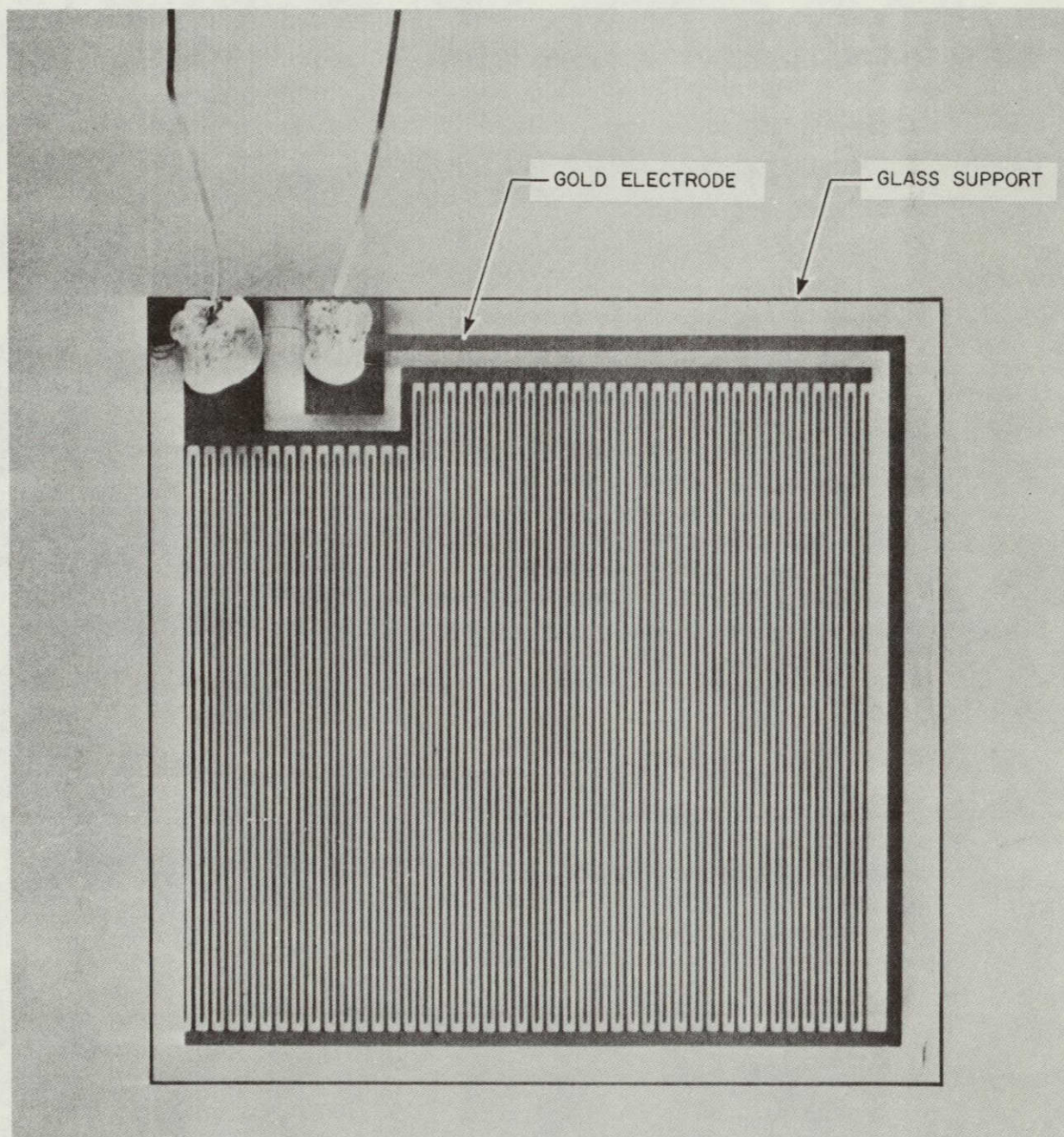
**Plate 3.  Close—up of Uncoated Sensing Electrode**

APPENDIX A

CHARGE-TRANSFER COMPLEXES

# Appendix A
## CHARGE-TRANSFER COMPLEXES

It is one thing for a polymer to have a high degree of conjugation for conduction along the backbone; however, this type of conductivity, especially for interchain effects, can be considerably enhanced with charge-transfer complexes. By-and-large, the greatest number of investigations in organic semi-conductors has been with charge transfer-complexes -either simple organic or polymeric[A1-A4].

In conjugated polyenes, the electron and/or hole migration in an electric field, i.e., the charge carrier, is an intrinsic property of the molecule. In charge transfer complexes, this is not the case. These systems are comprised of mixtures of compounds that are separately insulators, but when combined in a particular ratio demonstrate enhanced conductivity due to an induced delocalization and increased mobility of electrons. For example, anthracene-iodine, p-phenylenediamine-chloranil, quinoline (as the quinolinium ion)-tetracyanoquinodimethan (TCNQ) complexes, and others are representative of the simple organic type of charge-transfer complex, and whose electrical conductivities are as much as six to nine orders of magnitude higher than those of the organic compounds from which they were derived. In all instances, they have involved the combination of compounds that are electron donors and electron acceptors. Among the types of molecular electron acceptors exhibiting the greatest complexing behavior are two similar materials - tetracyanoethylene (TCNE) and the aforementioned TCNQ.

For weak donors and acceptors, the molecular complex AD is formed by ion bonding van der Waals type forces and is, at first approximation, a singlet state with a slight admixture of a state in which electron transfer takes place giving rise to an ionic compound of the type $A^-D^+$. The adduct AD has a characteristic optical absorption spectrum which is found in neither the donor nor acceptor molecule alone. The electron transfer process is assumed to be responsible for the optical absorption which leads to the first

excited level in which the contribution of the ionic state is greater. In a case where the molecules in the complex AD have sufficient donating and accepting power, electron transfer can take place in the ground state. Then the system, besides having characteristic optical absorption, will show paramagnetic behavior and free radical characteristics.

In quantum mechanical terms [A5] the wave function of the ground state of the molecular compound AD can be written as

$$\Psi_T = a\Psi_0 + b\Psi_1 + \ldots \tag{1}$$

where $\Psi_0$ is a non-bond wave function $\Psi(A,B)$ which has the form $\Psi_0 = \Psi(A,B) = \alpha \Psi_A \Psi_B$ and is antisymmetric in all the electrons.

The wave function $\Psi_1$ corresponds to the electron transfer from B to A in the complex such as $\Psi_1 = \Psi(A^-,B^+) + \ldots$ . The $+ \ldots$ sign indicates additional terms in c $\Psi_2$ . . . . However, here the $\Psi_T$ will be approximated by the first two terms alone.

By normalizing $\Psi_T$ so that $\int \Psi_T^2 \, dv = 1$, the coefficients a and b can be related by

$$a^2 + 2ab\,S + b^2 = 1 \tag{2}$$

where

$$S = \int \Psi_0 \Psi_1 \, dv$$

For loose complexes, second-order perturbation theory gives a good approximation. Thus,

$$W_T = \int \Psi_T H \Psi_T \, dv$$

$$\cong W_0 - \frac{(H_{01} - SW_0)^2}{(W_1 - W_0)} + \ \cdots \tag{3}$$

where

$$W_0 \equiv \int \Psi_0 \, H \Psi_0 \, dv ; \quad W_1 \equiv \int \Psi_1 \, H \Psi_1 \, dv$$

and
$$H_{01} \equiv \int \Psi_0 \, H \Psi_1 \, dv$$

H is the exact Hamiltonian operator for the nuclei and electrons in the system.

$W_0$ is equal to the sum of separate energies of A and B, modified by any energy of attraction arising from the interaction of A and B molecules. $W_1$ includes the attraction energy of ionic and covalent bonding.

Then the energy of formation, Q, of the AB complex is given by

$$Q = \left( W_A + W_B \right) - W_T = \left( W_A + W_B - W_0 \right) + \left( W_0 - W_T \right) \tag{4}$$

Assuming that there will be an excited state, the appropriate wave function will be

$$\Psi_E = a^* \Psi_1 - b^* \Psi_0 + \ \cdots$$

$$a^* \approx a ; \quad b^* \approx b \tag{5}$$

and
$$a^{*2} - 2a^* b^* \, S + b^{*2} = 1 \tag{6}$$

and using the approximation of the second-order perturbation theory

$$W_E = W_1 + \frac{(H_{01} - SW_1)^2}{(W_1 - W_0)} + \ \cdots \tag{7}$$

The frequency of the absorption for the molecular complex is given by

$$h\upsilon = W_E - W_T = W_1 - W_0 + \frac{\left(H_{01} - SW_1\right)^2 + \left(H_{01} - SW_0\right)^2}{\left(W_1 - W_0\right)}$$

(8)

Then the strong absorption spectrum can be assigned to the $\Psi_T \rightarrow \Psi_E$ transition.

Further, one can write

$$W_1 - W_0 = I_B - E_A - \left(e^2/r\right) + C_{AB}$$

(9)

where $I_B$ is the ionization energy of molecule B, $E_A$ is the electron affinity of the A and $e^2/r$ is the coulomb energy of the excited state with a separation of charge equal to $r$, and $C_{AB}$ is the difference in energy in the non-bond and ionic bond forms.

The frequencies of the absorption spectrum for several molecular complexes have been found to be in good agreement with the predicted values according to the above theory.

In the case of very strong acceptors, complete electron transfer could occur, and the system becomes paramagnetic in its ground electronic state. For the system in the solid state, charge-transfer interactions are extensive and provide an electron conduction mechanism.

One of the most interesting features of these organic charge-transfer complexes is the semiconduction characteristics found in several systems; the hydrocarbon-halogen complexes[A6] are representative of these systems. These systems are good semiconductors and show strong electron paramagnetic resonance absorption. A detailed study of the EPR characteristics resulted in a complete elucidation of the electronic structure of the complexes and also a correlation between the electrical and magnetic properties. For example, the agreement between the activation energies of spin concentration and conduction for the hydrocarbon-halogen systems

indicated that the unpaired electrons (responsible for the EPR absorption) are the charge carriers in these semiconductors. It has been shown rather clearly that EPR techniques are very useful in studying these systems.

In the case of hydrocarbon-halogen systems, a delocalized $\pi$ electron from the hydrocarbon goes over to a vacant antibonding orbital in the halogen (iodine) molecule. This charge transfer results in the formation of two radical molecular ions. Since these species show EPR absorption, one can perform a detailed study on these systems and hopefully understand the electrical and magnetic properties. Stamires [A7, A8] has done an extensive amount of work in the area of charge-transfer complexes using EPR techniques. In some cases, a hyperfine structure was resolved and radical ions completely characterized, i.e., triphenylamine (donor) - $I_2$ (acceptor), or other amines such as diazabicyclo (2.2.2) octane $(N(CH_2CH_2)_3N)$ with other acceptors, such as, halogens, tetracyanoethylene or chloranil. It appears to be a logical continuation of these types of measurements, therefore that one studies electron transfer reactions between various type of amines and unsaturated conjugated polymeric systems. Amines, in general, are considered good donors.

REFERENCES

A1. Kronick, P. L. and Labes, M. M., in Organic Semiconductors, ed. by Brophy, J. S. and Buttrey, J. W., The Macmillan Co., New York (1962), p. 36.

A2. Kepler, R. G., Bierstedt, P. E. and Merrifield, R. E., Ibid., p 45.

A3. Menefree, E. and Pao, Yoh Han, Ibid., p. 49.

A4. Sehr, R., Labes, M. M., Bose M., Ur, H. and Wilhelm, F., in Symposium on Elecrical Conductivity in Organic Solids, ed. by Kallmann, H. and Silver, M.; Interscience Publishers, New York (1961), p. 309.

A5. Mulliken, R. S., J. Am. Chem. Soc. 74, 811 (1952).

A6. Singer, L. S. and Kommandeur, J., J. Chem. Phys. 34, 133 (1961).

A7. Stamires, D. N. and Turkevich, J., J. Am. Chem. Soc. 85, 2557 (1961).

A8. Ibid., 86, 749, (1964).

APPENDIX B

DECISION MECHANISMS FOR
CONTAMINATION RECOGNITION

# APPENDIX B

## DECISION MECHANISMS FOR CONTAMINANT RECOGNITION

### B.1 Introduction

The development of sensors whose outputs are affected by the presence of a contaminant provides a basis for its detection. The exploitation of this basis requires the development of a mechanism which will combine the information provided by several sensors to provide a decision concerning the presence of contaminant. The approach to be taken in specifying the decision mechanism depends on the exact nature of the operational environment, the number and similarities of the contaminants to be encountered, and the efficacy of the sensors. In the following pages, a variety of different decision mechanisms will be discussed for situations of increasing complexity. It is anticipated that the actual situation will be more complex than any of these listed, and will require the most sophisticated techniques available for generating a decision mechanism.

### B. 2 Standard Uncontaminated vs Standard Contaminated Atmosphere Problem

The simplest situation envisioned for a contaminant recognition device is one in which the environment has but two states, a standard atmosphere and a standard atmosphere with a single contaminant in standard quantity. To further idealize this system, assume absolutely accurate sensors, so that each sensor will take on one and only one value for each of the two states of the environment. This situation is illustrated by the geometric interpretation of Figure B-1. A space may be defined from the voltage readings of the sensors. The standard uncontaminated atmosphere is represented in this space as a point, whose coordinates are the values of the sensors output measurements when exposed to this standard atmosphere. Similarly, the contaminated atmosphere is symbolized as another point in the space, defined by the output readings it produces in the sensors. A decision in this simplified case consists of determining which of the two environmental states coincides with the actual measurement point.

A simple mechanism to solve this problem is diagramed in Figure B-2. The sensors are shown on the left side of the page. Each sensor drives a binary device that is "on" for the reading given by the contaminated atmosphere and "off" for the reading given by the uncontaminated atmosphere. (Such binary operation may be

achieved, of course, by proper design of the sensors without external hardware.)
Two diode logic gates are shown; one responds positively for contaminated atmos-
pheres, and one responds positively to uncontaminated atmospheres. Either can
be implemented with one resistor, one diode per sensor, and one amplifier.

B. 3 Statistical, Standard Single Contaminant Problem .

The simplest generalization of this example merely assumes statistical variations
from standard values. Such variations might arise from measurement errors in the
sensors, or from statistical variations in atmospheric composition. The geometric
interpretation of this problem is shown in Figure B-3. A number of different
measurement values may actually be recorded, and they are distributed in some
fashion about the ideal measurement values.

A probability distribution can be assigned to give the probability of each set
of measurements which may be encountered under the conditions of presence or
absence of the contaminant. Such a distribution may be described by moments,
such as means and variances, measurable from experimental samples.

This situation has been studied in great detail. The Neyman-Pearson lemma
provides an optimum decision mechanism. One selects the decision; contaminated
or uncontaminated, which, if true, would provide the highest probability to the
actual observed measurements.

To delineate the regions in the measurement space which are to be associated with
the decisions contaminated and uncontaminated, the statistical distributions must
be known in detail. A standard procedure is to assume a form for these distri-
butions, such as Gaussian, while leaving a number of moments of these distributions
unspecified. The estimation of these moments from sample data provides the
decision boundary.

A very common assumption is that the distributions are both Gaussian with different
mean vectors, but equal covariance matrices. Such an assumption gives rise to a
linear decision boundary, illustrated in Figure B-3 by a straight line. Linear
surfaces in multidimensional spaces (the dimensionality is equal to the number
of sensors) is called a hyperplane. The linear function describing the hyperplane
is called a linear discriminant, for points on one side of the hyperplane give
positive values of the function.

The hardware implementations of the lineal discriminant may be accomplished inexpensively by means of circuits, such as those diagramed in Figure B-4. Using Ohms law:

$$I = E/R \qquad\qquad\qquad\qquad (B-1)$$

it can be seen that the current, I, supplied by each sensor to the summing device is the product of the voltage, E, generated by the sensor and the conductance, 1/R, of the weighting resistance. Using the coefficients in the discriminant to specify these conductances, a sum greater than some threshold is produced for points above the discriminant and less than the threshold for points below the discriminant. The decision element, therefore, is required only to compare the sum with the threshold to perform its binary classification.[1,2]

## B.4 Single Contaminant of Varying Concentration Problem

The shortcomings of the mechanisms, described above, stem from the simplified nature of the assumed situation. By adding complexities to the simplified situation, one may observe the increases in complexity, and lack of precision in the decision mechanism. The next complexity to be introduced is variability in the concentration of a single contaminant. When this complexity is introduced, the Neyman-Pearson lemma no longer provides an optimum decision mechanism. The mechanism, suggested below, is one of many possible schemes, but has the virtue of being reasonable and easily implemented. It illustrates a decision boundary which might result if it is assumed that there is a large cost associated with declaring a pollutant present when it is actually not present.

The vector associated with a particular contaminant may be considered as a point on a locus, for with increasing concentrations the measurement vector should be expected to move in a lawful manner away from the standard atmosphere's derived point. This is illustrated in Figure B-5, where the measurements obtained with increasing concentration of the pollutant are shown as increasingly distant from that obtained with the standard atmosphere. A simple linear locus, as illustrated, may actually be a good first approximation to those found experimentally, if the sensors have similar response curves and the overall range of contaminant concentrations is low.

It deserves explicit statement that the situation here is different in nature from those of the preceding example. The outputs of each sensor vary over wide ranges of values, so that the actual reading from any of the sensors alone would be expected to be a poor indicator of the presence of the contaminant. However, the locus of points described by the measurements of the contaminated atmosphere is depicted by a mathematical formula. For the sensor 2 case, illustrated:

$$S_2 - S_{o2} = m (S_1 - S_{o1}) \hspace{3cm} \text{(B2)}$$

is the formula of a straight line. In this functional definition, the parameter, m, is determined by the contaminant present, and serves to identify it. The complex decision devices, discussed from this point on, operate on this specification of the relationship between different sensor measurements, rather than on the measurements themselves.

Returning to the geometric model of the problem, a recognition criterion for such a locus of measurements may be of the form shown in Figure B-6. The classification region is defined by a number of hyperplanes. One hyperplane recognizes that a measurable deviation from the standard atmosphere must be present for identification of contamination. Other hyperplanes encompass the contamination measurement locus and an area around it to allow for statistical variations from the ideal measurements.

This geometric form, generated by the hyperplane, is suggested because of the ease of implementation of hardware for its achievement. The mechanization of this decision device is illustrated in Figure B-7.

## B.5 Simultaneous Multiple Contaminant Problem

Even when the locus of vectors associated with a single contaminant is a straight line, the actual locus traveled by a set of sensors in operation may be quite complex. If combinations of two or more contaminants may be encountered, the set of possible vectors becomes planar, or higher dimensional, rather than a straight line. Again, this may be illustrated by reference to the simplified two-dimensional geometric model, Figure B-8. Here the sets of measurements of vectors for each of two different contaminants are shown, and the entire area between them is shown as possible measurements achieved by combinations of the two contaminants in the atmosphere. (In cases where further reactions occur in the joint presence of two contaminants and the sensor compounds, this set can be even more complex.) If the sets of measurements for different combinations of contaminants do not overlap, the situation may be handled with the simple combination of hyperplanes and the simple two-level discriminant devices described above. Such a set of discriminants is diagramed in Figure B-9. This, however, is a strong requirement on the measurement space. It means that there can exist no two different sets of contaminants capable of producing the same measurement vector, even with statistical variation. Utilizing very large numbers of independent sensors, so that the measurement space may be expected to be very sparsely populated, provides an approach toward achieving this end for discrete

concentration levels. This technique is quite difficult in the early stages of sensor research.

The restriction of sensor linearity may be reduced by providing more complex discriminant devices. One possibility would be to measure the rate of change of contaminant concentrations, and integrate over time to determine the actual concentrations. When the introduction of contamination is a random infrequent process, with contaminants being introduced independently, this technique should be quite effective. Similarly, the second derivatives can be measured to provide accurate contaminant records even when several contaminants are introduced simultaneously, if the rates of introduction are independent, continuous-random variables. The implementation of such a scheme would necessarily be at least partially digital (done perhaps by a control computer), since long-term integration necessitates digital storage. However, the actual measurements of contamination rates could be accomplished by resistance networks similar in structure to those of the simple discriminant devices.

To illustrate this kind of operation, a geometric model is shown in Figure B-10. Here a standard atmosphere was present for the first eight measurements of the system, and then a concentration of contaminant began to build. The concentration. achieved steady state by the 12th sample time, and the system stayed in steady state until the 20th sample, after which contaminant began to add to the contamination. Again, steady state was achieved by the 23rd sample and was not disturbed until the 30th sample when contaminant became evident. This may be observed from the slopes of the changes in measurement vectors. The important fact is that, for all measurements after the 20th sample, the actual measurement point could have been achieved by a wide variety of different combinations x, y, and z, and the uncertainty was eliminated by a record of the history of the system.

If one desires to avoid the digital hardware necessitated by the historical approach, or if the system is not well behaved enough to make such records useful, or if the historical records are not available for some reason, the only alternative left is to use more classification regions. and more powerful techniques for their design.

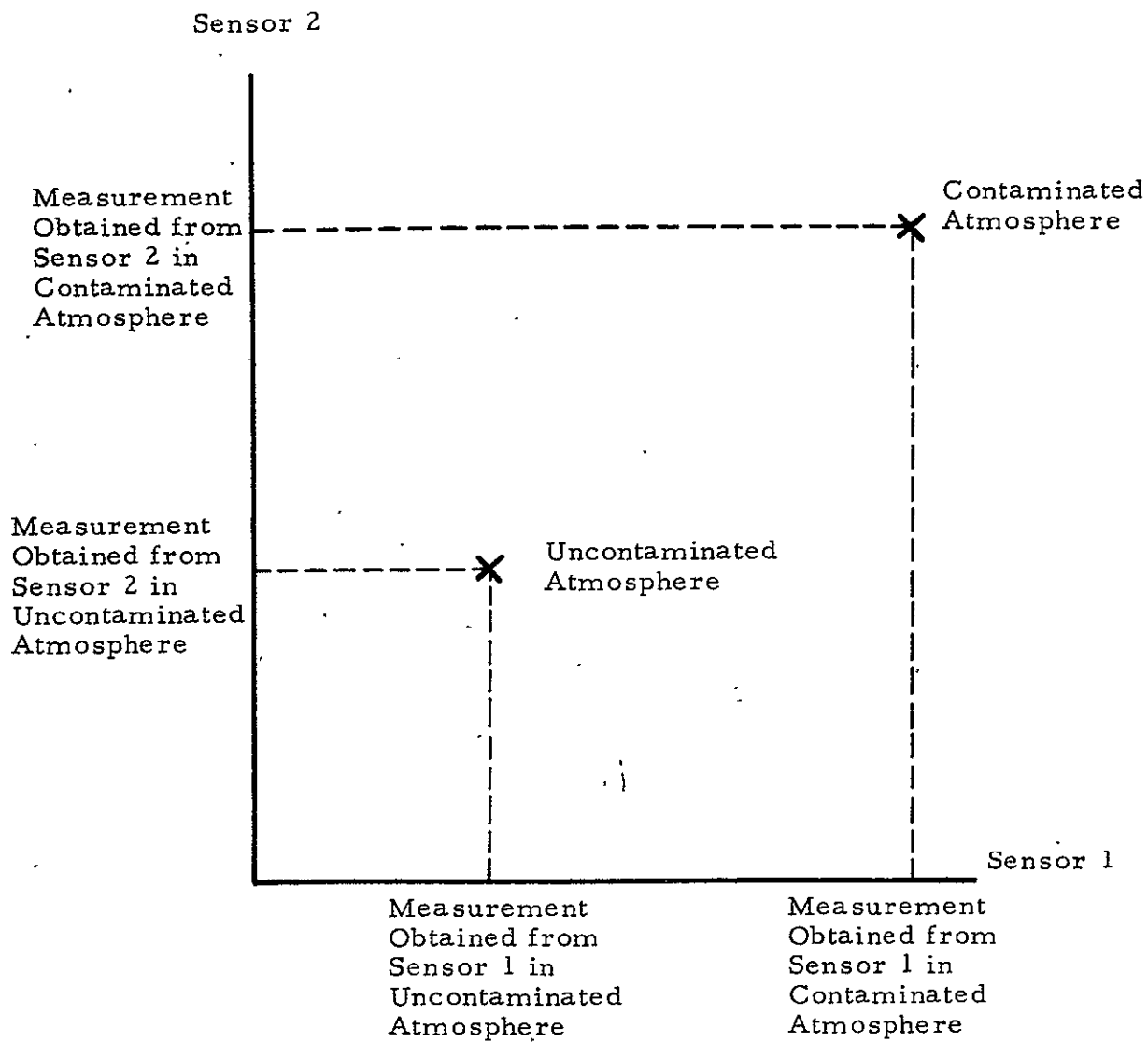## B.6  General Classification Problem

The most sophisticated of current discriminant analytic techniques, for the partitioning of a measurement space into regions identified with classes of

136

inputs have been developed (References 3 and 4). Their use to provide the most likely classifications of contaminants on the basis of the set of organic semi-conductor sensors is virtually mandatory for early systems research which may be expected to depend on relatively few sensors, yet must be required to respond to a wide variety of envrionmental conditions and to specify a fair number of distinct contaminants.

The techniques which have been developed use polygonal classification regions, generated by iterative, non-parametric statistical analyses, that may be implemented on digital computers. Measurement samples are taken on the environment in which the machine is to operate, and classified. The sample of such measurements must be large to provide reliability in the machine design. A cost function is defined, taking into account the cost of errors and the probability of marginally correct classifications being turned into errors due to system degradations. A hyperplane is generated which minimizes the cost with respect to all the classifications desired. Another hyperplane is then generated to minimize the remaining cost, and the two are combined in an optimal fashion. The process continues to generate hyperplanes to minimize the remaining cost, and to integrate the hyperplanes into the optimum polygonal discriminant.

The form of polygonal discriminants was selected for easy implementation by two-level resistor-transistor-logic systems, such as that shown in Figure B-7. For small numbers of required hyperplanes, and suitable restrictions on these hyperplane, these are relatively inexpensive and reliable mechanisms capable of complex and fine discrimination in real time. Recent work (Reference 1) has developed a modification of these mechanisms more efficient for complex polygonal discriminants. For still more complex techniques, general purpose digital computers are the mechanization of choice. Douglas Aircraft Co. has also had considerable experience in studies of these systems (Reference 5).

Figure B-1. Geometric Interpretation of the Idealized Standard
Atmosphere vs Standard Contaminant Problem

"ON" if Atmosphere
Contaminated

"OFF" Otherwise

Output =

"ON" if Atmosphere
Uncontaminated

"OFF" Otherwise

Output =

Sensors

Binary
Devices

Diode

Output = {
"ON" if the sensor output is that
for contaminated atmosphere

"OFF" if the sensor output is that for
uncontaminated atmosphere
}
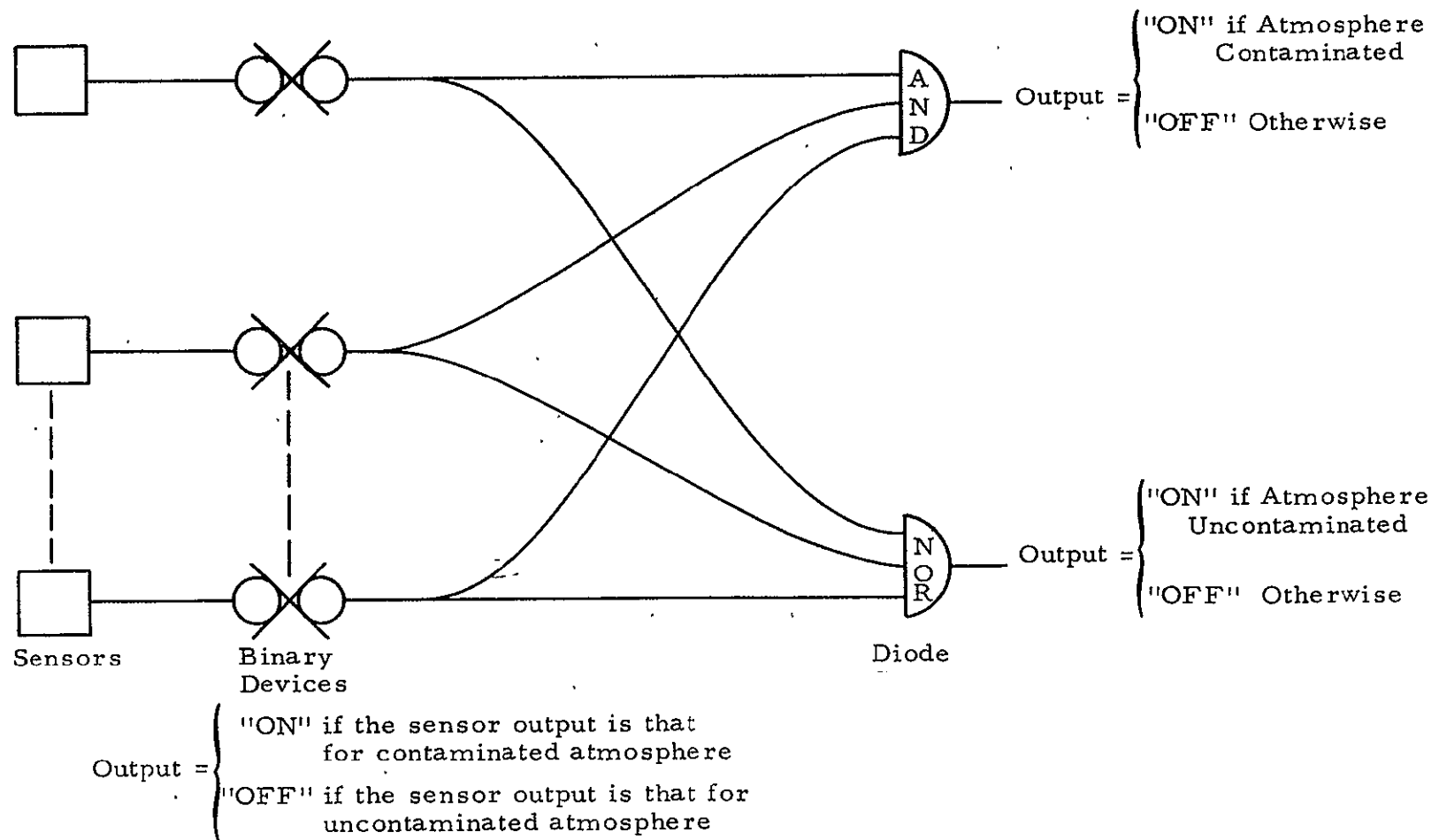
CO368

Figure B-2.  Sample Mechanization for Standard Atmosphere -
Standard Contaminant Problem
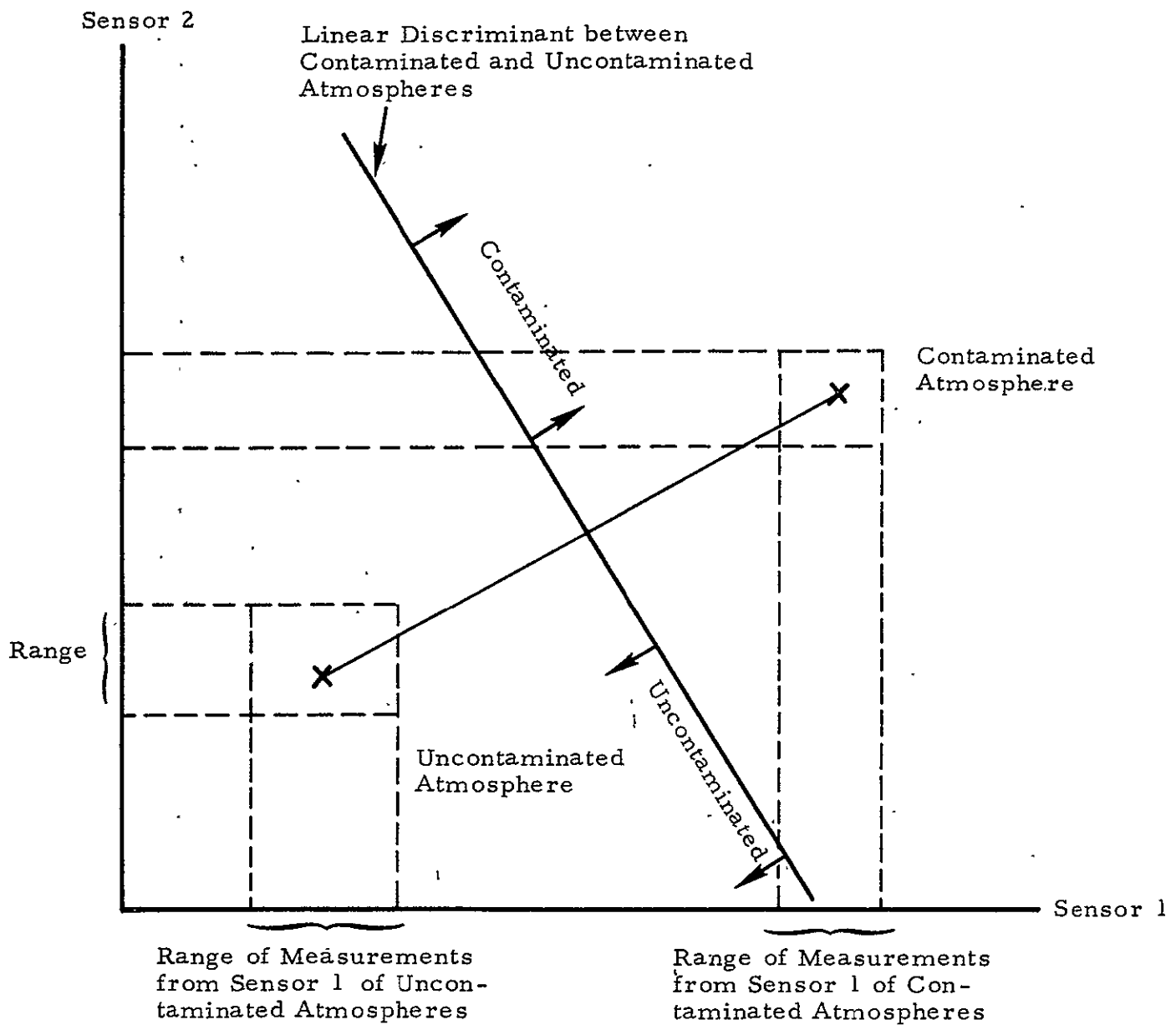
Figure B-3.   Geometric Interpretation of Statistical Standard
Atmosphere vs Standard Contaminant Problem

*CO367*

| Sensors<br>(Voltage<br>Generating) | Resistor<br>Weighing<br>Network | Summing<br>Device | Binary Decision<br>Element |
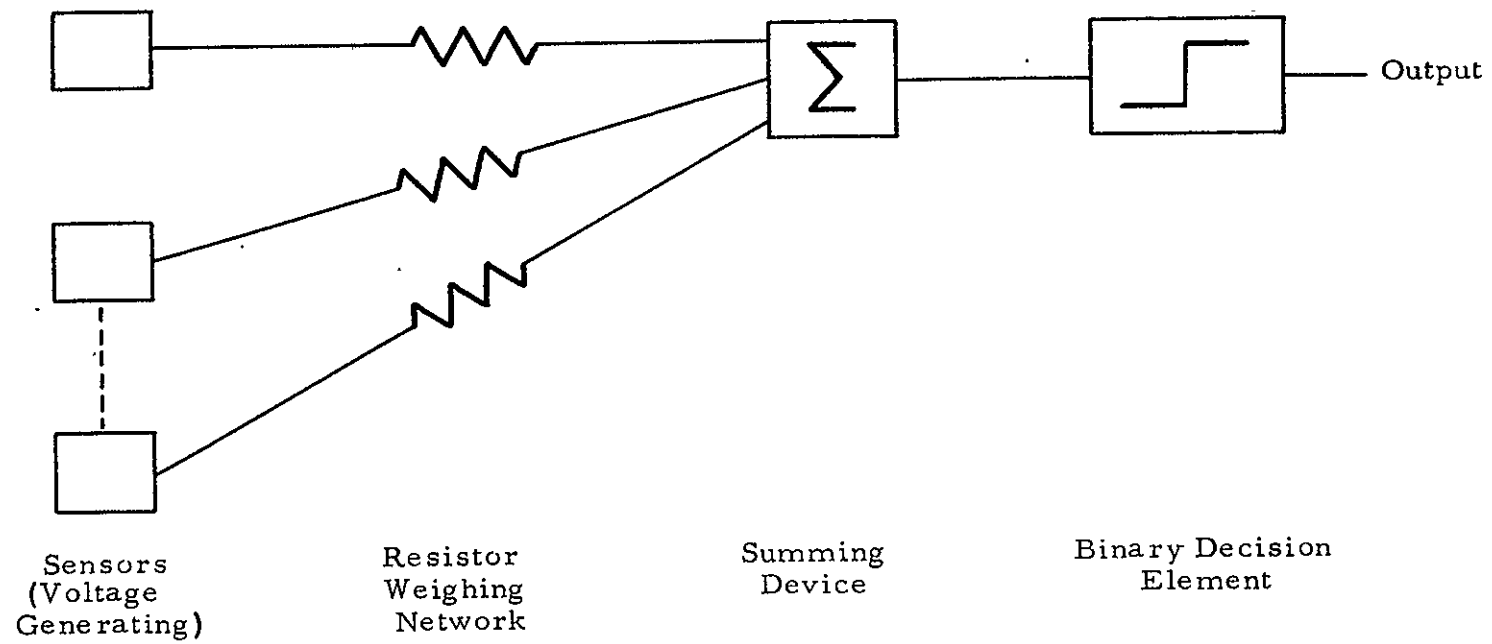
Figure B-4.   Diagram of Linear Discriminant Device
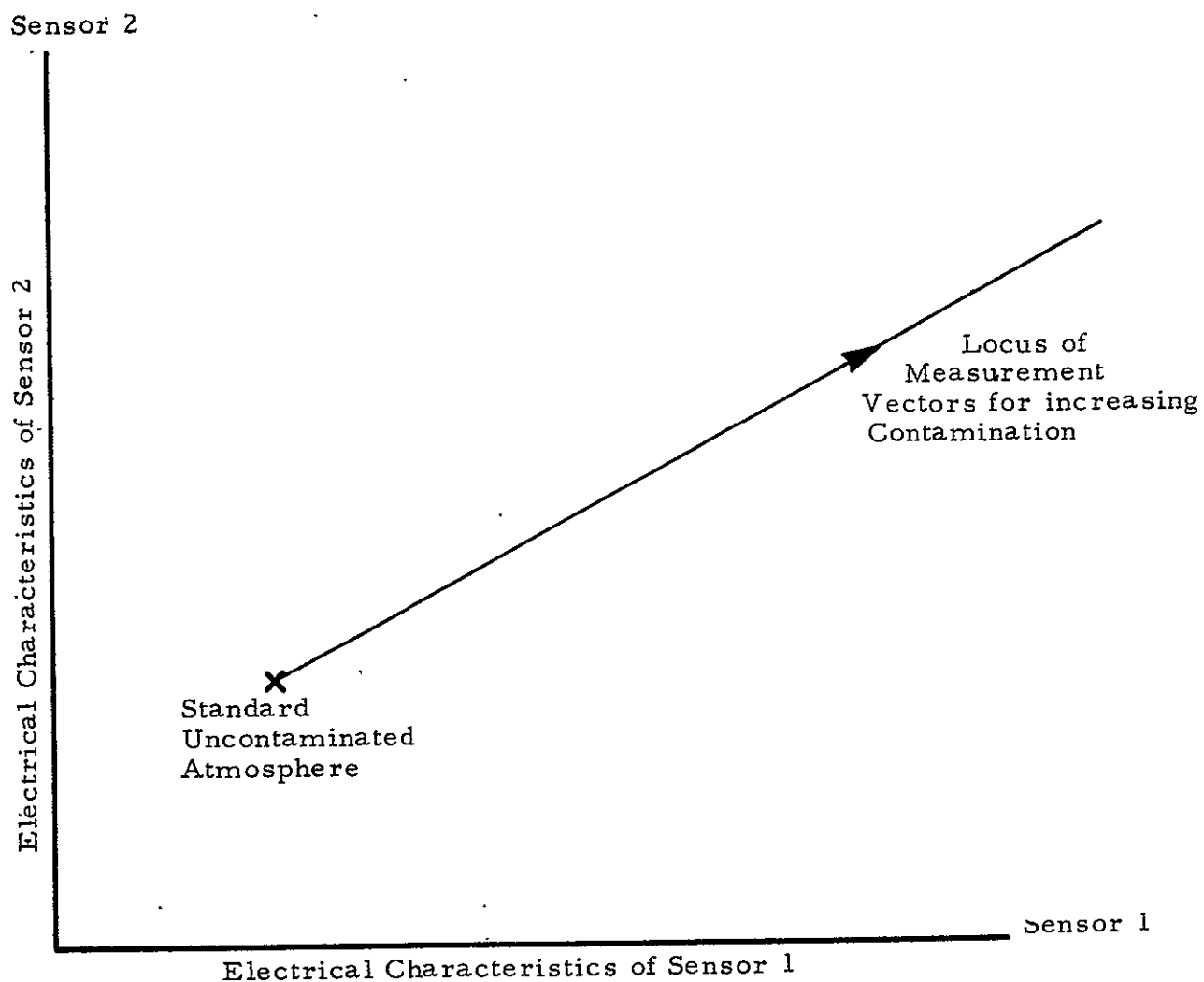
Figure B-5. Locus of Measurements for Increasing Concentration of
a Single Contaminant in a Standard Atmosphere
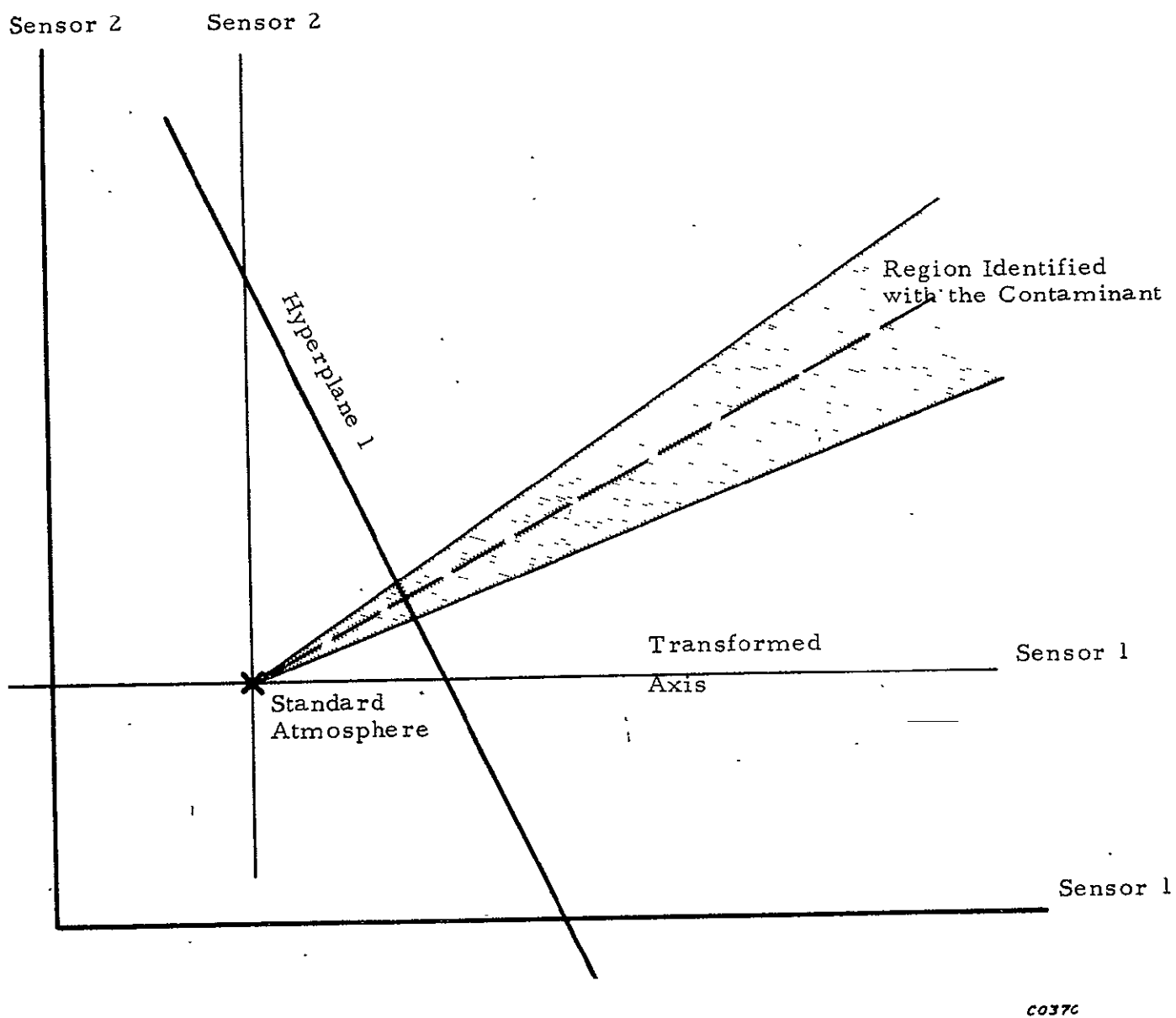
Figure B-6.  Classification Region for Recognition of
a Signal Contaminant of Variable Concentration
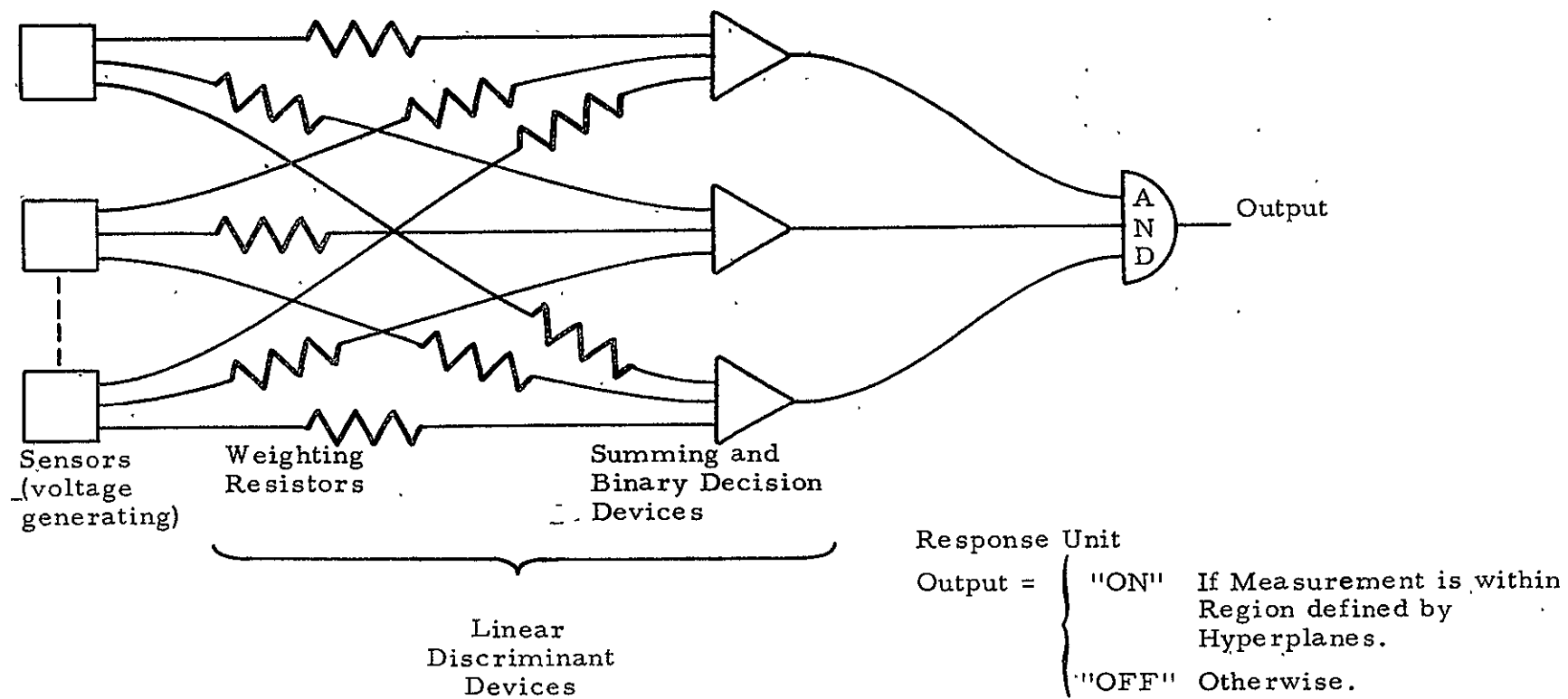
Figure B-7. Diagram of Discriminant Device for Recognition of a Single Contaminant of Variable Concentration
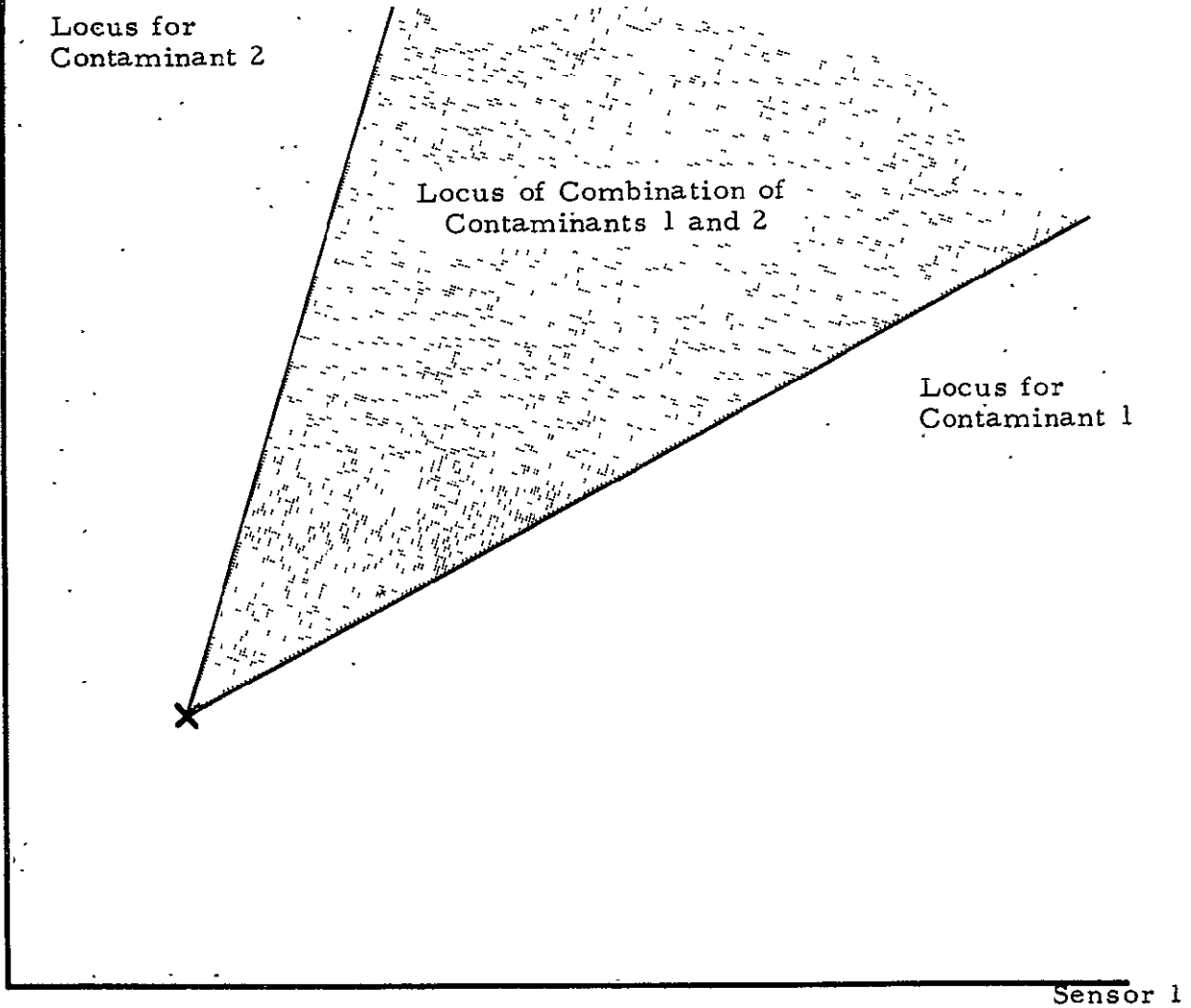
Figure B-8. Locus of Measurements Possible with Combinations of
Two Different Contaminants
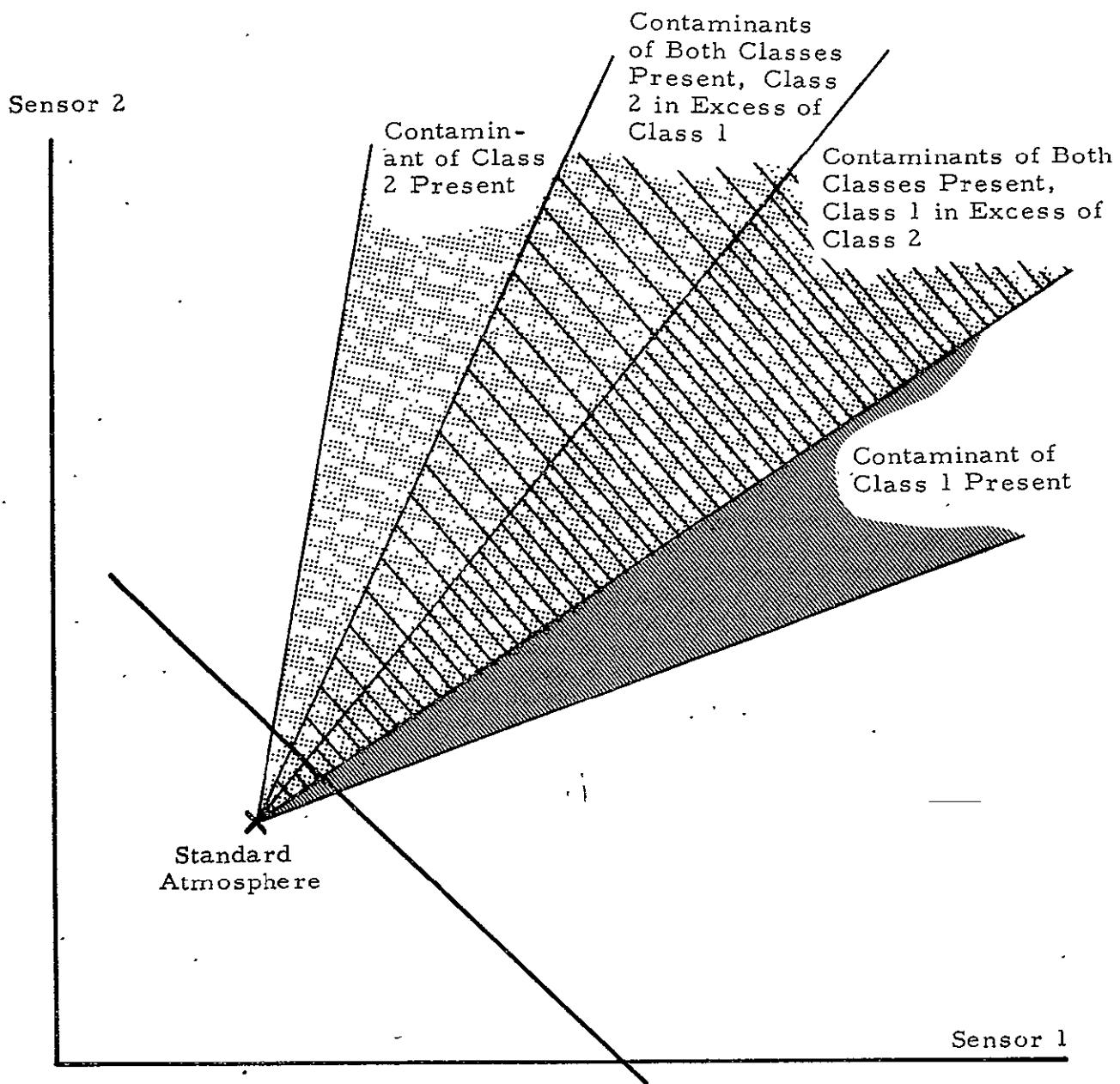
Figure B-9. Classification Regions for Simple Two
Contaminant Problem
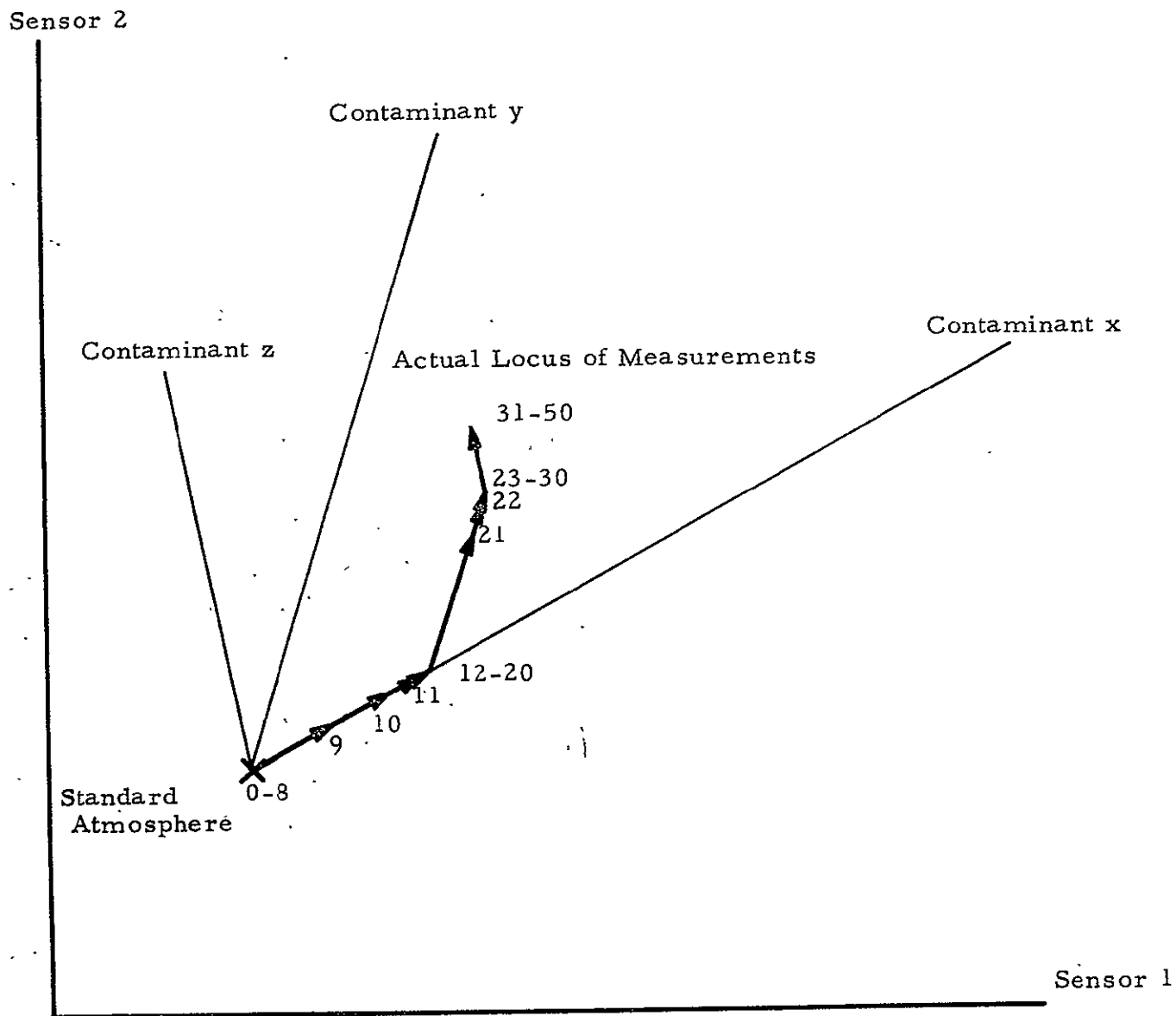
Figure B-10.  Example of Possible Locus of Measurements Taken in a System with Three Possible Contaminants

# APPENDIX B

## REFERENCES

1. Astropower Laboratory, Douglas Aircraft Co. - RADC-TDR-64-206 <u>Adaptive</u> <u>Techniques as Applied to Textual Data Retrieval</u>, Chapter 5, "Hardware Considerations"

2. Joseph, R. D.; Kelly, P. M.; Vigilone, S. S. "An Optical Decision Filter," <u>Proc. IEEE 51</u> (1963) p. 1098

3. Astropower Laboratory, Douglas Aircraft Co. - RADC-TDR-64-206 <u>op.cit.</u> App. IX, "Pattern Recognition Using Time-Varying Theshold Logic"

4. Daly, J. A.; Joseph, R. D.; Ramsey, D. M. <u>An Iterative Design Technique for Pattern Classification</u>, presented WESCON, San Francisco 1963

5. Joseph, R. D.; Vigilione, S. S.; Wolf, H. F. <u>Cloud Pattern Recognition,</u> Astropower Laboratory; Douglas Aircraft Co. paper, TP-1967 presented ACM. Philadelphia (Aug. 25, 1964)

## REFERENCES

1. Byrd, N. R., _Space Cabin Atmosphere Contaminant Measurement Techniques,_ Contract NAS12-15, NASA Electronics Research Center, Cambridge, Mass., Report SM-48446-F, NASA CR-86047, July 1968.

2. Byrd, N. R. and Sherattte, M. B., _Synthesis and Evaluation of Polymers for Use in Early Warning Fire Alarm Devices,_ Contract NAS3-17515, NASA Lewis Research Center, Cleveland, O., Final Report, NASA CR-134693, February 1975.

3. Senturia, S. D., _Fabrication and Evaluation of Polymeric Early-Warning Fire-Alarm Devices,_ Contract NAS3-17534, NASA Lewis Research Center, Cleveland, O., Final Report, NASA CR-134764, 1975.

4. Labes, M. M. and Rudyj, O. N., J. Am. Chem. Soc. _85,_ 2055 (1963).

5. Reucroft, P. J., Rudyj, O. N. and Labes, M. M., Ibid, 2059 (1963).

6. Heilmeir, G. H., _Discussion Seminar on Organic Semiconductors, Stanford University,_ June 5-6 (1964).

7. Schneider, W., Ibid.

8. Aftergut, S., Ibid.

9. Terenin, A., Proc. Chem. Soc., _1961,_ 321.

10. Alexander, E. R., _Principles of Ionic Organic Reactions, John Wiley_ and Son, Inc., New York (1950), P. 155.

11. Garrett, C. G. B., in _Semiconductors,_ ed. by Hannas, N. B., Reinhold Publ. Co., New York (1959), pp. 640-641.

12. Bijl, D., Kainer, H and Rose-Innes, A. C., J. Chem. Phys. _30,_ 765 (1959).

13. Kainer, H., Bijl, D. and Rose-Innes, A. C., Naturwissenchaften _41,_ 303 (1954).

14. Matsunaga, Y., J. Chem. Phys. _30,_ 855 (1959).

15. Krieg, B. and Manecke, G., Makromol. Chem _108,_ 210 (1967).

16. Osgerby, J. M. and Pauson, P. L., J. Chem. Soc. _1961,_ 4607.

17. Zeschmar, W., Brit. Pat. 1, 149, 293 (1970).

18. Garrett, C. G. B., Radiation Res. Suppl. _2,_ 340 (1960).

19. Byrd, N. R. and Sheratte, M. B., _Semiconducting Polymers for Gas Detection,_ Contract NAS3-18919, NASA Lewis Research Center, Cleveland, O., First Quarterly Progress Report for the Period 28 June 1974 - 29 September 1974.

20. Mochalin, V. B. and Ivanova, N. G., Zh. Obsch. Khim. _32,_ 1493 (1962).

21. Gilman, H. and Morton, J. W. in _Organic Reactions,_ ed. by Adams, R., Vol. 8, John Wiley and Sons, New York (1964), p. 285.

22. Gol'dfarb, Ya., et al. Ivz. Akad. Nauk. SSSR Ser. Khim _1963,_ 2172.

23. Ogliaruso, M. A. and Becker, E. I., J. Org. Chem. _30,_ 3358 (1965).

24. Linstead, R. P. and Elridge, J. A., J. Chem. Soc. _1952,_ 5000.

25. Zechsmar, W., Swiss Pat. 484,216 (1967).

26. Griffin, R.N., _Development of High Temperature Resistant Graphite Fiber Coupling Agents,_ Contract NAS3-17788, NASA Lewis Research Center, Cleveland, O., Final Report, 1975, NASA CR-134725.

BLANK PAGE

# REPORT DISTRIBUTION LIST

| Addressee | | Number of Copies |
|---|---|---|
| | | |

1. National Aeronautics & Space Administration
   Lewis Research Center
   21000 Brookpark Road
   Cleveland, Ohio 44135

| Attn: | Contracting Officer | MS 500-313 | 1 |
|---|---|---|---|
| | Technical Report Control Office | MS 5-5 | 1 |
| | Technology Utilization Office | MS 3-16 | 1 |
| | AFSC Liaison Office | MS 4-1 | 2 |
| | Library | MS 60-3 | 2 |
| | Office of Reliability and Quality Assurance | MS 500-111 | 1 |
| | G. M. Ault | MS 3-13 | 1 |
| | R. H. Kemp | MS 49-1 | 1 |
| | Polymer Section | MS 49-1 | 15 |
| | H. L. Dore | MS 49-1 | 1 |
| | R. W. Hall | MS 49-1 | 1 |
| | J. C. Freche | MS 49-1 | 1 |
| | H. Allen, Jr. | MS 3-19 | 1 |
| | P. E. Foster | MS 3-19 | 1 |
| | S. Weiss | MS 6-2 | 1 |

2. National Aeronautics & Space Administration
   600 Independence Avenue, S.W.
   Washington, D. C. 20546

| Attn: | J. T. Hamilton (HQ/KT) | 1 |
|---|---|---|
| | J. T. Wakefield (HQ/KT) | 1 |
| | W. L. Smith (HQ/KT) | 1 |
| | L. Sirota (HQ/KT) | 1 |
| | R. J. Miner (HQ/KT) | 1 |
| | R. G. Bivens | 1 |
| | B. G. Achhammer (HQ/RWM) | 1 |
| | W. L. Hanbury (HQ/DDS) | 1 |
| | G. Morgan (HQ/DBS) | 1 |
| | J. Marsh (HQ/MHE) | 1 |
| | J. H. Enders (HQ/ROO) | 1 |

3. National Aeronautics & Space Administration
   Scientific & Technical Information Facility
   Acquisitions Branch
   College Park, MD                                              10

4. National Aeronautics & Space Administration
   Ames Research Center
   Moffett Field, California 94035                                1

   Attn:  John Parker

| Addressee | Number of Copies |
|---|---|

5. National Aeronautics & Space Administration      1
   Flight Research Center
   P.O. Box 273
   Edwards, California 93523

   Attn: Library

6. National Aeronautics & Space Administration      1
   Goddard Space Flight Center
   Greenbelt, Maryland 20771

   Attn: Library

7. National Aeronautics & Space Administration      1
   John F. Kennedy Space Center
   Kennedy Space Center, Florida 32889

   Attn: Library

8. National Aeronautics & Space Administration
   Langley Research Center
   Langley Station
   Hampton, Virginia 23665

   Attn: V. L. Bell                               1
   N. J. Johnston                          1
   S. Burke                                      1
   J. Samos                MS 139A          1

9. National Aeronautics & Space Administration
   Manned Spacecraft Center
   Houston, Texas 77001

   Attn: Library                                   1
   Code EP                                       1

10. National Aeronautics & Space Administration
    George C. Marshall Space Flight Center
    Huntsville, Alabama 35812

    Attn: J. Curry                                  1
    J. Stuckey                               1

11. Jet Propulsion Laboratory                 1
    4800 Oak Grove Drive
    Pasadena, California 91103

    Attn: Library

| Addressee | Number of Copies |
|---|---|

12. Office of the Director of Defense           1
    Research & Engineering
    Washington, D.C. 20301

    Attn:  H. W. Schulz, Office of Assistant Direct
          (Chem. Technology)

13. Defense Documentation Center           1
    Cameron Station
    Alexandria, Virginia 22314

14. Research & Technology Division           1
    Bolling Air Force Base
    Washington, D. C. 20332

    Attn:  RTNP

15. Air Force Materials Laboratory           1
    Wright-Patterson Air Force Base
    Dayton, Ohio 45433

    Attn:  T. J. Reinhart, Jr.

16. Commander           1
    U. S. Naval Missile Center
    Point Mugu, California 93041

    Attn:  Technical Library

17. Commander           1
    U. S. Naval Ordnance Test Station
    China Lake, California 93557

    Attn:  Code 45

18. Director (Code 6180)           1
    U. S. Naval Research Laboratory
    Washington, D. C. 20390

    Attn:  H. W. Carhart

19. Picatinny Arsenal           1
    Dover, New Jersey

    Attn:  SMUPA-VP3

20. SCI           1
    Azusa, California 91703

    Attn:  Ira Petker

| Addressee | Number of Copies |
|---|---|

21. Aeronautic Division of Philco Corporation          1
    Ford Road
    Newport Beach, California 92600

    Attn: L. H. Linder, Manager
          Technical Information Department

22. Aeroprojects, Inc.                                 1
    310 East Rosedale Avenue
    West Chester, Pennsylvania 19380

    Attn: C. D. McKinney

23. Aerospace Corporation                              1
    P.O. Box 95085
    Los Angeles, California 90045

    Attn: Library-Documents

24. Office of Aerospace Research (RROSP                 1
    1400 Wilson Blvd.
    Arlington, Virginia 22209

    Attn: Major Thomas Tomaskovic

25. Arnold Engineering Development Center              1
    Air Force Systems Command
    Tullahoma, Tennessee 37389

    Attn: AEOIM

26. Air Force Systems Command                          1
    Andrews Air Force Base
    Washington, D. C. 20332

    Attn: SCLT/Capt. S. W. Bowen

27. Air Force Rocket Propulsion Laboratory             1
    Edwards, California 93523

    Attn: RPM

28. Air Force Flight Test Center                       1
    Edwards Air Force Base, California 93523

    Attn: FTAT-2

29. Air Force Office of Scientific Research            1
    Washington, D. C. 20333

    Attn: SREP/J. F. Masi

| Addressee | Number of Copies |
|---|---|

30. Commanding Officer      1
    U.S. Army Research Office (Durham)
    Box GM, Duke Station
    Durham, North Carolina 27706

31. U. S. Army Missile Command      1
    Redstone Scientific Information Center
    Redstone Arsenal, Alabama 35808

    Attn: Chief, Document Section

32. Bureau of Naval Weapons      1
    Department of the Navy
    Washington, D. C. 20360

    Attn: DLI-3

33. Chemical Propulsion Information Agency      1
    Applied Physics Laboratory
    8621 Georgia Avenue
    Silver Spring, Maryland 20910

34. University of Denver      1
    Denver Research Institute
    P.O. Box 10127
    Denver, Colorado 80210

    Attn: Security Office

35. Dow Chemical Company      1
    Security Station
    Box 31
    Midland, Michigan 4864

    Attn: R. S. Karpiuk, 1710 Building

36. Ultrasystems, Inc.      1
    2400 Michelson Drive.
    Irvine, California 92664

    Attn: K. Paciorek/R. Kratzer

37. General Dynamics/Astronautics      1
    P.O. Box 1128
    San Diego, California 92112

    Attn: Library & Information Service (128-00)

38. General Electric Company      1
    Re-Entry Systems Department
    P.O. Box 8555
    Philadelphia, Pennsylvania 19101

    Attn: Library

| Addressee | Number of Copies |
|---|---|

39. General Technologies Corporation                1
    708 North West Street
    Alexandria, Virginia

    Attn:  H. M. Childers

40. Allied Chemical Corporation                     1
    General Chemical Division
    P.O. Box 405
    Morristown, New Jersey 0796C

    Attn:  Security Office

41. American Cyanamid Company                        1
    1937 West Main Street
    Stamford, Connecticut 06902

    Attn:  Security Office

42. ARO, Incorporated                                1
    Arnold Engineering Development Center
    Arnold Air Force Station, Tennesse 37389

    Attn:  B. H. Goethert, Chief Scientist

43. AVCO Corporation                                 1
    Space Systems Division
    Lowell Industrial Park
    Lowell, Massachusetts 01851

    Attn:  Library

44. Battelle Memorial Institute                      1
    505 King Avenue
    Columbus, Ohio 43201

    Attn:  Report Library, Room 6A

45. The Boeing Company                               1
    Aero Space Division
    P.O. Box 3707
    Seattle, Washington 98124

    Attn:  Ruth E. Perrenboom (1190)

46. Celanese Research Company                        1
    Morris Court
    Summit, New Jersey 07901

    Attn:  J. R. Leal

47.  Monsanto Research Corporation                              1
     Dayton Laboratory
     Station B, Box 8
     Dayton, Ohio

     Attn:  Library

48.  North American Rockwell Corporation                        1
     Space & Information Systems Division
     12214 Lakewood Blvd.
     Downey, California 90242

     Attn:  Technical Information Center, D/096-722 (AJ01)

49.  Northrop Corporate Laboratories                            1
     Hawthorne, California 90250

     Attn:  Library

50.  Rocket Research Corporation                                1
     520 South Portland Street
     Seattle, Washington 08108

51.  Rocketdyne, A Division of                                  1
     North American Rockwell Corporation
     6633 Canoga Avenue
     Canoga Park, California 91304

     Attn:  Library, Dept. 596-306

52.  Rohm & Haas Company                                        1
     Redstone Arsenal Research Division
     Huntsville, Alabama 35808

     Attn:  Library

53.  Sandia Corporation                                         1
     Livermore Laboratory
     P. O. Box 969
     Livermore, California 94551

     Attn:  Technical Library (RPT)

54.  Thiokol Chemical Corporation                               1
     Alpha Division, Huntsville Plant
     Huntsville, Alabama 35800

     Attn:  Technical Director

55.  United Aircraft Corporation                                1
     United Aircraft Research Laboratories
     East Hartford, Connecticut 06118

     Attn:  D. A. Scola

| Addressee | Number of Copies |
|---|---|
| 56. Hercules Powder Company<br>Allegheny Ballistics Laboratory<br>P.O. Box 210<br>Cumberland, Maryland 21501<br><br>Attn: Library | 1 |
| 57. Hughes Aircraft Company<br>Culver City, California<br><br>Attn: N. Bilow | 1 |
| 58. Institute for Defense Analyses<br>400 Army-Navy Drive<br>Arlington, Virginia 22202<br><br>Attn: Classified Library | 1 |
| 59. ITT Research Institute<br>Technology Center<br>Chicago, Illinois 60616<br><br>Attn: A. M. Stake, Manager<br>Polymer Chemistry Research | 1 |
| 60. Lockheed Missiles & Space Company<br>Propulsion Engineering Division (D.55-11)<br>1111 Lockheed Way<br>Sunnyvale, California 94087 | 1 |
| 61. Lockheed Propulsion Company<br>P. O. Box 111<br>Redland, California 92374<br><br>Attn: Miss Belle Berlad, Librarian | 1 |
| 62. United Aircraft Corporation<br>Pratt & Whitney Aircraft<br>East Hartford, Connecticut<br><br>Attn: Library | 1 |
| 63. United Aircraft Corporation<br>United Technology Center<br>P. O. Box 358<br>Sunnyvale, California 94088<br><br>Attn: Library | 1 |
| 64. Westinghouse Electric Corporation<br>Westinghouse Research Laboratories<br>Pittsburgh, Pennsylvania<br><br>Attn: Library | 1 |

65. TRW Equipment Lab
    Cleveland, Ohio

    Attn:  W. E. Winters                                           1
           P. J. Cavano                                            1

66. Horizons Incorporated                                         1
    23800 Mercantile Road
    Cleveland, Ohio 44122

    Attn:  K. A. Reynord

67. Air Force Aero Propulsion Laboratory                          1
    Wright-Patterson Air Force Base, Building 18-R-D105
    Dayton, Ohio 45433

    Attn:  B. P. Botteri

68. Gillette Research Institute                                   1
    Harris Research Laboratories
    1413 Research Blvd.
    Rockville, MD 20850

    Attn:  J. P. Wagner, Research Supervisor

69. University of Massachusetts                                   1
    Department of Chemical Engineering
    Amherst, Mass.  01002

    Attn:  J. W. Eldridge

70. Johnson Service Company
    507 East Michigan Street
    Milwaykee, Wisconsin 53201

    Attn:  C. F. Klein                                            1
           S. R. Buchanan                                         1

71. Honeywell                                                     1
    Commercial Division
    2701 Fourth Avenue, South
    Minneapolis, MN 55408

72. Office of Building Research & Technology                      3
    Department of Housing & Urban Development (MS 98)
    Washington, D. C. 20411

    Attn:  Orville Lee

73. National Bureau of Standards (MS 3)                           1
    Washington, D. C. 20234

    Attn:  R. L. P. Custus

| Addressee | Number of Copies |
|---|---|

74. General Service Administration (MS 29)         1
    Washington, D. C. 20405

    Attn:  T. E. Goonan

75. Massachusetts Institute of Technology       2
    Bldg. 13, Room 3061
    77 Massachusetts Avenue
    Cambridge, Mass. 02139

    Attn:  S. D. Senturia
           Associate Professor of Electrical En

76. ABT Associates                                  1
    55 Wheeler Street
    Cambridge, Mass. 02138

    Attn:  D. J. MacFadyen

77. Technical Information Systems Company      1
    National Aeronautics & Space Administration
    Scientific & Technical Information Facility
    P.O. Box 33
    College Park, Maryland 20740

    Attn:  T. Anuskiewics

78. E. J. Schwoegler Laboratories, Inc.       1
    7533 State Line Avenue
    Munster, Ind. 46321

79. Electro Signal Lab., Incorporated        1
    10222 Hingham Street
    Rockland, MA 02370

    Attn:  D. F. Steele

80. Exxon Research & Engineering Company     1
    P.O. Box 8
    Linden, New Jersey 07036

    Attn:  R. R. Bertrand

81. Technology and Economics, Inc.           1
    127 Mount Auburn Street
    Cambridge, MA 02138

    Attn:  A. Ackerman

82. Mel Lowry                                     1
    4709 Baum Blvd., Contraves Goerz
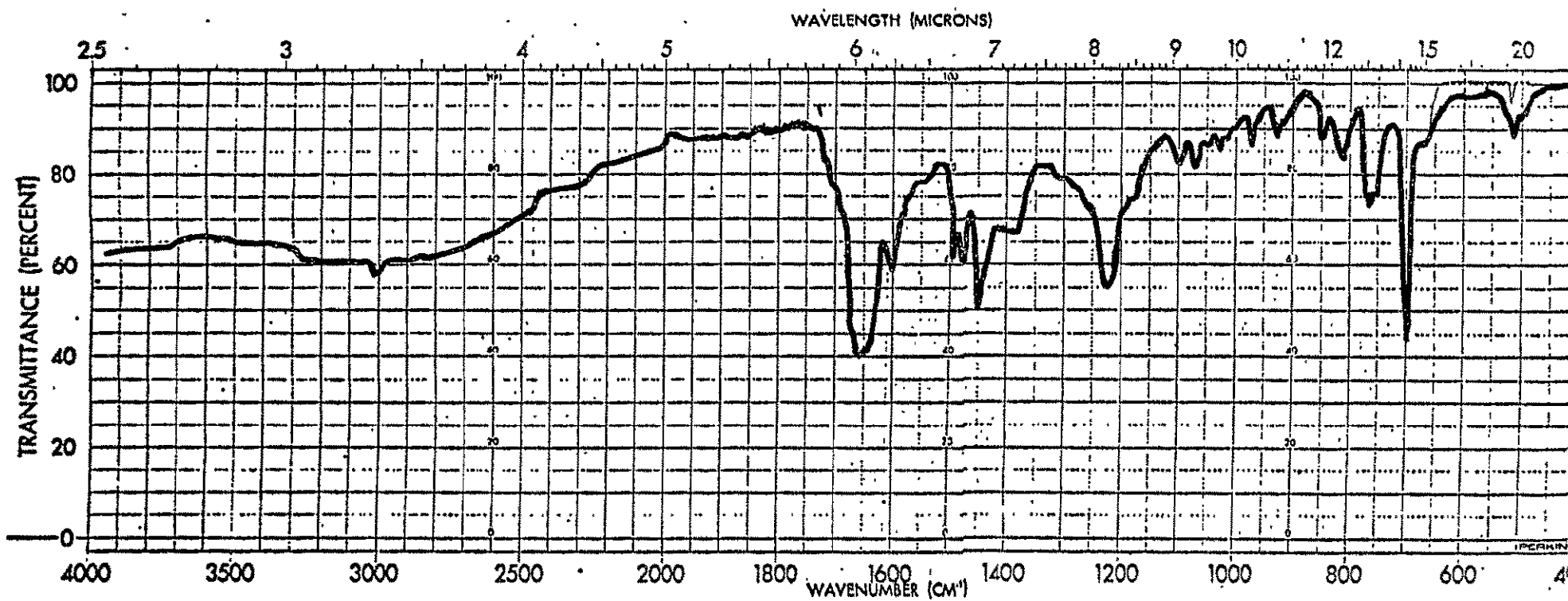    Pittsburgh, PA 15213

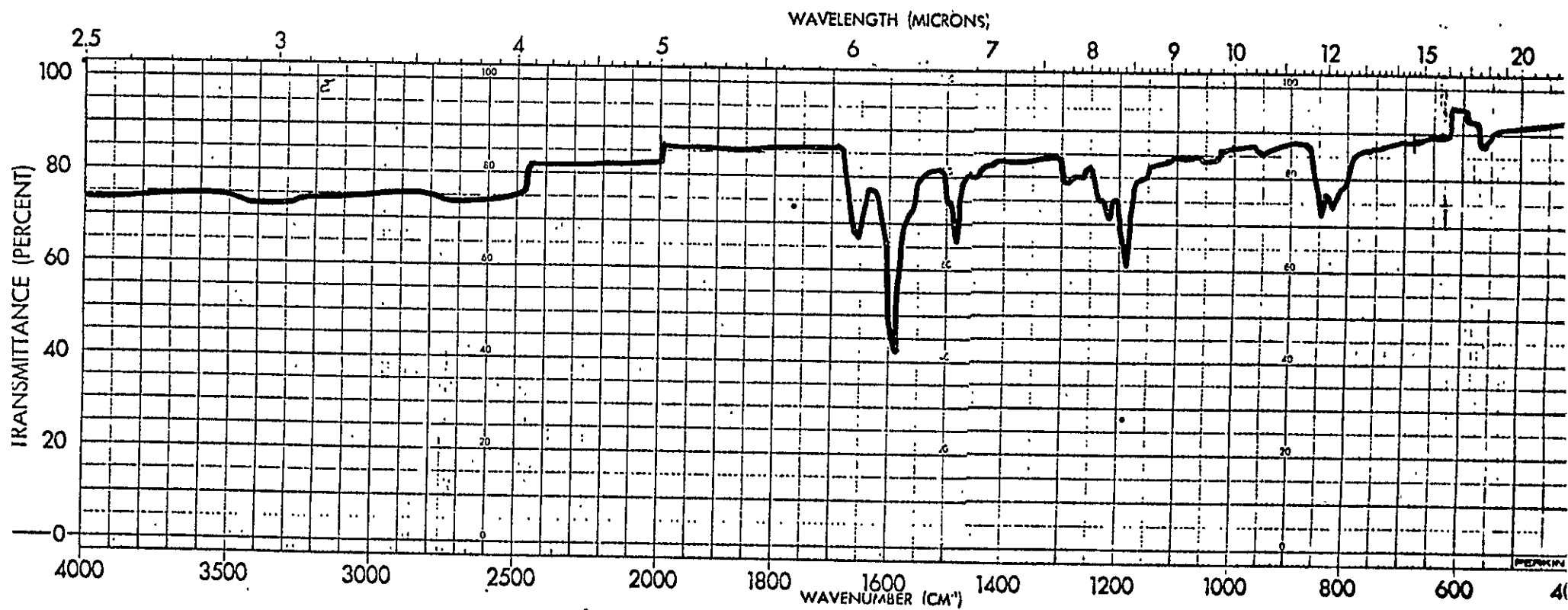FIGURE 47. INFRARED SPECTRUM OF POLYIMIDAZOLE FROM 1,4-BIS(PHENYLGLYOXYLOYL)

FIGURE 48. INFRARED SPECTRUM OF POLY(SCHIFF'S BASE) FROM p – PHENYLENEDIAMINE AND THIOPHENE–2,5–DICARBOXALDEHYDE
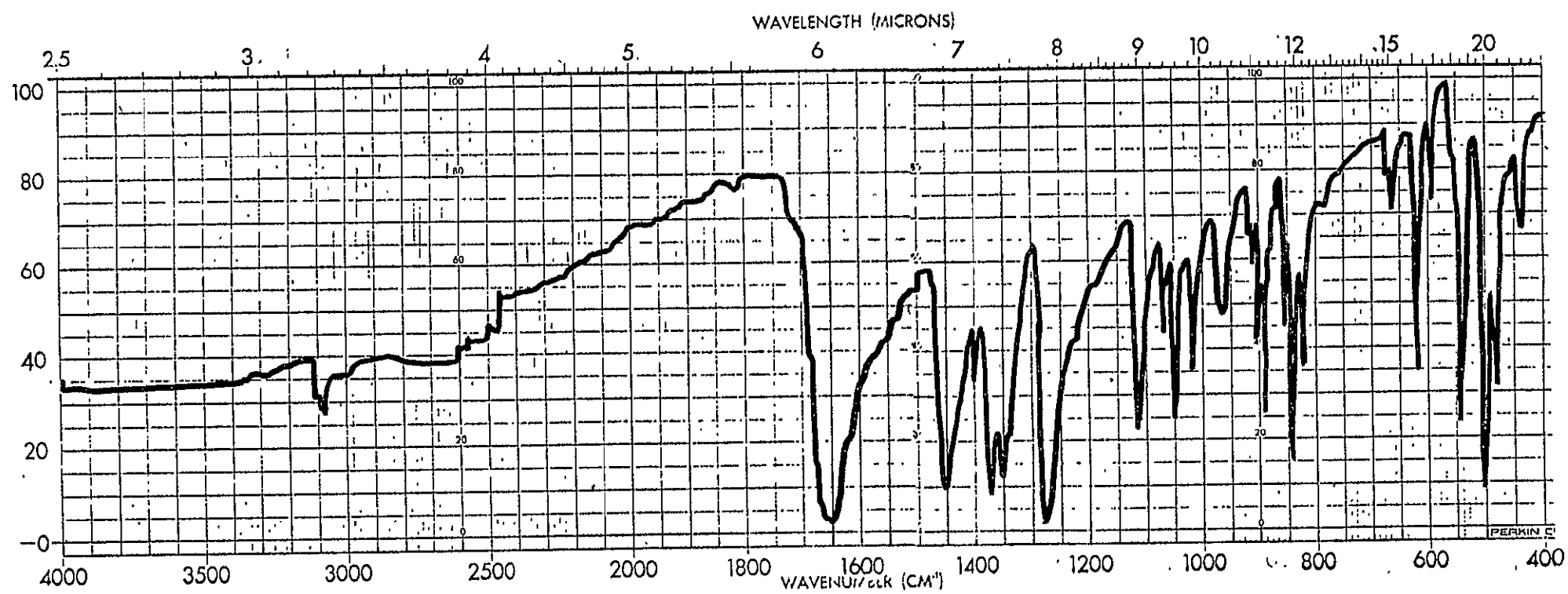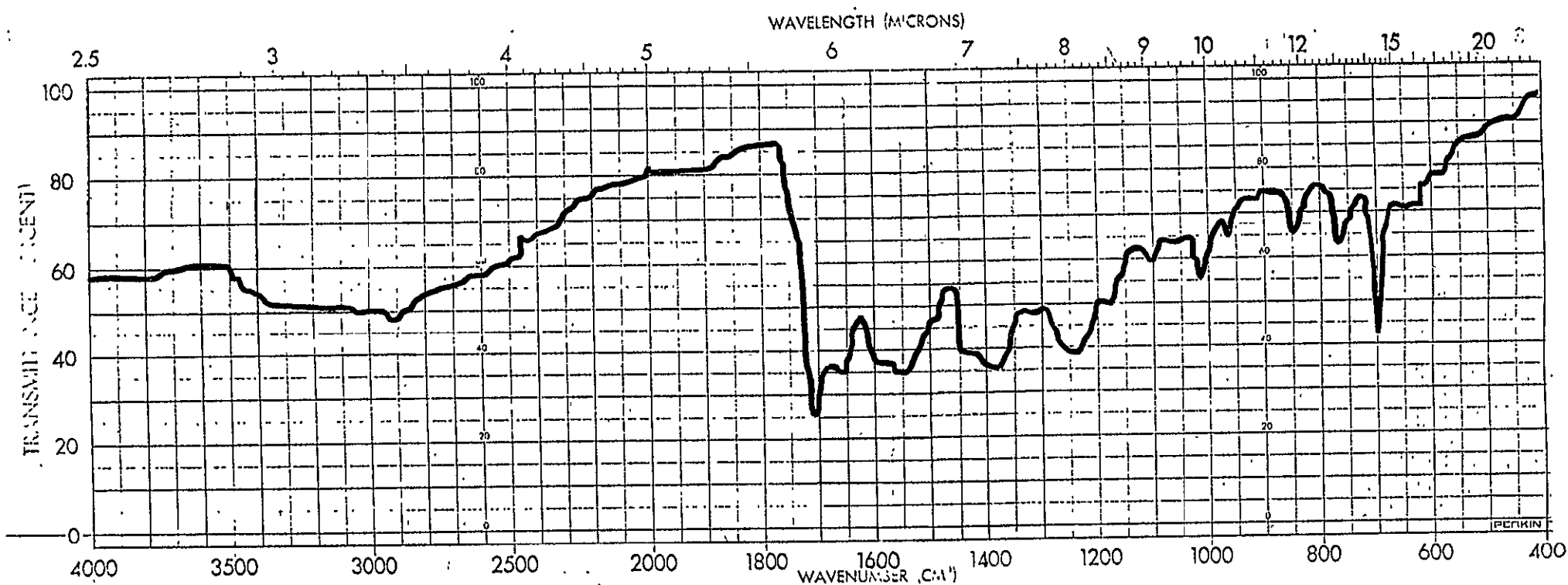
FIGURE 49. INFRARED SPECTRUM OF FERROCENE-1,1'-DICARBOXALDEHYDE

FIGURE 50. INFRARED SPECTRUM OF FERROCENE/IMIDAZOLE POLYMER